UNIVERSITY OF CAPE TOWN

MASTER'S THESIS

Modeling Compact Objects with Effective Field Theory

Author:
Irvin Martínez

Supervisor:
Amanda Weltman

A thesis submitted in fulfillment of the requirements
for the degree of Master of Science

in the

High Energy Physics, Cosmology & Astrophysics Theory Group
The Department of Mathematics and Applied Mathematics

October 17, 2022

Declaration of Authorship

I, Irvin Martínez, declare that this thesis titled, "Modeling Compact Objects with Effective Field Theory" and the work presented in it are my own. I confirm that:

- This work was done wholly or mainly while in candidature for a research degree at this University.
- Where any part of this thesis has previously been submitted for a degree or any other qualification at this University or any other institution, this has been clearly stated.
- Where I have consulted the published work of others, this is always clearly attributed.
- Where I have quoted from the work of others, the source is always given. With the exception of such quotations, this thesis is entirely my own work.
- I have acknowledged all main sources of help.
- Where the thesis is based on work done by myself jointly with others, I have made clear exactly what was done by others and what I have contributed myself.

Signed: Signed by candidate

Date:

"Feet on the ground, eyes on the sky."

Amanda Weltman

UNIVERSITY OF CAPE TOWN

Abstract

Faculty of Science
The Department of Mathematics and Applied Mathematics

Master of Science

Modeling Compact Objects with Effective Field Theory

by Irvin Martínez

In this master's thesis we have developed a worldline Effective Field Theory of compact objects, by extending the model of spinning extended objects derived using the coset construction [1], from which one can derive the effective theory from symmetry principles. To massive spinning extended objects, we have added electromagnetic charge and the finite-size structure including dissipation, such that we describe charged spinning compact objects, the most general compact object allowed in a theory of gravity such as General Relativity with classical electrodynamics.

To the derived effective action, we have matched the coefficients of the theory from the literature and obtained the leading order post-Newtonian expansion of our effective description of compact objects to show its predictability. We have expanded on the theoretical foundations of the effective theory for spinning extended objects by showing that the developed theory can be equivalent to the currently used theories as a special case. Nonetheless, the effective theory itself is more general and does not require additional degrees of freedom to be introduced, other than the ones derived from symmetries. We bring new results on the interaction and internal structure of charged spinning compact objects.

On the numerical side, based on the Effective Field Theory reasoning, we have introduced a framework for evolving a compact object binary. Within this approach, we obtain the leading order waveform emitted by the binary during its late inspiral and compare it to a waveform from standard methodologies. Then, by performing illustrative numerical experiments of systems that the LIGO-Virgo observatories have already detected, we show the role of the stellar structure and their coefficients in the phase evolution of the waveform, as well as the order in which they arise and the sensitivity required for the gravitational wave observatories to measure them. If these coefficients are to be measured, tight constraints on fundamental physics can be placed.

Acknowledgements

I am very grateful to Amanda Weltman for all her support and guidance on building this project, and to Enrico Ramírez-Ruiz, for introducing me into the field of compact objects and gravitational waves. I am particularly thankful to Tanja Hinderer, Riccardo Penco, Jan Steinhoff, Walter Goldberger, S. Mougiakakos, A. Luna, G. Creci, I. Meijer for very valuable discussions on the theoretical side, and to Johan Samsing and Aldo Batta, on the numerics. I am very thankful with all the people that spend time with me talking about Effective Field Theories and Compact Objects, Samaya Nissanke, Lavinia Heisenberg, Stephan Rosswog, Cliff Burgess, Michele Levi, Rafael del Porto, Ricardo Yarza, Horng Sheng Chia, Gustavo Niz, Alberto Diez, Raj Patil and Luis Lehner.

I am deeply grateful to my loving family, who have supported me through the years, and without them this would not have been possible. To my dad, who gave me wings to fly the furthest I could. To my mom, who has always kept me flying, even join on board and have spent some of the best time ever with her. To my sister, who is my best friend and is always there.

I also would like to acknowledge all the amazing people that shared with me and listen to me in México, South Africa and Europe. To Ian, who is an inspiration in life and physics and has always been present. To those whom I spent time in the mountains: To Maciej, Guy, Olaf and Pete, and to Hugo, Beto, Lu, Chris, Rojo, Ale, María, who are all an inspiration to me. Thank you for all the adventures. And to all my friends not mentioned here, who have always been interested on what I do, asking questions and wanting to know more about the universe. Thank you all.

Contents

To my loving sister May and mom Aurora. In memory of my beloved father Fabián.

Chapter 1

Introduction

1.1 Compact Objects in the Universe

We live in a time with access to data from the most energetic "particle" collisions in the universe. The astonishing first detection of gravitational waves (GWs) by the LIGO-Virgo observatories from a binary black hole (BBH) merger [2], the multi-messenger detection from a binary neutron star (BNS) collision [3, 4, 5], and the recent detection of the coalescence of black hole (BH) - neutron star (NS) binaries [6], provide us with ample opportunities to test fundamental physics in the strong regime of gravity.

These detections of binary systems through GWs have already allowed us to better understand the properties of compact objects [7, 8]. With more sensitivity upgrades planned for the LIGO-Virgo observatories [9], the upcoming third generation Einstein Telescope [10, 11] and the space based detector, LISA [12], the era of precision gravity is upon us, and with it the potential for great discovery using multi-messenger astronomy to better understand the universe on all scales. On the theoretical side, the development of improved tools to model the dynamics of any astrophysical source to extract the gravitational wave signature, can only aid in this discovery.

One of the key potentials with GW observations is to test fundamental physics by probing the internal structure of the compact objects. For example, the equation of state of matter for NSs is still unknown, and it has been suggested that it can be constrained by matching the Love numbers of the NSs with GW observations [13, 14]. The Love numbers are dimensionless parameters that measure the rigidity and tidal deformation of the stellar object, and different values for the Love numbers correspond to different equations of state of matter [15]. The measurement of dynamical tides will lead to stringent constraints on the equation of state of matter [16, 17].

On the other hand, BHs within the theory of General Relativity are described by only three parameters, its mass, spin and charge, and the Love numbers vanishes [18, 19]. Any finding of deviation of this description or discovery of a new parameter that describes the BH must show hints of a more complete underlying gravitational theory [20, 21]. Therefore, modified theories of gravity can be constrained with Love numbers as well [22]. Exotic compact objects have been proposed, such as fuzzballs [23], gravastars [24], wormholes [25] and boson stars [26], and its stellar structure in terms of Love numbers [22].

Finally, it is worth mentioning that, within the framework used in this thesis, it has been proposed the possibility to test physics beyond the standard model, such as ultralight bosons [27], and dark matter [28]. As one can see with our brief introduction to the kind of compact objects that could possibly exists in our universe, having access to GW observations, there is room for great discoveries.

1.2 The Theoretical Model

The modeling of compact objects and their interactions must take into account different effects, such as the spin, charge, and the stellar structure of the various stellar types. In this work we bring the tools of effective field theory (EFT) for extended objects [29, 30, 1] to model BHs and NSs as point particles, with additional effects encoded as higher order corrections in the action.

Although at first it might seem counter intuitive to model such massive objects as point particles, there is in fact, a lot of similarity in the description of compact objects and elementary particles [31, 32]. For instance, the no hair theorem implies that a BH effectively behaves as a point particle, and it has been shown that, by matching on to the effective action of a spinning point particle, a spinning BH is described relativistically to all orders in the multipole expansion from minimal coupling in the amplitudes formalism [33, 34].

Using the coset construction [35, 36, 37, 38] in the Effective Field Theory (EFT) framework for extended objects [29, 30, 1], we build the most general effective action allowed in an effective theory of gravity such as General Relativity with electrodynamics. In this theory, BHs can be described by only three parameters, its mass, spin and charge, behaving effectively as a point particle [31, 32]. One of the advantages of using the EFT for extended objects is that we can model the compact objects as point particles, with its additional effects and internal structure encoded as higher order corrections in the action, which are made up of the allowed invariant operators given the symmetries of the objects. These operators are accompanied by the coefficients of the effective theory, which encapsulates the internal properties of the compact objects. In this sense, we construct the lowest order effective action for the most general allowed compact object in the point particle approximation, which is one that is charged and spinning.

The coset construction is a very general technique from the EFT framework that can be used whenever there is a symmetry breaking. With this technique, it is possible to derive the covariant building blocks that transform correctly under the relevant symmetries, which then can be used to form invariant operators to build up an effective action. Any state other than vacuum will break some of the space-time symmetries, and by correctly identifying the pattern of the symmetry breaking, we can derive its effective action. Within this approach, we can treat the coefficients that appears in front of the invariant operators as free parameters to be fixed by experiments or observations. In this sense, we are interested to know what was the full symmetry group, G, of the EFT, and what subgroup, H, was realized non-linearly, parametrized by the coset, G/H [39].

An effective theory of gravity, such as General Relativity, can be derived using the coset construction by weakly gauging the space-time symmetry group of gravity, the Poincaré group ISO(3,1), and realizing translations nonlinearly, which is parametrized by the coset ISO(3,1)/SO(3,1) [1], with SO(3,1) the Lorentz group. From this coset parametrization, it is possible to derive the widely known Einstein's vierbein theory of curved space or tetrad formalism, which is a generalization of the theory of General Relativity that is independent of a coordinate frame. Once the underlying theory of gravity is developed, one can proceed to identify the symmetries that an extended object breaks to derive its effective action. For instance, a point particle breaks spatial translations and boosts, while a spinning point particle breaks spatial translations and the full Lorentz group [1].

Due to the Goldstone's theorem [40] and the inverse Higgs constraint [38], the

symmetry breaking pattern for a spinning object implies the existence of a Nambu-Goldstone field, that takes the role of the angular velocity [1], yielding a very natural construction for the action of spinning objects. Although it has been pointed out that this is a theory for "slowly" spinning compact objects, given that from construction the effective action corresponds to the low energy dynamics of the theory, we show that we can safely consider the current observed compact objects through GWs as slowly spinning.

Therefore, in this work we review and build on the EFT for spinning extended objects introduced in [1]. We derive in detail the building blocks of the effective theory and its constraints, which allows us to build up the tower of invariant operators and form the effective action to all orders. We have extended the model by considering the electromagnetic charge U(1) symmetry, as an internal symmetry in the coset parameterization, which allows us to derive the Einstein-Maxwell action. Then, by identifying the symmetry breaking pattern of charged spinning object, we construct the corresponding corrections to the point particle. We show that the spin corrections considered in the effective theory for spinning extended objects in [41], which are used to obtain state of the art results needed for GW extraction, are encoded in the allowed boson couplings.

For the internal structure of the objects, we take into account size [29], and dissipative effects [30, 42]. The coefficients accompanying the operators of these effects, encode the microphysics of the object, and based on results in the literature, we can identify them without having to do the explicit computations. Tidal effects for the case of spinning compact objects have been taken into account in [43, 44, 45], as well as for noncompact objects in [46], by considering only rotationally invariant operators and associating departures from sphericity with higher order corrections. The coefficients due to tidal effects for compact objects can be matched from [18, 19, 14, 47, 48]. We consider quasi-static dynamical tides on the NS as well, and match the coefficient to [49].

We consider the size effects induced by charge as well, known as the polarizability, for which some of the coefficients are unknown. On the dissipative effects for spinning BHs, we consider the absorption of gravitational and electromagnetic waves [30], as well as the dissipation generated by the spin [42, 50, 46, 19], for which coefficients have been matched by analytical means [30, 19]. For a NS, dissipation accounts for the energy loss due to the viscosity of the star, and state of the art hydrodynamical simulations are needed to match the coefficients.

1.3 The Coalescence of a Binary

In the lifetime of a binary made out of compact objects, if the orbital distance of initial formation is short enough, relativistic effects will make the orbit of the binary to shrink due to GW radiation until they collide. The description of the coalescence of binary systems is divided into four stages: the inspiral, plunge, merger and ringdown, which is depicted in fig. 1.1. The inspiral phase is described using the post-Newtonian (PN) expansion, which is a perturbative series in terms of the expansion parameter $v/c < 1$, with v the relative velocity of the binary [29, 51]. The transition from the inspiral to the plunge can be modelled analytically [52], although it is usually modelled altogether with the merger by solving the full Einstein's equations numerically [53], which is computationally expensive. After merging, if the final outcome is a BH, it enters into a ringdown phase that can be modelled analytically using perturbation theory [54]. Although the derived action can be used for

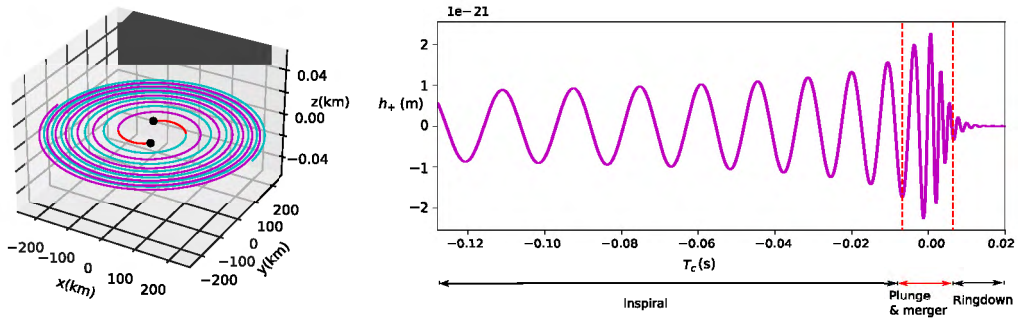

FIGURE 1.1: The coalescence of an equal mass BBH system, each with mass, $M = 20\,M_\odot$, and initial gravitational wave frequency, $f_{GW} = 50$Hz. The left figure represents the dynamics of the binary until the collision of the BHs using our numerical code for point particles, with the purple and cyan line the trajectories followed by each of the BHs. The orbital trajectory once the LSO is reached is shown in red until the radii of the holes interact. The system decays due to GW radiation by including the leading order 2.5 PN correction in the equations of motion. The figure on the right is the gravitational waveform extracted from the merger of the same binary but using the EOB method from the LIGO Algorithm Library [58]. The coalescence is divided into four different phases: inspiral, plunge, merger and ringdown.

different regimes in the coalescence of binaries, in this thesis we restrict ourselves to the inspiral, described by PN expansion.

The need to extract efficient and accurate waveforms for all of the phases of the coalescence led to the development of the Effective One Body (EOB) framework [55], which is a combination of analytical methods based on the Hamiltonian, that uses the PN expansion as an input for the inspiral, and non-perturbative methods and numerical relativity results to model the merger semi-analytically. Since the introduction of the EOB many additional improvements have been done to include the stellar structure, such as tidal effects [56, 16, 17] for NSs, and BHs horizon GW absorption or dissipative effects [57]. The EOB is the current framework used for gravitational wave extraction and comparison to observations. In fig. 1.1, we show a waveform from an equal mass BBH extracted using the EOB method from the LIGO library [58].

The properties of the internal structure of the compact objects play an important role mostly in the late inspiral phase of the coalescence [45], before the plunge and merger (or collision) of the components of the binary. During the inspiral, the dynamics are well described by the post-Newtonian (PN) approximation [51], which reproduces the dynamics of the full theory of General Relativity to high accuracy until the last stable orbit (LSO) is reached [59, 60]. The LSO is the closest distance at which a point particle has a stable orbit around the stellar object and it will set the limit of our theory. Once the LSO has been reached, the binary enters into the plunge phase.

In the PN expansion, one obtains general relativistic corrections to the dynamics as a perturbative series in terms of the expansion parameter, $v/c \ll 1$, with v the relative velocity of the binary. For each n-PN order, the expansion of the Lagrangian is of order v^{2n}. In figure 1.1, we show the dynamics of the coalescence of an equal mass BBH in a quasi-circular orbit made with our simulations, and show where our

theory breaks down. Although high order PN corrections are necessary for a precise description of the interaction, in this thesis we consider only the leading order correction to each of the relevant terms in the action, and neglect any higher order conservative PN correction to the point particle interaction, which only contribute to a shift of the orbit and do not contribute to the decay of the binary. For the GW decay, we consider only the leading order PN correction due to gravitational wave radiation, the 2.5−PN term [29].

A very powerful framework that has led to the derivation of many new results on the dynamics of binary systems, is the effective field theory (EFT) for extended objects in nonrelativistic General Relativity [29, 30]. In this worldline effective theory, extended objects are treated as point particles, with its properties and internal structure encoded in higher order invariant operators that are allowed by the symmetries of the objects. Within this framework, it is possible to build a tower of EFTs [61], which follows a clear hierarchy of scales: $\ell \ll r \ll \lambda$, with ℓ, the radius of the compact object, r, the orbital separation of the binary, and $\lambda = r/v$, the wavelength of the GW radiation [29]. In this EFT approach, given the hierarchy of scales, we can organise the PN expansion in a systematic way by using the usual diagrammatic tools from EFTs.

Since the introduction of the EFT for extended objects, in which finite size [29] and dissipative effects [30] are taken into account for nonspinning objects, the framework has gone through a remarkable progress in the past few years. For instance, it was shown in [62], that the computations simplifies by considering the time dimension as compact, and parametrizing the gravitational interaction in terms of nonrelativistic fields. Furthermore, spinning [43, 41, 1] and charged [30, 63, 64] compact objects were introduced, and the effective theory that describes the long wavelength gravitational radiation from compact binary systems was derived [65]. Tidal effects for spinning objects were considered in [43, 41, 46], while dissipative effects for slowly spinning in [50, 46], and for maximally spinning in [42]. In this thesis we have introduced charged spinning compact objects, in which the polarizability and the electromagnetic dissipation of the charged spinning objects are considered.

Therefore, we obtain the leading order (LO) PN expansion of the theory of charged spinning compact objects that we have derived in this thesis. In this effective theory, the covariant building blocks are derived by giving the symmetries of a compact object as the only input, from which we can build the invariant operators to build the effective action. Within this procedure, the coefficients of the derived effective theory from a coset are to be matched from the known full theory, and ultimately from observations. In this work we have matched the coefficients from the known theories [29, 30, 43, 41, 63, 42], which allows us to show the predictivity of our theory by recovering well known results.

To connect to the results of the PN expansion for spinning extended objects [43, 41, 66], we introduce the spin degree of freedom as the conjugate of the relativistic angular velocity, and show that from construction, our effective theory contains all the necessary ingredients to obtain the well known LO results in phase space. After recovering such results on spinning objects, by including the invariant operators corresponding to the corrections due to the electrodynamics, we re-derive the 1 PN correction to the interaction of charged point particles in curved space-time [63] in terms of non-relativistic fields, which simplifies the computation. Then, by considering the internal structure of an extended object in an external electromagnetic field, we bring new LO PN results on the polarizability and dissipation of charged spinning compact objects.

Although in this thesis we obtain the LO corrections due to the different effects that play a role in the dynamics, and the 1 PN correction of the electromagnetic and gravitational interaction for nonspinning point particles, the EFT framework for extended objects [29, 30] has been extensively used to recover well known results, to obtain higher order PN corrections, and to derive new results on the effects due to spin, charge and the internal structure of the compact objects, which are required for meaningful gravitational waveform extraction. We briefly summarize the history and current state of the PN expansion.

The first PN correction dates back to Einstein [67]. Before the introduction of the EFT for extended objects [29, 30], extraordinary efforts led to the obtention of the 3 PN expansion to the dynamics without spin [51], but the computation of higher order terms became very challenging. Then, within the EFT framework, the known results up to 3 PN order were reproduced [68], and new results for the 4 PN [68, 69] and 5 PN [70] corrections to the dynamics were derived. On spinning objects, the PN contributions from the spin-orbit and spin-spin coupling were derived [43], which received further corrections in [71, 72, 73, 74, 75, 41]. The current state of the art of the PN expansion for spinning objects is the complete 4 PN corrections [66], and partial results up to 5 PN order [76, 77, 78, 79]. The PN expansion for charged objects was considered until recently [63], in which partial results of the 1 PN correction were derived. A review on the PN expansion using EFT can be found in [80, 81].

Although high order PN corrections are necessary for a precise description of the interaction, in the numerical section of this thesis, we consider only the LO PN correction due to the internal structure of the compact objects, to do a systematic study of their properties and imprints in the waveform. In our computations of the PN expansions, we have not considered the radiation of gravitons, and therefore to take into account for the decay of the binary due to GW radiation, we extract from the literature the LO correction due to radiation, which is the 2.5 PN term [29, 65, 51], to then implement it numerically.

1.4 Numerical Experiments

Taking into account the aforementioned ingredients but neglecting charge, and with the point particle approximation in mind, we obtain the equations of motion for the effective action and introduce a known methodology for simulating stellar dynamics as point particles [82] into the framework of EFT for compact objects. Our implementation of the coalescence of a binary is tested with analytical results, and the stellar structure effects are internally tested by matching the coefficients of the theory during the simulation. Solving numerically for the point particle as well as for its additional effects, allows us to evolve the system with high accuracy for low computational cost.

We perform a systematic investigation of the matching of the coefficients of the effective theory from Newtonian hydrodynamical simulations, in which we have found that, at least for a non-compact star, the static tidal effects does not reproduce the expected results, and a better treatment of dynamical tides as in [17] needs to be done. We have not been able to compare the coefficient of a NSs as we did for a non-compact object, given the relativistic velocities in which they interact in a parabolic encounter. Nevertheless, in this thesis we implement numerically the quasi-static tidal effects, for which results can be seen as a lower bound on the more accurate dynamical effects.

We propose a hybrid method for extracting gravitational waveforms as a function of the orbital frequency of the binary, ω_s, input which is generated numerically and then evaluated in the analytical formula of the waveform. Our method for GW extraction reproduces LO results from known methodologies that evaluates the coalescence time, t_c, of the binary. Nevertheless, for a correct high order PN waveform extraction that can match observations, the conservative PN expansion in the center of mass frame needs to be derived and incorporated, which is beyond the scope of this thesis.

We perform illustrative numerical "experiments" of the inspiral of the different detected binaries to study the imprints of the stellar structure in the dynamics. With these, we show the role of the stellar structure and its coefficients in the waveform, given that the addition of the stellar properties in the equations of motion generates changes in the orbital frequency, which can be measured as a phase shift in the waveform. We show the order at which the stellar structure effects arise in the waveform, and the sensitivity that the current LIGO-Virgo observatories will need to detect them.

We suggest that the matching of the coefficients due to the internal structure of spinning NSs, n_Ω, is the first to be matched from observations, given that it can be the LO effect, making a wave shift in the waveform of order up to, $\Delta\varphi \simeq O(10)$, given our considered spinning objects. Moreover, we perform a systematic study of the internal structure of the objects, and show that, at least at this level of the implementation, in order to constrain the coefficients of all the LO effects due to the internal structure of the compact objects, current and future GW observatories need to measure wave shifts with an accuracy of at least, $\Delta\varphi \simeq O(10^{-4})$ radians.

The plausibility for LIGO-Virgo observatories and the Einstein telescope to detect such effects, is of course dependent on the frequency where the dephasing is accumulated in the signal relative to the most sensitive band of the detectors. At current sensitivity, if the phase shift is of order $O(10^0)$ radians in the most sensitive band, then the effect could be measurable and a systematic study needs to be carried out, i.e. using Fisher matrix estimates [83]. With upcoming sensitivity upgrades, a systematic study needs to be done to put bounds on the measurability of such effects, and whether all the effects due to the internal structure of the compact object can be constrained.

1.5 The Effective Theory of Compact Objects

This thesis has the purpose to build on the theoretical foundations in the description of compact objects as an EFT, and to systematically study the imprints of the stellar structure in the inspiral regime of the binary. We have built the LO effective action for compact objects using symmetry arguments with the coset construction, and matched the coefficients of the theory from the literature, such that we do not have to do any explicit computation on the derivation of the coefficients.

In the EFT framework, a compact object is described as a point particle, with its properties encoded in higher order corrections in the action. Our action describes a relativistic point particle, with relativistic corrections due to spin, charge, and corrections due to the internal structure of the objects. In our description of compact objects, we have clarified on the EFT for spinning objects, and introduced the electromagnetic charge such that we can describe charged spinning compact objects.

We have considered the inspiral phase of the coalescence to study the imprints of the internal structure of the objects in the waveform. Therefore, we have obtained

the LO PN expansion of each of the relevant terms in the action. We have shown the predictivity of our theory by comparing to known results, and then obtained new ones on the LO PN expansion of the stellar structure of charged spinning compact objects.

Within the point particle approximation, we have developed a numerical framework to extract GWs and measure the imprints of the stellar structure. Although our current implementation is lacking of precise waveform extraction, our results, which are the phase shifts generated by the different effects due to the internal structure to lowest order, give an insight of the order at which the effect will arise in the waveform. Therefore, we have shown the role of the different effects and their coefficients by performing different numerical examples with the current detected compact object binaries. Using an EFT perspective, we have set lower bounds on the accuracy needed for GW detectors the measure such effects.

This work is the first step on the development of the complete EFT for compact objects, in which we have focused on the inspiral regime. Nevertheless, by the time this thesis is finished, we are further developing the model to extract the dynamics without introducing additional degrees of freedom, and exploiting the power of the vierbein formalism in a modern fashion. In this approach, the effective action can be equally used for both the post-Minkowskian expansion and the PN. Moreover, the formalism can be used in the EOB framework. These work is under construction. The ultimate goal, in order to test fundamental physics, is to create a framework based on the state of the art theoretical and numerical tools, to match the coefficients from observations.

The outline of this thesis is the following. In chapter 2, we provide a brief introduction to the concepts and tools from EFTs necessary to develop the EFT for compact objects. Then, in chapter 3, we develop in detail the Effective Field Theory for Compact Objects. In chapter 4, work in the inspiral regime of a compact object binary and obtain the LO post-Newtonian expansion of the derived effective action. In chapter 5, we implement our results in numerical experiments to extract GWs and study the role of the stellar structure during the late inspiral. Finally, in chapter 6, we summarize and conclude.

Chapter 2

Effective Field Theory

In the observable universe there exists a wide variety of scales, from the quantum world to the cosmological structure. In this scale range we can find all kind of physical phenomena, for which the dynamics will be different from one scale to another. There is an important property of nature, known as decoupling, that has allowed us to understand the physical phenomena emerging at the different scales. The decoupling of physical effects means that most of the details, or short distance physics, are irrelevant for the description of larger distance phenomena.

The theoretical framework we have developed for modeling the laws of nature is known as field theory, both at quantum and classical level. Field theories also have the property that short distances mostly decouple from larger ones, and the set of tools that have been developed to show the symmetries, hierarchy of scales and decoupling of physical effects, are known as effective field theories. These tools, with the appropriate knowledge of the symmetry pattern, relevant scales and hierarchies, allows us to simplify the description of different systems.

In this chapter we introduce the concepts of EFTs by formulating an effective action for charged point particles in flat space-time. We derive the effective action using the coset construction.

2.1 Conventions

We differentiate between space-time and local Lorentz indices as in [1]:

- μ, ν, σ, ρ... denote space-time indices.
- a, b, c, d... denote Lorentz indices.
- i, j, k, l... denote spatial components of the Lorentz indices.

We denote the time of occurrence and the location in space of an event with the four component vector, $x^a = (x^0, x^1, x^2, x^3) = (t, \vec{x})$, and define the flat space-time interval, $\mathrm{d}s$, between two events, x^a and $x^a + \mathrm{d}x^a$, by the relation

$$\mathrm{d}s^2 = -c^2\mathrm{d}t^2 + \mathrm{d}x^2 + \mathrm{d}y^2 + \mathrm{d}z^2, \tag{2.1}$$

which we write using the notation

$$\mathrm{d}s^2 = \eta_{ab}\mathrm{d}x^a\mathrm{d}x^b\,; \qquad \eta_{ab} = \mathrm{diag}(-1, +1, +1, +1). \tag{2.2}$$

In the last expression we have introduced the summation convention, which states that any index that is repeated in an expression, is summed over the range of values taken by the index.

2.2 Worldline Point Particle Dynamics

The most important consideration when modelling compact objects with EFTs is that they can be treated as point particles with higher order corrections. To describe the dynamics of point particles, it is necessary to specify a continuous sequence of events in the space-time by giving the coordinates, $x^a(\sigma)$, of the events along a parametrized curve, defined in terms of a suitable parameter, σ. There is one curve among all possible curves in the space-time, which describes the trajectory of a material particle moving along some specified path, known as the worldline. We can consider it as a curve in the space-time, with $\sigma = ct$, acting as a parameter so that $x^a = (ct, \vec{x}(t))$. The existence of a maximum velocity $|\vec{u}| < c$, which requires the curve to be time-like everywhere, $\mathrm{d}s < 0$, allows us to have a direct physical interpretation for the arc length along a curve.

Consider a clock attached to the particle frame, or the proper frame $\tilde{\mathrm{F}}$, which is moving relative to some other inertial frame F on an arbitrary trajectory. As measured in the frame F, during a time interval between t and $t + \mathrm{d}t$, the clock moves through a distance $|\mathrm{d}\vec{x}|$. The proper frame $\tilde{\mathrm{F}}$, which is moving with same velocity as the clock, will have $\mathrm{d}\vec{\tilde{x}} = 0$. If the clock indicates a lapse of time, $\mathrm{d}t \equiv \mathrm{d}\tau$, the invariance of the space-time interval, eq. (2.1), implies that

$$\mathrm{d}s^2 = -c^2\mathrm{d}t^2 + \mathrm{d}x^2 + \mathrm{d}y^2 + \mathrm{d}z^2 = \mathrm{d}\tilde{s}^2 = -c^2\mathrm{d}\tau^2. \tag{2.3}$$

Thus, we obtain the lapse of time in a moving clock

$$\mathrm{d}\tau = \mathrm{d}t\sqrt{1 - \frac{v^2}{c^2}}, \tag{2.4}$$

along the trajectory of the clock. The total time that has elapsed in a moving clock between two events, known as the proper time τ, is denoted as

$$\tau = \int \mathrm{d}\tau = \int_{t_1}^{t_2} \mathrm{d}t\sqrt{1 - \frac{v^2}{c^2}}. \tag{2.5}$$

We now proceed to build the action of a free point particle. The Lagrangian must be constructed from the trajectory, $x^a(\tau)$, of the particle, and should be invariant under Lorentz transformations. The only possible term should be proportional to the integral of $\mathrm{d}\tau$, yielding the action

$$\mathcal{S} = -\alpha \int_\tau \mathrm{d}\tau = -\alpha \int \sqrt{1 - \frac{v^2}{c^2}}\mathrm{d}t, \tag{2.6}$$

where α is a dimensionful constant. To recover the action of a free point particle from non-relativistic mechanics, we take the limit $c \to \infty$, for which the Lagrangian yields $\mathcal{L} = \alpha v^2/2c^2$. By comparing our point particle Lagrangian with the non-relativistic one, $\mathcal{L} = (1/2)mv^2$, with m the mass of the particle, we find that, $\alpha = mc^2$. Thus, the action for a relativistic point particle is

$$\mathcal{S} = -mc^2 \int \mathrm{d}\tau, \tag{2.7}$$

which corresponds to the arc length of two connecting points in the space-time.

2.3 Symmetries in Classical Field Theory

We consider symmetries that can be labelled by a continuous parameter, θ. Working with the Lie algebras of a group G, we write a group element as a matrix exponential

$$U = e^{i\theta^u T_u}, \tag{2.8}$$

where the generators T_u, with $u = 1, ..., n$, form a basis of the Lie algebra of G. The T's generators are hermitian if U is unitary. For each group generator, a corresponding gauge field arises, which in this case is the field θ.

The properties of a group G are encoded in its group multiplication law

$$[T_u, T_v] = T_u T_v - T_v T_u = i c_{uvw} T_w, \tag{2.9}$$

where, c_{uvw}, are the structure constant coefficients. The last expression defines the Lie algebra of the group G. The Lie bracket is a measure of the non-commutativity between two generators.

It is also possible to consider in the local framework of field theory, continuous symmetries that have a position dependent symmetry parameters, $\theta = \theta(x)$. The space-time dependent symmetry transformation rules are called local or gauge symmetries. For global symmetries, θ do not depend on space-time position. There is also a distinction between internal symmetries and space-time symmetries, on whether they act or not on space-time position. An example of an internal symmetry, where x is unchanged, is

$$\phi^u(x) \to U\phi^u(x)U^{-1} = \mathcal{U}_v{}^u \phi^v(x), \tag{2.10}$$

while an example for a space-time symmetry is the transformation

$$\phi^u(x) \to V\phi^u(x)V^{-1} = \mathcal{V}_v{}^u \phi^v(x'), \tag{2.11}$$

with $x'^u = \mathcal{V}_v{}^u x^v$. Both internal and space-time symmetries can arise in global or gauged varieties.

Symmetries of Special Relativity

The symmetry of Special Relativity is determined by the Poincaré symmetry. Its Lie group, known as the Poincaré group, G = ISO(3,1), is the group of Minkowski space-time isometries that includes all translations and Lorentz transformations.

The Lorentz Group

The Lorentz group, SO(3,1), is the group of linear coordinate transformations

$$x^a \to x'^a = \Lambda^a{}_b x^b, \tag{2.12}$$

that leave invariant the quantity

$$\eta_{ab} x^a x^b = -(ct)^2 + x_1^2 + x_2^2 + x_3^2, \tag{2.13}$$

with $\det\Lambda = 1$. In order for eq. (2.13) to be invariant, Λ must satisfy

$$\eta_{ab} x'^a x'^b = \eta_{ab}(\Lambda^a{}_c x^c)(\Lambda^b{}_d x^d) = \eta_{cd} x^c x^d, \tag{2.14}$$

which implies the transformation of the metric as

$$\eta_{cd} = \eta_{ab}\Lambda^{a}{}_{c}\Lambda^{b}{}_{d}. \tag{2.15}$$

Consider an infinitesimal Lorentz transformation, with the Lorentz generators J_{ab}, and its corresponding field α_{ab}. We can expand

$$\Lambda^{a}{}_{b} = (e^{\frac{i}{2}\alpha^{cd}J_{cd}})^{a}{}_{b} = (e^{\alpha})^{a}{}_{b} \approx \delta^{a}{}_{b} + \alpha^{a}{}_{b}, \tag{2.16}$$

where the factor of, $\frac{1}{2}$, is taking into account the sum over all a and b. From equation (2.15) we find

$$\alpha_{ab} = -\alpha_{ba}, \tag{2.17}$$

which is an antisymmetric 4x4 matrix with six components that are independent. Thus, the six independent parameters of the Lorentz group from the antisymmetric matrix, α_{ab}, corresponds to six generators which are also antisymmetric $J^{ab} = -J^{ba}$.

Under Lorentz transformations, a scalar field is invariant,

$$\phi'(x') = \phi(x). \tag{2.18}$$

A covariant vector field, V^{a}, transforms in a representation of the Lorentz group as

$$V^{a} \to (e^{\frac{i}{2}\alpha_{cd}J^{cd}})^{a}{}_{b}V^{b}, \tag{2.19}$$

where the exponential is the matrix representation of the Lorentz group. If we consider an infinitesimal transformation, the variation of V^{a} reads,

$$\delta V^{a} = \frac{i}{2}\alpha_{cd}(J^{cd})^{a}{}_{b}V^{b}, \tag{2.20}$$

which is an irreducible representation.

The explicit form of the matrix $(J^{ab})^{c}{}_{d}$, reads

$$(J_{ab})^{c}{}_{d} = -i(\delta^{c}{}_{a}\eta_{bd} - \delta^{c}{}_{b}\eta_{ad}). \tag{2.21}$$

Using the form of the generator in eq. (2.21), we can compute the commutator

$$[J_{ab}, J_{cd}] = i(\eta_{ac}J_{bd} - \eta_{bc}J_{ad} + \eta_{bd}J_{ac} - \eta_{ad}J_{bc}), \tag{2.22}$$

to find the Lie algebra, SO(3,1). The components of J^{ab} can be rearranged into two spatial vectors

$$J_{i} = \frac{1}{2}\epsilon_{ijk}J^{jk}, \quad K^{i} = J^{i0}, \tag{2.23}$$

with, J^{ij} and K^{i}, the generators of rotations and boosts, respectively.

The Lorentz group has six parameters: Three rotations in three $2D$ planes that can be formed with the (x, y, z) coordinates that leave ct invariant, which is the SO(3) rotation group, and three boost transformations in the (ct, x), (ct, y) and (ct, z) planes that leave invariant $-(ct)^2 + x^2$, $-(ct)^2 + y^2$ and $-(ct)^2 + z^2$, respectively. We parametrize the Lorentz matrix as

$$\Lambda^{0}{}_{0} = \gamma, \quad \Lambda^{0}{}_{i} = \gamma\beta_{i}, \quad \Lambda^{i}{}_{0} = \gamma\beta^{i}, \quad \Lambda^{i}{}_{j} = \delta^{i}{}_{j} + (\gamma - 1)\frac{\beta^{i}\beta_{j}}{\beta^{2}}, \tag{2.24}$$

with $\gamma = (1 - v^2/c^2)^{-1/2}$, the Lorentz factor, and β^i, the velocity

$$\beta^i \equiv \frac{\eta^i}{\eta} \tanh \eta, \tag{2.25}$$

where η is the rapidity, defined as the hyperbolic angle that differentiates two inertial frames of reference that are moving relative to each other.

Therefore, the four vectors, V^a and V_a, transforms under the Lorentz group as

$$V^a(x) \to V'^a(x') = \Lambda^a{}_b V^b(x), \qquad V_a(x) \to V_a'(x') = \Lambda_a{}^b V_b(x), \tag{2.26}$$

with $\Lambda_a{}^b = \eta_{ac}\eta_{bd}\Lambda^c{}_d$. The vectors are related via $V_a = \eta_{ab}V^b$. A tensor, T^{ab}, transforms as

$$T^{ab}(x) \to T'^{ab}(x') = \Lambda^a{}_c \Lambda^b{}_d T^{cd}(x). \tag{2.27}$$

In general, any tensor with arbitrary upper and lower indices transforms with a $\Lambda^a{}_b$ matrix for each upper index, and with $\Lambda_a{}^b$ for each lower one. We will simple denote Lorentz transformations as, $V'^a = \Lambda^a{}_b V^b$ and $T'^{ab} = \Lambda^a{}_c \Lambda^b{}_d T^{cd}$.

The Poincaré Group

To complete the Poincaré group, in addition to Lorentz invariance, we also require invariance under space-time translations. We can write a general element of the group of translations in the following form,

$$U = e^{iz^a P_a}, \tag{2.28}$$

where z^a are the components of the translation,

$$x^a \to x^a + z^a, \tag{2.29}$$

and P^a its generators. Lorentz transformations plus translations form the Poincaré group, ISO(3,1). The Poincaré group algebra reads

$$[P_a, P_b] = 0 \tag{2.30}$$
$$[P_a, J_{bc}] = i(\eta_{ac}P_b - \eta_{ab}P_c) \tag{2.31}$$
$$[J_{ab}, J_{cd}] = i(\eta_{ac}J_{bd} - \eta_{bc}J_{ad} + \eta_{bd}J_{ac} - \eta_{ad}J_{bc}). \tag{2.32}$$

Gauge Symmetry of Classical Electromagnetism

The gauge symmetry of classical electromagnetism is invariance under the U(1) gauge transformation. This is an internal symmetry for which the charge generator, Q, correspond to a time invariant generator, with its corresponding gauge field, $A_\mu(x)$, which is the electromagnetic gauge field. The local gauge symmetry is parametrized by a parameter $\theta = \theta(x)$, and the group element is

$$U(x) = e^{\theta(x)}. \tag{2.33}$$

The gauge field, A_μ, transforms under the U(1) symmetry as

$$A_\mu(x) \to A_\mu(x) + \partial_\mu \theta(x). \tag{2.34}$$

Therefore, under Lorentz and U(1) transformations, the gauge field transforms as

$$A_\mu(x) \to \Lambda_\mu{}^\nu A_\nu(x) + \partial_\mu \theta(x, \Lambda). \tag{2.35}$$

The commutations relations of the charge generator, Q, with the generators of the Poincaré group, are constrained by the Coleman-Mandula theorem [84]. This theorem constrains the kinds of continuous space-time symmetries that can be present in an interacting relativistic field theory, and states that the most general possible transformations are determined by

$$U = \exp\left\{ i \left(z^a P_a + i\sigma^a \mathcal{O}_a + \frac{i}{2}\omega^{ab} J_{ab} \right) \right\}, \tag{2.36}$$

with P_a, the generators of translations, J_{ab}, of Lorentz transformations, and $\mathcal{O}_a$, the rest of the generators. The generators, $\mathcal{O}_a$, must be from internal symmetries, and although they can fail to commute with themselves, $[\mathcal{O}_a, \mathcal{O}_b] \neq 0$, they must always commute with the space-time symmetry generators $[P_a, \mathcal{O}_b] = 0$ and $[J_{ab}, \mathcal{O}_c] = 0$. Nevertheless, the charge operator for the U(1) symmetry of electromagnetism, commutes with itself, thus obtaining the commutation relations: $[P_a, Q] = 0$, $[J_{ab}, Q] = 0$ and $[Q, Q] = 0$.

Transformation Properties of Gauge Fields

The transformation properties of the gauge fields $\breve{e}^a_\mu$, $\breve{A}_\mu$ and $\breve{\omega}^{ab}_\mu$, under local translations, $e^{iz^a P_a}$, local Lorentz transformations, $e^{\frac{i}{2}\alpha_{cd}J^{cd}}$ and the local U(1) transformation, $e^{i\theta}$, read

$$\begin{aligned}
U = \ e^{i\theta} \ &: \begin{cases} \breve{A}_\mu \ \to \ \breve{A}_\mu - \partial_\mu \theta, \\ \breve{e}^{\ a}_\mu \ \to \ \breve{e}^{\ a}_\mu, \\ \breve{\omega}^{ab}_\mu \to \ \breve{\omega}^{ab}_\mu. \end{cases} \\
U = \ e^{icP} \ &: \begin{cases} \breve{A}_\mu \ \to \ \breve{A}_\mu, \\ \breve{e}^{\ a}_\mu \ \to \ \breve{e}^{\ a}_\mu - \breve{\omega}^{\ a}_{\mu b} z^b - \partial_\mu z^a, \\ \breve{\omega}^{ab}_\mu \to \ \breve{\omega}^{\ ab}_\mu. \end{cases} \\
U = e^{i\alpha J} \ &: \begin{cases} \breve{A}_\mu \ \to \ \Lambda_\mu{}^\nu \breve{A}_\nu, \\ \breve{e}^{\ a}_\mu \ \to \ \Lambda^a{}_b \breve{e}^{\ b}_\mu = \ \breve{e}^{\ a}_\mu + \alpha^a{}_b \breve{e}^{\ b}_\mu, \\ \breve{\omega}^{ab}_\mu \ \to \ \Lambda^a{}_c \Lambda^b{}_d \breve{\omega}^{cd}_\mu + \Lambda^a{}_c \partial_\mu (\Lambda^{-1})^{cb} = \breve{\omega}^{ab}_\mu + \breve{\omega}^{ac}_\mu \alpha^b{}_c + \breve{\omega}^{cb}_\mu \alpha^a{}_c - \partial_\mu \alpha^{ab}. \end{cases}
\end{aligned} \tag{2.37}$$

where the indices are lowered and raised using the metric η_{ab}. The gauge field, $\breve{e}$, transforms inhomogeneously under local translations. Under Lorentz transformations, $\breve{e}$ and $\breve{A}$, transforms linearly, while $\breve{\omega}^{ab}_\mu$ transforms as a connection. Under the U(1) transformation, only the gauge field, $\breve{A}$, transforms.

Finally, the electromagnetic field, the vierbein and spin connection, under diffeomorphisms transforms as

$$\begin{aligned} A_\mu(x) &\xrightarrow{\text{diffeo}} A_\mu(x) - A_\nu(x)\partial_\mu\xi^\nu - \xi^\nu(x)\partial_\nu A_\mu(x), \\ e^a_\mu(x) &\xrightarrow{\text{diffeo}} e^a_\mu(x) - e^a_\nu(x)\partial_\mu\xi - \xi^\nu(x)\partial_\nu e^a_\mu(x), \\ \omega^{ab}_\mu(x) &\xrightarrow{\text{diffeo}} \omega^{ab}_\mu(x) - \omega^{ab}_\nu(x)\partial_\mu\xi - \xi^\nu(x)\partial_\nu\omega^{ab}_\mu. \end{aligned} \tag{2.38}$$

Noether's Theorem

In Classical Field Theory, the symmetries of a Lagrangian and conserved quantities are closely related by Noether's theorem. This theorem allows us to obtain conserved quantities from the symmetries of the laws of nature. For instance, time translation symmetry gives conservation of energy, space translation symmetry gives conservation of momentum, rotation symmetry gives conservation of angular momentum, and the U(1) symmetry gives conservation of the electric charge .

Noether's theorem states that, on a classical solution of the equations of motion, there is a conserved current j^a_u, for each generator of a symmetry transformation [85]. Thus, for a field theory with the fields ϕ^a, the N currents j^a_u are conserved

$$\partial_a j^a_u = 0, \tag{2.39}$$

where $u = 1, ..., N$. We can define the charges Q_u

$$Q_u = \int \mathrm{d}^3x j^0_u(x^a), \tag{2.40}$$

The current conservation implies that Q_u is conserved.

Spontaneous Symmetry Breaking

In field theories, the ground state can fail to be invariant. In fact, any system other than vacuum will break at least some of the symmetries. If the ground state of a system is not invariant under a symmetry of its action, the symmetry is said to be spontaneously broken. If the symmetry is spontaneously broken, another state is produced once a transformation is applied to the ground state. The new state must have the same energy and is a candidate ground state. When the ground state is changed by a symmetry, the spontaneously broken symmetries come with consequences that are described by Goldstone's theorem.

The Goldstone's theorem [40] summarizes very general implications for the low energy theory whenever the ground state of a system does not respect one of the global continuous symmetries of the system. It states that a system, for which a continuous global symmetry is spontaneously broken, the system must contain a state, $|G\rangle$, denoted as Nambu-Goldstone (NG) boson or Goldstone mode. This mode is created from the ground state, $|\hat{0}\rangle$, by a space-time independent symmetry transformation. $|G\rangle$ is defined by the condition that the matrix element

$$\langle G|j^0|\hat{0}\rangle \neq 0, \tag{2.41}$$

does not vanish, with j^0 the density for the symmetry's conserved charge in eq. (2.40). All properties of the Goldstone boson follow from the matrix element definition (2.41) and eq. (2.40). The Goldstone state is a symmetry transformation of

the ground state, which makes it completely indistinguishable from the vacuum, thus creating a new ground state.

The Goldstone boson should decouple completely from all its interaction in the limit in which its momentum vanishes, such that the state $|G\rangle$ must be gapless. This means that its energy vanishes in the limit where the momentum vanishes,

$$\lim_{p\to 0} E(p) = 0. \tag{2.42}$$

For a relativistic system, where $E(p) = \sqrt{p^2 + m^2}$, with m the rest mass of the particle, the gapless condition implies the masslessness of the Goldstone particle.

In the group theoretical approach, for the description of a symmetry breaking pattern where the group G breaks to H, we can choose a basis for the generators such that we include the generators of H as a subset, $\{T_u\} = \{t_v, X_\alpha\}$, where the t's generate the Lie algebra of H, and the X_α constitutes the rest.[1] The broken generators X_α typically do not also generate a group, but it can be regarded as generating the space of cosets G/H. We expect a Goldstone mode for each choice of α.

The closure of H under multiplication ensures

$$[t_u, t_v] = ic_{uvw}t_w, \tag{2.43}$$

with no X's on the right hand side. It is also possible to choose a basis of generators such that

$$[t_u, X_\alpha] = ic_{u\alpha\beta}X_\beta, \tag{2.44}$$

with no t's on the right-hand side. The implication of this, is that the X_α's falls into a representation of H, which when exponentiated to a finite transformation, can be expressed as linear transformation

$$hX_\alpha h^{-1} = M_\alpha{}^\beta X_\beta, \tag{2.45}$$

for some coefficients $M_\alpha{}^\beta$, and for any $h = \exp(i\theta^u t_u) \in H$.

2.4 The Coset Construction

We start with the basics of the coset construction to develop this thesis. A brief but more comprehensive review can be found in [1, 39]. We use the notation as in [1] to consider the breaking of internal [36, 35] and space-time symmetries [37, 86] alike.

The coset construction is a very general technique from the EFT framework that can be used whenever there is a symmetry breaking. The breaking of some of the symmetries implies the existence of additional degrees of freedom, known as Nambu-Goldstone bosons or simple as Goldstone fields.[2] The coset construction is then used to derive building blocks for the Goldstone fields that transform correctly under the relevant symmetries, and that can be used to build up invariant operators to form an effective action. Any state other than vacuum breaks at least some of the

[1] We have chosen greek indices to differentiate from those of the unbroken group

[2] Goldstone theorem [40] implies the existence of a Goldstone field for each broken internal symmetry, but for the case in which space-time symmetries are broken, there can be a mismatch on the number of degrees of freedom and broken symmetries, for which additional constraints are needed. See the Inverse Higgs constraint below.

symmetries, and by appropriately identifying the pattern of the symmetry breaking, we can use it as a guide to derive the effective action.

We can formulate an EFT using the symmetry breaking pattern as the only input, knowing the full symmetry group G that is broken, and the subgroup H that is non-linearly realized [39]. If the group is broken, G → H, due to a spontaneous symmetry breaking, the coset recipe [1, 39] tells us that we can classify the generators into three categories:

$$\begin{aligned} P_a &= \text{generators of unbroken translations,} \\ T_A &= \text{generators of all other unbroken symmetries,} \\ X_\alpha &= \text{generators of broken symmetries,} \end{aligned} \tag{2.46}$$

where the broken generators, X_α, and the unbroken ones, T_A, can be of space-time symmetries as well as of internal ones. We have chosen different indices to differentiate between generators, but all of them run over Lorentz indices.

Whenever the set of generators for broken symmetries is nonzero, some Goldstone fields will arise. Thus, we must build an effective action for the Goldstone fields that is invariant under the whole symmetry group of consideration. The power of the coset construction, is that we can formulate an invariant EFT in which the broken symmetries and the unbroken translations are realized nonlinearly on the Goldstone fields [1].

Following the coset recipe [1, 39], we do a local parametrization of the coset, G/H_0, with H_0, the subgroup of H generated by the unbroken generators, T's. The coset is parametrized as

$$g(x,\pi) = e^{iy^a(x)P_a} e^{i\pi^\alpha(x)X_\alpha}, \tag{2.47}$$

where the factor, $e^{iy^a(x)P_a}$, describes a translation from the origin of the coordinate system to the point, x_a, at which the Goldstone fields, $\pi^\alpha(x)$, are evaluated. This factor ensures that the π's transform correctly under spatial translation. The group element g, which is generated by the X's and the P's, is known as the coset parametrization. For the case of flat space-time, the translation is simply parametrized by, $e^{ix^aP_a}$, with $y(x) \equiv x$.

To derive the building blocks that depend on the Goldstone bosons and that have simple transformation rules, we first note that the Goldstone fields, when appearing in the Lagrangian, they are coupled through its derivatives. Then, we introduce the Maurer-Cartan form, $g^{-1}\partial_\mu g$, a very convenient quantity that is an element of the algebra of G, and that can be written as a linear combinations of all the generators [1, 39],

$$g^{-1}\partial_\mu g = (e_\mu{}^a P_a + \nabla_\mu \pi^\alpha X_\alpha + C_\mu{}^B T_B). \tag{2.48}$$

The coefficients e^a_μ, $\nabla_\mu\pi^\alpha$ and C^B_μ, in general are nonlinear functions of the Goldstones, $\pi's$, and form the building blocks to build the EFT, with $\nabla_\mu{}^\alpha = e_\mu{}^a\nabla_a{}^\alpha$ and $C_\mu{}^B = e_\mu{}^a C_a{}^B$. As we shall see, we can compute the explicit expression of the building blocks with the algebra of the group G.

From the coset recipe, we can use the coefficients, C's, and its operators, T's, to define the covariant derivative that acts on matter fields [1, 39],

$$\nabla_a \equiv (e^{-1})_a^{\ \mu}(\partial_\mu + iC_\mu^B T_B). \tag{2.49}$$

This covariant derivative can be used on the building blocks, as well as to consider higher covariant derivatives of the Goldstone fields.

Furthermore, in gauge symmetries, it is necessary to promote the partial derivative to a covariant one in the Maurer-Cartan form, $\partial_\mu \to D_\mu$ [1]. Consider the gauged generator, E_I, from a subgroup, $G' \subseteq G$, with corresponding gauge field, w_μ^I. Thus, by replacing the partial derivative with a covariant one, we obtain the modified Maurer-Cartan form,

$$g^{-1}\partial_\mu g \to g^{-1}D_\mu g = g^{-1}(\partial_\mu + iw_\mu^I E_I)g. \tag{2.50}$$

This modification of the Maurer-Cartan form can also be written as a linear combination of the generators as in eq. (2.48), with a new building block made up of the gauge field, w_μ^I, accompanying the gauged generator, E_I. Now the building blocks can also depend on the gauge fields. The modified Maurer-Cartan form, $g^{-1}D_\mu g$, is invariant under local transformations, and its explicit components can be obtained using the commutation relations of the generators.

Inverse Higgs Constraint

The Goldstone's theorem [40], which states that a Goldstone mode exists for each broken generator, is only valid for internal symmetries. If space-time symmetries are spontaneously broken, there can be a mismatch in the number of broken generators and the number of bosons [87]. Nevertheless, we can preserve all the symmetries by imposing additional local constraints, which can be solved to write down some of the Goldstone's modes in terms of others. Using the inverse Higgs constraint [38], we can set to zero one or more of the coset covariant derivatives, whenever X and X', are two multiplets of the broken generator, such that the commutators of the unbroken translations, $\bar{P}$, and the broken generator, X', yields a different broken generator, X: $[\bar{P}, X'] \supset X$. If this is the case, we can set some of the covariant derivatives of the Goldstones to zero. By imposing all possible inverse Higgs constraints, one obtains the only relevant building blocks.

2.5 Electrodynamics of Spheres

2.5.1 Classical Electromagnetism

It is well known that a classical theory of electromagnetism obeys the symmetries of Special Relativity determined by the Poincaré group, ISO(3,1), as well as the symmetries of the U(1) charge symmetry group. Thus, the full group is, G = U(1)×ISO(3,1), which contains the generators for Lorentz transformations, J^{ab}, and gauge field, $\check{\omega}_\mu^{ab}$, the generators of translations, P_a, and gauge field, $\check{e}_\mu^a$, and the generator of charge, Q, and a gauge field $\check{A}_\mu$.[3] Charge corresponds to a time invariant generator of the internal symmetry group, U(1), while the symmetry of the Poincaré group is a space-time symmetry (See appendix 2.3 for more details).

[3]Note that we have defined the gauge fields, $\check{o}$'s, compared to [1], in which the gauge fields are defined as $\tilde{o}$'s. We will reserve the $\sim$ symbol to refer to quantities in the comoving frame.

Therefore, we parametrize the coset, U(1)×ISO(3,1)/U(1)×SO(3,1), separating translations from the rest of the group. The coset parametrization in flat space-time is given by the group element

$$g = e^{ix^a \bar{P}_a} = e^{ix^a P_a} e^{ix^0 Q}, \tag{2.51}$$

which contains all the unbroken translation, $\bar{P}_a = \bar{P}_0 + P_i = P_a + Q$, with $\bar{P}_0 = P_0 + Q$. Then, the Maurer-Cartan form reads

$$\begin{aligned} g^{-1} D_\mu g &= e^{-ix^a \bar{P}_a} \left(\partial_\mu + i \check{A}_\mu Q + i \check{e}_\mu{}^a P_a + \frac{i}{2} \check{\omega}_\mu^{ab} J_{ab} \right) e^{ix^a \bar{P}_a} \\ &= \partial_\mu + i A_\mu Q + i e_\mu{}^a P_a + \frac{i}{2} \omega_\mu^{ab} J_{ab}, \end{aligned} \tag{2.52}$$

where we have used the commutation relation rules of the symmetries (See appendix 2.3) to obtain

$$e_\mu{}^a = \check{e}_\mu{}^a + \partial_\mu x^a + \check{\omega}_\mu^{ab} x_b, \tag{2.53}$$

$$A_\mu = \check{A}_\mu + \partial_\mu \xi(x), \tag{2.54}$$

$$\omega_\mu^{ab} = \check{\omega}_\mu^{ab}. \tag{2.55}$$

Before going any further, we consider the case of flat space-time. From a geometrical perspective, this limit implies that the curvature and the torsion tensor are equal to zero, which can be measured from the commutator of the two covariant derivatives, $[D_\mu, D_\nu]$. By considering the covariant derivative appearing in the Maurer-Cartan form, (2.52), we can cast the commutator as,

$$\begin{aligned} [D_\mu, D_\nu] =& i \check{F}_{\mu\nu} Q + i \check{T}^a_{\mu\nu} P_a + \frac{i}{2} \check{R}^{ab}_{\mu\nu} J_{ab}, \\ =& i \left(\partial_\mu \check{A}_\nu - \partial_\nu \check{A}_\mu \right) Q + i \left(\partial_\mu \check{e}^a{}_\nu - \partial_\nu \check{e}^a{}_\mu + \check{e}_{\mu b} \check{\omega}_\nu^{ab} - \check{e}_{\nu b} \check{\omega}_\mu^{ab} \right) P_a \\ &+ \frac{i}{2} \left(\partial_\mu \check{\omega}_\nu^{ab} - \partial_\nu \check{\omega}_\mu^{ab} + \check{\omega}^a_{\mu c} \check{\omega}_\nu^{cb} - \check{\omega}^a_{\nu c} \check{\omega}_\mu^{cb} \right) J_{ab}. \end{aligned} \tag{2.56}$$

Given that in flat space-time, $\check{T}^{\mu\nu}_a = 0$ and $\check{R}^{\mu\nu}_{ab} = 0$, it implies that

$$\check{\omega}_\mu^{ab} = 0 \quad \text{and} \quad \check{e}_\mu^a = 0, \tag{2.57}$$

for which eq. (2.53), takes the simple form

$$e_\mu{}^a = \partial_\mu x^a = \delta_\mu{}^a. \tag{2.58}$$

The field, e_μ^a, is known as the vierbein, which is used for deriving an invariant volume element $\mathrm{d}^4x \det e$, and which for the case of flat space-time is simply d^4x. Given the coset recipe, we can use the coefficients of the unbroken U(1) generator in eq. (2.52), to define the gauge covariant derivative,

$$\nabla_a \equiv \partial_a + iQA_a, \tag{2.59}$$

which is the usual covariant derivative in a Classical Field Theory of electromagnetism. Having defined the vierbein and the gauge covariant derivative, we can proceed to build invariant actions [1].

The first building block can be extracted from the commutator of the covariant derivatives, eq. (2.56), which in the flat space-time limit,

$$g^{-1}[D_\mu, D_\nu]g = i(\partial_\mu A_\nu - \partial_\nu A_\mu)Q = iF_{\mu\nu}Q, \tag{2.60}$$

with $F_{\mu\nu} = \partial_\mu A_\nu - \partial_\nu A_\mu$, the electromagnetic tensor. Thus, the first invariant term that can be build with our covariant building block, $F_{\mu\nu}$, is,

$$\mathcal{S} = -\alpha \int \mathrm{d}^4 x F_{\mu\nu} F^{\mu\nu}. \tag{2.61}$$

As pointed out earlier, the coefficients of the theory can be treated as free parameters that are to be fixed by experiments or from the literature. Thus, to reproduce Maxwell's theory, we find the coefficient, $\alpha = (4\mu_0)^{-1}$, with μ_0, the magnetic permeability of vacuum, such that we have the well known Maxwell action,

$$\mathcal{S} = -\frac{1}{4\mu_0} \int \mathrm{d}^4 x F_{ab} F^{ab}, \tag{2.62}$$

where we have used, $F^{ab} = e_\mu{}^a e_\nu{}^b F^{\mu\nu}$. Eq. (2.62) lives in the bulk, while the action that describes the sphere, lives in the worldline.

2.5.2 Charged Spheres

With the underlying theory of classical electromagnetism, we identify the symmetry pattern for a charged point particle, and derive its building blocks to construct an effective action. Then, by considering spherical objects at rest, and departures from sphericity, we add size effects to describe charged spheres.

Charged Point Particles

In general, a point particle breaks spatial translations, and boosts by choosing a preferred reference frame. Under a U(1) symmetry, the state of a charged point particle is an eigenstate of the charge, and does not break U(1) the symmetry. Thus, the symmetry breaking pattern reads

$$\begin{aligned} \text{Unbroken generators} &= \begin{cases} \bar{P}_0 \equiv P_0 + Q & \text{time translations,} \\ J_{ij} & \text{spatial rotations.} \end{cases} \\ \text{Broken generators} &= \begin{cases} P_i & \text{spatial translations,} \\ J_{0i} \equiv K_i & \text{boosts,} \end{cases} \end{aligned} \tag{2.63}$$

where we have included the charge generator as a time invariant generator of translations [1]. Given this pattern, we can parametrize the coset as

$$g = e^{ix^a(\sigma)\bar{P}_a} e^{i\eta^i(\sigma)K_i} = e^{ix^a(\sigma)\bar{P}_a}\bar{g}. \tag{2.64}$$

with σ, the worldline parameter that traces out the trajectory of the particle, η^i, the Goldstone mode, and $\bar{g} = e^{i\eta^i(\sigma)K_i}$.

The important building blocks are contained in the Maurer-Cartan form projected into the particle's trajectory, $\dot{x}^\mu g^{-1} D_\mu g$. It can be casted as a linear combination of the generators,

$$\begin{aligned}
\dot{x}^\mu g^{-1} D_\mu g &= \dot{x}^\mu g^{-1}(\partial_\mu + i\check{A}_\mu Q + i\check{e}_\mu{}^a P_a) g \\
&= \dot{x}^\mu \bar{g}^{-1}(\partial_\mu + iA_\mu Q + ie_\mu{}^a P_a)\bar{g} \\
&= i\dot{x}^\mu (A_\nu \Lambda^\nu{}_\mu Q + e_\mu{}^b \Lambda_b{}^0 P_0 + e_\mu{}^b \Lambda_b{}^i P_i) + i(\Lambda^{-1})^0_c \dot{\Lambda}^{ci} K_i, \\
&= iE\left(P_0 + AQ + \nabla\pi^i P_i + \nabla\eta^i K_i\right),
\end{aligned} \tag{2.65}$$

where the dot means derivative with respect to the worldline parameter, σ, and $\Lambda^a{}_b = \Lambda^a{}_b(\eta) \equiv (e^{i\eta^j K_j})^a{}_b$, being the boost matrix of the Lorentz transformations, which is a function of the Goldstone field, η^i. Thus, the covariant quantities are

$$\begin{aligned}
e &= \dot{x}^\mu e_\mu{}^b \Lambda_b{}^0, \\
A &= e^{-1}\dot{x}^\mu A_\nu \Lambda^\nu{}_\mu, \\
\nabla\pi^i &= e^{-1}\dot{x}^\mu e_\nu{}^b \Lambda_b{}^i, \\
\nabla\eta^i &= e^{-1}(\Lambda^{-1})^0_c \dot{\Lambda}^{ci}.
\end{aligned} \tag{2.66}$$

These are some of the building blocks that we will use to build up an invariant action. Nevertheless, as pointed out before, given that we are working with space-time symmetries, there are some subtleties with the counting of Goldstone fields, for which the Inverse Higgs constraint can be placed.

In this case, the commutator between boosts and unbroken time translations gives broken spatial translations [1]. Therefore, by imposing the inverse Higgs constraint, we set to zero the covariant derivative, $\nabla\pi^i = 0$, such that we obtain the relation

$$\nabla\pi^i = e^{-1}\dot{x}^\mu e_\mu{}^b \Lambda_b{}^i = e^{-1}(\dot{x}^\mu e_\mu{}^0 \Lambda_0{}^i + \dot{x}^\mu e_\mu \Lambda_j{}^i) = 0. \tag{2.67}$$

Solving for this constraint, we obtain the velocity (See eq. 2.25)

$$\beta^i \equiv \frac{\eta^i}{\eta}\tanh\eta = \frac{\dot{x}^\nu e_\nu{}^j}{\dot{x}^\nu e_\nu{}^0}, \tag{2.68}$$

where we have used the fact that, in flat space-time, $e_\nu{}^a = \delta_\nu{}^a$. Using the inverse Higgs constraint we have expressed the η's in terms of the π's. This result can be interpreted as the Goldstones, η's, or in terms of the, β's, as parametrizing the boost necessary to get into the moving particle rest frame [1].

We can also rewrite the inverse Higgs constraint in a way that the physical interpretation is transparent [1]. This is done by expressing eq. (2.67), in terms of the velocity in the proper frame, u^a, as

$$u^a \Lambda_a{}^i = 0, \tag{2.69}$$

and defining the set of Lorentz vectors, $\hat{n}^a{}_{(b)}$,

$$\hat{n}^a{}_{(0)} \equiv u^a = \Lambda^a{}_0(\eta)\ , \quad \hat{n}^a_{(i)} \equiv \Lambda^a{}_i(\eta). \tag{2.70}$$

This set of Lorentz vectors define an orthonormal basis in the particle's comoving frame.

Then, we analyse the covariant derivative of the boost Goldstone, η^i, in eq. (2.66), which can be rewritten as

$$\nabla\eta^i = \hat{n}^{(i)}_a \partial_\tau u^a = \hat{n}^{(i)}_b e_\mu{}^b a^\mu = a^i, \tag{2.71}$$

with, a^i, the acceleration of the particle in the comoving frame. Thus, the covariant derivatives, $\nabla\eta^i$, corresponds to the component of the acceleration projected on the i-th vector defined by the set of Lorentz vectors, $\hat{n}^a_{(b)}$, measured in the proper frame of the particle [1]. In the absence of external forces, $\nabla\eta^i = 0$. Nevertheless, this building block is needed to take into account for a full description of the system, i.e. when the charge from an external body is relevant, such that the acceleration is nonzero.

Thus, we are left with the building blocks,

$$\begin{aligned} e &= \dot{x}^\mu e_\mu{}^0, \\ A &= e^{-1}\dot{x}^\mu A_\mu, \\ \nabla\eta^i &= e^{-1}a^i, \end{aligned} \tag{2.72}$$

which are to be used in order to build an invariant action. We start with the building block, $e = |e| = \sqrt{e^2}$, and rewrite it as

$$\begin{aligned} |e| &= \sqrt{(e\nabla\pi^i)^2 + (e^2 - (e\nabla\pi^i)^2)} \\ &= \sqrt{(e\nabla\pi^i)^2 - (\dot{x}^\nu e_\nu{}^a \dot{x}^\mu e_\mu{}^b)}, \\ &= \sqrt{-\eta_{ab} e_\nu{}^a e_\mu{}^b \dot{x}^\nu \dot{x}^\mu} = \sqrt{-\eta_{ab}\dot{x}^a\dot{x}^b} = \frac{\mathrm{d}\tau}{\mathrm{d}\sigma}, \end{aligned} \tag{2.73}$$

where we have imposed the inverse Higgs constraint, and used the orthogonality property of the boost matrices, $\Lambda_a{}^b\Lambda^a{}_c = \delta^b{}_c$, and $e_\mu{}^a = \delta_\mu{}^a$. We can build an invariant term made up of the building block e,

$$\mathcal{S} = c_E \int \mathrm{d}\sigma e = c_E \int \mathrm{d}\sigma \frac{\mathrm{d}\tau}{\mathrm{d}\sigma} = -mc^2 \int \mathrm{d}\tau, \tag{2.74}$$

and match the coefficient, $c_E = -mc^2$, to the action of a free relativistic point particle with mass, m. The last expression shows the action for a free relativistic point particle to all orders in the absence of external forces [1].

With the covariant block, A, we add the point particle correction due to charge as,

$$\mathcal{S} = \int \mathrm{d}\sigma e(-mc^2 + c_A A) = \int \mathrm{d}\tau(-mc^2 + qu^a A_a), \tag{2.75}$$

with, q, the net charge of the charged particle, where the coefficient, c_A, has been matched from the classical theory of electrodynamics. Therefore, equation (4.66), is the action in the proper frame that describes charged point particles in classical electromagnetism. We now move into the description of size effects, to describe a charged sphere.

Size Effects

In the context of the EFT for extended objects, the addition of size effects in the action of a point particle was introduced in [29], which can be done in a systematic fashion. Size corrections must respect the symmetries of the theory, Lorentz and gauge U(1) symmetry, and thus contained in an infinite series expansion of all possible invariant operators made up of the covariant building blocks. To build up invariant terms made out of F_{ab}, we first define its transformation properties under local Lorentz transformations. By considering the Lorentz parametrization of eq. (2.64), g_L, the electromagnetic tensor transforms as

$$F \equiv g_L^{-1}\, \tilde{F}, \tag{2.76}$$

such that F is transformed in a linear representation under a Lorentz transformation as expected. The explicit transformation reads

$$F_{ab} = (\Lambda^{-1})_a{}^c (\Lambda^{-1})_b{}^d \tilde{F}_{cd}. \tag{2.77}$$

Having the correct transformation rules, we can form rotationally invariant objects made out of F_{ab}, u^a, and a^b, to build up the invariant action. These corrections in the action reads,

$$\mathcal{S} = \sum_n \int \mathrm{d}\tau c_n \mathcal{O}_n(F_{ab}, u_c, a_d), \tag{2.78}$$

with, $\mathcal{O}_n$, the invariant operators, c_n, its corresponding coefficients, and n, being chosen to the desired accuracy. The leading order, electric parity terms are

$$\mathcal{S} = \int \mathrm{d}\tau \left(n_q F^{ba} F_{ca} u_b u^c + n_{qa} u_a a_b F^{ab} + \dots \right), \tag{2.79}$$

where the ellipsis denotes higher order corrections. The first term correspond to the induced, electric parity, dipolar moment, while the second term can be seen as a higher order correction to the latter due to the acceleration of the body.

The electric parity building block is identified, $E_a = F_{ba} u^b$ [30], such that the first term in the last equation, $\propto E^a E_a$. For the moment we restrict to operators with electric parity only. Nevertheless, a term with magnetic parity, $B_a = \frac{1}{2}\epsilon_{abcd} F^{bc} u^d$, can be build as well, $\propto B^a B_a$. The leading order corrections in (2.79), with its corresponding coefficients, c_q, and c_{qa}, encode the short distance information, or the size structure, which are responsible for the polarization. The polarizability accounts for the deformation of the sphere in the presence of an external electromagnetic field. In general,

the coefficients, c_q and c_{qa}, are dependent on the radius of the sphere, therefore taking into account for the fact that a sphere is an extended object. The specific form of these coefficient for a charged sphere is beyond the scope of this work.

Dissipative Effects

Dissipation in the EFT of extended objects was introduced in [30]. Dissipative effects of the sphere takes into account for its absorption of electromagnetic waves. These large number of degrees of freedom can be encoded in operators allowed by the symmetries of the object. For instance, for a rigid sphere, the allowed operators for rotations, SO(3), as well as parity eigenvalue, allows us to build the action [30]

$$S = \int \mathrm{d}\tau \mathcal{P}^a(\tau) u^b F_{ab}, \tag{2.80}$$

with $\mathcal{P}(\tau)$, a composite dynamical operator corresponding to the electric parity, electromagnetic dipole moment. The specific form of the operator, $\mathcal{P}(\tau)$, and its coefficient are discussed in detail in the next section.

2.5.3 The Effective Action

Finally, by considering, the electric parity only, we write down the leading order effective action of a charged sphere in a classical theory of electromagnetism,

$$\mathcal{S}_{eff} = \int \mathrm{d}\tau \left(-mc^2 + q u^a A_a + c_q E^a E_a + c_{qa} E^a a_a + \mathcal{P}^a F_{ab} u^b + \dots \right) + \mathcal{S}_0, \tag{2.81}$$

with

$$\mathcal{S}_0 = -\int \mathrm{d}^4 x \frac{1}{4\mu_0} F_{ab} F^{ab}. \tag{2.82}$$

Eq. (2.81) describes our effective theory. We have developed a theory of classical electromagnetism and described a charged sphere as a charged point particle with the finite size structure encoded in higher order operators in the action. In this approach, the description of the sphere lives in the worldline, while the interaction, eq. (2.82), lives in the bulk.

2.6 The Dynamics of Interacting Spheres

To obtain the leading order dynamics of two interacting spheres, we first recall that the propagators can be read off from the terms that are quadratic in the fields. For instance, for a scalar field, the propagator is encoded in

$$\mathcal{L} = \int \mathrm{d}^4 x \partial_a \phi \partial^a \phi = -\int \mathrm{d}^4 x \phi \Box \phi, \tag{2.83}$$

where we have integrated by parts and neglected the boundary term.

For the photon field, we start with the Maxwell action with the gauge fixing term

$$\mathcal{L} = -\frac{1}{\mu_0}\int \mathrm{d}^4x \left(\frac{1}{4}F_{ab}F^{ab} + \frac{1}{2\xi}(\partial_a A^a)\right). \tag{2.84}$$

The gauge fixing term is included to remove redundant degrees of freedom. We will use the Feynman gauge, which set $\xi = 1$. Integrating by parts, we can cast the Lagrangian as

$$\mathcal{L} = -\frac{1}{2\mu_0}\int \mathrm{d}^4x \left(A^a\eta_{ab}\Box A^b + \left(\frac{1}{\xi} - 1\right)A^a(\partial_a\partial_b A^b)\right). \tag{2.85}$$

We read the propagator from the quadratic terms in the fields. The corresponding Green's function in configuration space

$$\eta_{ab}\Box D_F^{bc}(x-y) = \delta^{(4)}(x-y)\delta_a^c. \tag{2.86}$$

In momentum space

$$k^2\eta_{ab}D_F^{bc}(k) = \delta_a^c, \tag{2.87}$$

which can be inverted to obtain the propagator,

$$iD_F^{ab}(k) = \frac{i}{k^2}\eta^{ab}. \tag{2.88}$$

We separate the time dimensions of the photon field from the spatial ones. Therefore, from the above analysis, the leading order propagator for the electromagnetic interaction reads

$$\text{-·-·-·-·-·-} = \langle A_0(x_1)A_0(x_2)\rangle = -\mu_0\,\delta(t_1-t_2)\int \frac{\mathrm{d}^3\vec{k}}{(2\pi)^3}\frac{e^{i\vec{k}\cdot\vec{r}}}{\vec{k}^2}. \tag{2.89}$$

The electromagnetic charge coupling from the worldline action reads,

$$\mathcal{S}_q = \int \mathrm{d}t q v^a A_a = -\int \mathrm{d}t q A_0 + \int \mathrm{d}t q v^i A_i. \tag{2.90}$$

which to leading order, we extract the vertex,

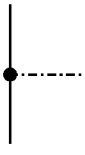

$$= -\,q\int \mathrm{d}t A_0. \tag{2.91}$$

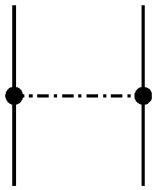

FIGURE 2.1: Leading order electromagnetic interaction, which is the Coulomb interaction

Therefore, we obtain the interaction of two point charges, which is the Coulomb interaction

$$\begin{aligned} \text{Figure 2.1} &= \int \mathrm{d}t_1 q_1 A_0(x_1) \times \int \mathrm{d}t_2 q_2 A_0(x_2) \\ &= \int \mathrm{d}t \left(-\frac{\mu_0}{4\pi}\frac{q_1 q_2}{r}\right), \end{aligned} \tag{2.92}$$

where we have used,

$$\int \frac{\mathrm{d}\vec{k}^3}{(2\pi)^3}\frac{e^{i\vec{k}\cdot\vec{r}}}{\vec{k}^2} = \frac{1}{4\pi}\frac{1}{r}. \tag{2.93}$$

Chapter 3

Compact Objects in Effective Field Theory

3.1 Compact Objects in General Relativity

Following the same methodology as in the previous section, before constructing a theory for compact objects, we review how a theory of gravity can be derived from the coset construction as in [1], where a frame independent generalization of General Relativity, known as Einstein's vierbein field theory, is derived. The difference of our construction compared to the one in [1], is the inclusion of the gauge symmetry group, $U(1)$, which allows us to derive the Einstein-Maxwell action in the vierbein formalism, as well as the correction to the point particle due to charge. Once the underlying theory of gravity has been developed, then we derive the leading order action for charged spinning compact objects in the effective theory of General Relativity (vierbein formalism). This is a theory that can naturally incorporate spinning objects.

3.1.1 Effective Theory of Gravity

There are two symmetries in gravity to consider: Diffeomorphisms invariance, and Poincaré symmetry, determined by the Poincaré group, ISO(3,1), which contains the generators for translations, P_a, and Lorentz transformations, J_{ab}, with their corresponding gauge fields, $\check{e}^a_\mu$ and $\check{\omega}^{ab}_\mu$. Both of the aforementioned symmetries of the system can be separated by considering the principal bundle, P(M,G), with base manifold, M, and structure group, G. In this way, we realize the matter fields as sections of their respective fiber bundle [1]. The coordinates, x^μ, describing the position on the considered manifold, M, are not affected by the local Poincaré group, but it is transformed under diffeomorphisms. The local Poincaré transformations act along the fiber, while diffeomorphisms can be considered as relabeling the points on the manifold.

To incorporate electrodynamics in the theory of gravity [1], we add the U(1) symmetry of electromagnetism with its gauge field, $\check{A}_\mu$, and generator Q, and proceed with the coset construction by gauging the Poincaré group and realizing translations non-linearly [86]. The coset then reads, U(1) $\times$ ISO(3,1)/U(1) $\times$ SO(3,1), with the coset parametrization

$$g = e^{iy^a(x)\bar{P}_a}, \tag{3.1}$$

where $\bar{P}_a = \bar{P}_0 + P_i = P_a + Q$. We now compute the Maurer-Cartan form from the coset parametrization (3.1), which is expressed as a linear combination of the generators of the theory,

$$
\begin{aligned}
g^{-1}D_\mu g &= e^{-iy(x)^a \bar{P}_a}\left(\partial_\mu + i\check{A}_\mu Q + i\check{e}_\mu{}^a P_a + \frac{i}{2}\check{\omega}_\mu^{ab} J_{ab}\right) e^{iy(x)^a \bar{P}_a} \\
&= \partial_\mu + iA_\mu Q + ie_\mu{}^a P_a + \frac{i}{2}\omega_\mu^{ab} J_{ab},
\end{aligned}
\tag{3.2}
$$

where we have used the commutation relation rules of the symmetries (See section 2.3) to obtain

$$e_\mu{}^a = \check{e}_\mu^a + \partial_\mu y^a + \check{\omega}_\mu{}^a{}_b y^b, \tag{3.3}$$

$$A_\mu = \check{A}_\mu + \partial_\mu \xi(y), \tag{3.4}$$

$$\omega_\mu^{ab} = \check{\omega}_\mu^{ab}. \tag{3.5}$$

The field, e_μ^a, is the vierbein, that appears in the tetrad formalism, which defines the metric as $g_{\mu\nu} = \eta_{ab} e_\mu^a e_\nu^b$. It can be used to build up the invariant element, $\mathrm{d}^4x \det e$, as well as to change from orthogonal frame, i.e. $A_\mu = e_\mu^b A_b$. The field, $\omega_\mu{}^{ab}$, is known as the spin connection, and it is named given its transformation properties, which transforms as a gauge field [39] (See section 2.3).

Following the coset recipe, we can introduce the covariant derivative for matter fields by using the coefficients from the unbroken Lorentz generators, which transform in a linear representation under Lorentz transformations. The covariant derivative for matter fields reads

$$\nabla_a^g = (e^{-1})_a{}^\mu(\partial_\mu + \frac{i}{2}\omega_\mu^{bc} J_{bc}), \tag{3.6}$$

where the upper index g denotes gravity, which transforms as, $\nabla_a^g = \Lambda_a{}^b \tilde{\nabla}_b^g$, under Lorentz transformations. In a similar manner we can obtain the covariant derivative for charged fields, which transform in a linear representation under U(1) transformations, by using the coefficients from the unbroken U(1) generators. The covariant derivative for charged fields reads

$$\nabla_a^q = (e^{-1})_a{}^\mu(\partial_\mu + iA_\mu Q), \tag{3.7}$$

which transforms in the same way under Lorentz transformations as eq. (3.6). The only required ingredients to describe the non-linear realizations of translations and the local transformations of the Poincaré and U(1) group, are the covariant derivatives and the vierbein [1]. Having defined these elements, we proceed to extract building blocks from the curvature invariants.

The curvature invariants can be obtained from the covariant version of the commutator of the covariant derivative that appear in the Maurer-Cartan form,

$$
\begin{aligned}
g^{-1}[D_\mu, D_\nu]g &= iF_{\mu\nu}Q + iT_{\mu\nu}^a P_a + \frac{i}{2}R_{\mu\nu}^{ab} J_{ab}, \\
&= i\left(\partial_\mu A_\nu - \partial_\nu A_\mu\right) Q + i\left(\partial_\mu e_\nu^a - \partial_\nu e_\mu^a + e_{\mu b}\omega_\nu^{ab} - e_{\nu b}\omega_\mu^{ab}\right) P_a \\
&+ \frac{i}{2}\left(\partial_\mu \omega_\nu^{ab} - \partial_\nu \omega_\mu^{ab} + \omega_{\mu c}^a \omega_\nu^{cb} - \omega_{\nu c}^a \omega_\mu^{cb}\right) J_{ab},
\end{aligned}
\tag{3.8}
$$

with $T^a_{\mu\nu} = \check{T}^a_{\mu\nu} + \check{R}^{ab}_{\mu\nu} y_b$, and $R^{ab}_{\mu\nu} = \check{R}^{ab}_{\mu\nu}$, the covariant torsion and Riemann tensor respectively. The covariant quantities have been defined in this way, from, $[D_\mu, D_\nu] = i\check{F}_{\mu\nu}Q + i\check{T}^a_{\mu\nu}P_a + \frac{i}{2}\check{R}^{ab}_{\mu\nu}J_{ab}$, in eq. (2.56), such that by construction, T^a_μ and $R^{ab}_{\mu\nu}$ transforms independently under the local transformations [1].

We are interested in a gravitational theory as General Relativity where the torsion tensor is zero. Solving for the vanishing torsion tensor, we obtain an equation for the spin connection in terms of the vierbein [1],

$$\omega^{ab}_\mu(e) = \frac{1}{2}\left\{e^{\nu a}(\partial_\mu e_\nu{}^b - \partial_\nu e_\mu{}^b) + e_{\mu c}e^{\nu a}e^{\lambda b}\partial_\lambda e_\nu{}^c - (a \leftrightarrow b)\right\}. \tag{3.9}$$

From the expression for the torsion in eq. (3.8), one can read the Christoffel symbols, $T^a_{\mu\nu} = \Gamma^a_{\mu\nu} - \Gamma^a_{\nu\mu}$. Therefore, the Christoffel symbol reads

$$\Gamma^a_{\mu\nu} = \partial_\mu e_\nu{}^a - e_{\nu b}\omega^{ab}_\mu, \tag{3.10}$$

which can be used to express the Riemann tensor in terms of the Christoffel symbols as usual,

$$R^c{}_{dab} = \partial_a\Gamma^c_{bd} - \partial_b\Gamma^c_{ad} + \Gamma^c_{fa}\Gamma^f_{db} - \Gamma^c_{fb}\Gamma^f_{da}. \tag{3.11}$$

After imposing the condition that the torsion tensor vanishes, eq. (3.8), reads

$$g^{-1}[D_\mu, D_\nu]g = iF_{\mu\nu}Q + \frac{i}{2}R^{ab}_{\mu\nu}J_{ab}, \tag{3.12}$$

Therefore, we can use the tensors, $F_{\mu\nu}$ and $R^{ab}_{\mu\nu}$, to build up a Lagrangian that matches to the one of the theory of General Relativity, as well as electrodynamics in curved spacetime. Such action reads:

$$\mathcal{S} = \int \det e \; \mathrm{d}^4x \left\{-\frac{1}{4\mu_0}F_{ab}F^{ab} + \frac{1}{16\pi G}R + \dots\right\}, \tag{3.13}$$

with, $R = R^{ab}{}_{ab} = e^\mu_a e^\nu_b R^{ab}{}_{\mu\nu}$, the Ricci scalar, which is the low energy term of the theory of gravity. The second term is the well known Einstein-Hilbert action, and the first term is Maxwell's action in curved spacetime, with μ_0, the magnetic permeability of vacuum. The coefficients of eq. (3.13), have been matched from the known theory, which allows us to obtain the Einstein-Maxwell action in the vierbein formalism. The ellipsis stands for higher order terms from a more fundamental theory of gravity.

One can easily obtain the well known gravitational action by changing to the spacetime indices:

$$\mathcal{S} = \int \sqrt{-g}\; \mathrm{d}^4x \frac{1}{16\pi G}R, \tag{3.14}$$

with $R = R^{\mu\nu}{}_{\mu\nu} = e^\mu_a e^\nu_b R^{ab}{}_{\mu\nu}$, and where we have used $g_{\mu\nu} = e^a_\mu e^b_\nu \eta_{ab}$. Furthermore, one can also recover the Christoffel symbol, eq. (4.14), in terms of the metric via, $\Gamma^\alpha_{\mu\nu} = e^\alpha_a \Gamma^a_{\mu\nu}$.

3.1.2 Charged Spinning Compact Objects

Extended objects in the EFT framework was first introduced in [29, 30] for non-spinning objects, where size effects including dissipation are considered. Then, spin was introduce in [43], and then formulated as well in [71], whose ingredients differ. The effective theory for spinning objects derived using the coset construction was introduced in [1]. Although in [30], BHs electrodynamics is introduced as a toy model, it was until [63] that charge was considered in the EFT for compact objects to obtain the dynamics. In the following we will use the coset construction and extend the work on spinning objects in [1], to include the U(1) symmetry to describe charged spinning compact objects.

Charged Spinning Particles

In the previous section we constructed an invariant action for a charged extended object without spin in flat spacetime, by identifying the symmetry breaking pattern of a charged point particle, which breaks spatial translations and boosts. The state of a charged point particle is an eigenstate of the charge and does not break the U(1) symmetry. Now, in the curved spacetime case, we consider spinning objects which break the full Poincaré group, such that the system is described by the charged point particle with the additional breaking of rotations. BHs and NSs have their own internal symmetry, which characterizes the low energy dynamics of the effective theory. The additional symmetry group for a compact object is the internal symmetry group, S $\subseteq$ SO(3), so that G = U(1) $\times$ ISO(3,1) $\times$ S, with G the full symmetry before being broken [1]. In principle, S, can be a discrete group, but with the appropriate choice of the coset parametrization, we can treat in the same way both continuous and discrete symmetries.

By considering the comoving frame, the group G is broken into a linear combination of internal rotations, S_{ij}, and spatial rotations, J_{ij}, such that the symmetry breaking pattern for the charged spinning point particle reads,

$$\begin{aligned}
\text{Unbroken generators} = \begin{cases} \bar{P}_0 = P_0 + Q & \text{time translations,} \\ \bar{J}_{ij} & \text{internal and spacetime rotations.} \end{cases} \\
\text{Broken generators} = \begin{cases} P_i & \text{spatial translations,} \\ J_{ab} & \text{boosts and rotations,} \end{cases}
\end{aligned} \tag{3.15}$$

with, $\bar{J}_{ij}$, the sum of the internal and spacetime rotations [1], and where we have considered a spherical star at rest, such that, S_{ij}, are the generators of the internal $SO(3)$ group, and $\bar{J}_{ij} = S_{ij} + J_{ij}$. Translations are non-linearly realized the local Poincaré and U(1) transformations are consider to take place along the fiber. Given that Lorentz transformations can be parametrized as the matrix product of a boost and a rotation, the coset parametrization reads

$$g = e^{iy^a \bar{P}_a} e^{i\alpha_{ab} J^{ab}/2} = e^{iy^a \bar{P}_a} e^{i\eta^j J_{0j}} e^{i\xi_{ij} J_{ij}/2} = e^{iy^a \bar{P}_a} \bar{g}, \tag{3.16}$$

which implies a one to one correspondence between the Goldstone fields, α_{ab} and η_i, ξ_{ij} [1]. By parametrizing the coset with the generators of the broken spatial rotations, the Maurer-Cartan form can be computed without the need to specify the explicit unbroken generators of rotations, $\bar{J}_{ij}$.

We proceed as before to identify the relevant degrees of freedom from the projected Maurer-Cartan form to the worldline of the object,

$$\begin{aligned}\dot{x}^\mu g^{-1} D_\mu g =& \dot{x}^\mu g^{-1}(\partial_\mu + i\check{A}_\mu Q + i\check{e}_\mu{}^a P_a + i\check{\omega}_\mu{}^{ab} J_{ab}) g \\ =& \dot{x}^\mu \bar{g}^{-1}(\partial_\mu + iA_\mu Q + ie_\mu{}^a P_a + \frac{i}{2}\omega_\mu^{ab} J_{ab})\bar{g} \\ =& ie(P_0 + AQ + \nabla\pi^i P_i + \frac{1}{2}\nabla\alpha_{cd} J^{cd}).\end{aligned} \tag{3.17}$$

The building blocks of the low energy dynamics are,

$$e = \dot{x}^\mu e_\mu{}^a \Lambda_a{}^0 \tag{3.18}$$

$$A = e^{-1}\dot{x}^\mu A_\nu \Lambda^\nu{}_\mu \tag{3.19}$$

$$\nabla\pi^i = e^{-1}\dot{x}^\mu e_\mu{}^a \Lambda_a{}^i \tag{3.20}$$

$$\nabla\alpha^{ab} = e^{-1}\left(\Lambda_c{}^a \dot{\Lambda}^{cb} + \dot{x}^\nu \omega_\nu^{cd} \Lambda_c{}^a \Lambda_d{}^b\right) \tag{3.21}$$

with the Λ's, the Lorentz transformations parametrized by α, or equivalently by η and ξ. As one can observe, one of the advantages of using the parametrization (3.16), is that no connection proportional to $\bar{J}$ appears, which makes the building blocks independent of the residual symmetry group [1]. The residual symmetry, SO(3), requires all spatial indices to be contracted in an SO(3) invariant manner.

From the coset perspective, we can remove some of the Goldstones using the inverse Higgs constraint [38], given that the commutator between the unbroken time translations and boosts, gives spatial translations, $[K^i, P^0] = iP^i$. Thus, we set to zero the covariant derivative of the Goldstone,

$$\nabla\pi^i = e^{-1}(\dot{x}^\nu e_\nu^0 \Lambda_0{}^i + \dot{x}^\nu e_\nu^j \Lambda_j{}^i) = 0, \tag{3.22}$$

and solve this constraint, to express the boost as a function of velocities [1],

$$\beta_i \equiv \frac{\eta_i}{\eta}\tanh\eta = \frac{\dot{x}^\nu e_\nu{}^i}{\dot{x}^\nu e_\nu{}^0} \tag{3.23}$$

where, η, is identified as the rapidity (See appendix 2.3). To obtain the physical interpretation of last equation, we rewrite the building block, e, such that

$$\begin{aligned}e =& \sqrt{(e\nabla\pi^i)^2 - (\dot{x}^\nu e_\nu{}^a \Lambda_a{}^c \dot{x}^\mu e_\mu^b \Lambda_{bc})} \\ =& \sqrt{-\eta_{ab} e_\nu{}^a e_\mu{}^b \dot{x}^\nu \dot{x}^\mu} = \sqrt{-g_{\mu\nu}\dot{x}^\mu \dot{x}_\mu} = \frac{\mathrm{d}\tau}{\mathrm{d}\sigma},\end{aligned} \tag{3.24}$$

with, σ, the worldline parameter that traces out the trajectory of the particle. To obtain last equation we have imposed the inverse Higgs constraint, and the property of the boost matrices, $\Lambda_a{}^b \Lambda^a{}_c = \delta^b{}_c$.

Therefore, with eq. (3.24), we rewrite the constraint, eq. (3.22), in a way that makes manifest its physical interpretation [1]. For rotations, we can write, $\Lambda^0{}_a(\xi) = \delta^0_a$ and $\Lambda^i{}_j(\xi) = \mathcal{R}^i{}_j(\xi)$, with $\mathcal{R}(\xi)$ an $SO(3)$ matrix, such that the constraint (3.22) now reads

$$u^a \Lambda_a{}^i(\eta) \mathcal{R}_i{}^j(\xi) = 0. \tag{3.25}$$

with, $u^a \equiv e_\mu{}^a \partial_\tau x^\mu$, the Lorentz velocity measured in the local inertial frame defined by the vierbein. Given that the matrix $\mathcal{R}_j{}^i(\xi)$ is invertible, we obtain

$$u^a \Lambda_a{}^i(\eta) = 0. \tag{3.26}$$

These quantities have a clear geometrical interpretation: the set of local Lorentz vectors,

$$\hat{n}^a{}_{(0)} \equiv u^a = \Lambda^a{}_0(\eta)\,, \quad \hat{n}^a_{(i)} \equiv \Lambda^a{}_i(\eta), \tag{3.27}$$

that define an orthonormal local basis with respect to the local flat metric, η_{ab}, in the frame that is moving with the particle [1]. Orthogonality is obtained from the boost matrices, $\Lambda_a{}^b \Lambda^a{}_c = \delta^b_c$. This means that, the $\hat{n}^a_{(b)}$, is a set of vierbeins that defines the local inertial frame on the particle worldline. One can also define the orthonormal basis in terms of the spacetime vectors, $\hat{n}^\mu{}_{(b)} \equiv e^\mu_a \hat{n}^a_{(b)}$, with respect to the full metric, $g_{\mu\nu}$.

Moreover, an additional set of orthonormal vectors is obtained [1],

$$\hat{m}^b{}_{(a)} \equiv \Lambda^b{}_a(\alpha) = \Lambda^b{}_c(\eta) \mathcal{R}^c{}_a(\xi), \tag{3.28}$$

with the zeroth vector, $\hat{m}^b{}_{(0)} = \hat{n}^b{}_{(0)} = u^b$, the velocity of the compact object in the proper frame. The rest of the vectors differs by a rotation, $\mathcal{R}(\xi)$, compared to (3.27), from which one can observe that the set of vectors, $\hat{m}^b{}_{(a)}$, contain information about the rotation, parametrized by the three degrees of freedom of ξ.

With these definitions, the covariant derivatives, $\nabla\alpha^{0i}$, can be expressed as

$$\nabla\alpha^{0i} = \mathcal{R}_j{}^i(\xi) \Lambda_a{}^{(j)}(\eta)(\partial_\tau u^a + u^\mu \omega_\mu{}^a{}_c u^c) = \mathcal{R}_j{}^i(\xi) \Lambda^{(j)}_a(\eta) a^a = a^i, \tag{3.29}$$

which is a rotated version of the acceleration projected into the orthonormal basis defined by the $\hat{n}$'s basis in the proper frame of the particle. As in the case of charged spheres, in the absence of external forces, this building block is zero. Nevertheless, it must be considered to build up invariant terms when an external force, such as the one from an external gravitating object, or form the charge of another object, is strong enough to make this building block relevant to the dynamics.

The rest of the covariant derivatives for the Goldstone, reads

$$\nabla\alpha^{ij} = \Lambda_k{}^i(\eta^{kl}\partial_\tau + \partial_\tau x^\mu \omega^{kl}_\mu)\Lambda_l{}^j = \Omega^{ij}, \tag{3.30}$$

which is the relativistic angular velocity of the object in the proper frame. From the covariant quantity, Ω^{ij}, it is possible to define the angular velocity vector with the epsilon tensor, which reads

$$\Omega_i = -\frac{1}{2}\epsilon_{ijk}\Lambda_a{}^j(\eta^{ab}\partial_\tau + \partial_\tau x^\mu \omega^{ab}_\mu)\Lambda_b{}^k. \tag{3.31}$$

Thus, we are left with the building blocks

$$e = \mathrm{d}\tau/\mathrm{d}\sigma, \tag{3.32}$$
$$A = u^\mu A_\mu, \tag{3.33}$$
$$\nabla\alpha^{0i} = a^i \tag{3.34}$$
$$\nabla\alpha^{ij} = \Omega^{ij}, \tag{3.35}$$

with $A_\mu = A_\nu \Lambda^\nu{}_\mu$. We consider the blocks A and e, to derive the effective action of a charged point particle in curved space-time. The action takes the form

$$\mathcal{S} = \int \mathrm{d}\sigma e(-n_E + n_A A) = \int \mathrm{d}\tau(-mc^2 + q u^a A_a), \tag{3.36}$$

where we have matched the coefficient, $n_E = mc^2$, from the action of a point particle [29] with mass, m, and the coefficient, $n_A = q$, from the action of a charged point particle [29, 63] with net charge, q.

Now we include the building block, $\nabla\alpha^{ab}$, neglecting charge for simplicity. The leading order action reads [1],

$$\mathcal{S} = \int \mathrm{d}\sigma e \left(-mc^2 + n_\alpha \nabla\alpha_{ij}\nabla\alpha^{ij} + \dots\right) = \int \mathrm{d}\sigma e \left(-mc^2 + n_\Omega \Omega_{ij}\Omega^{ij}\right), \tag{3.37}$$

where a term linear in Ω, has been discarded by time reversal symmetry, and we have considered spherical objects at rest. The ellipses denotes higher order corrections made out of $\nabla\alpha^{ab}$. In the mechanics of rotational dynamics, to characterize a rigid sphere only two parameters are needed, which is the mass, m, and moment of inertia, I. By comparing our action to the one of a relativistic spinning point particle [88, 43], we match the coefficient, $n_\Omega = I/4$, to obtain the relativistic action for spinning particles in curved space-time [1, 46],

$$\mathcal{S} = \int \mathrm{d}\tau \left\{-m + \frac{I}{4}\Omega_{ab}\Omega^{ab} + \dots\right\}, \tag{3.38}$$

where we have defined, $\Omega_{0i} = 0$, as in [46]. A higher order correction made out of the Goldstone building block,

$$\mathcal{S} = \int \mathrm{d}\tau c_{\alpha,u} \nabla\alpha_{ac}\nabla\alpha^{cb}\frac{u^a u_b}{u^2} = \int \mathrm{d}\tau c_{\Omega,a}\Omega_{ij}a^i\frac{u^j u_0}{u^2} + \dots. \tag{3.39}$$

We can connect our action to the one used to obtain the PN expansion for spinning objects [72, 41], with the introduction of the relativistic spin degree of freedom [43, 41, 17]

$$S^{ab} = 2\frac{\partial\mathcal{L}}{\partial\Omega_{ab}}, \tag{3.40}$$

which is the conjugate variable of the angular velocity, with associated spin tensor $S^{ab} = \epsilon^{ab}{}_c S^c$. Then, by considering the action that describes a spinning extended object in the proper frame,

$$\mathcal{S} = \int \mathrm{d}\tau \left\{-mc^2 + \frac{I}{4}\Omega_{ab}\Omega^{ab} + c_{\Omega,a}\Omega_{ab}a^a\frac{u^b u_0}{u^2} + \dots\right\}, \tag{3.41}$$

we Legendre transform it to write it down in terms of the spin S^{ab}, and transform it to the lab frame, with

$$\tilde{\Omega}^{ab} = \Lambda^a{}_c \Lambda^b{}_d \Omega^{cd} = \Lambda^a{}_c \Lambda^b{}_d [\Lambda_e{}^c (\eta^{ef} \partial_\tau + \partial_\tau x^\mu \omega_\mu{}^{ef}) \Lambda_f{}^d] \tag{3.42}$$

$$= -\Lambda^a{}_c \partial_\tau \Lambda^{bc} + \partial_\tau x^\mu \omega_\mu{}^{ab}, \tag{3.43}$$

and $\tilde{S}^{ab} = \Lambda^a{}_c \Lambda^b{}_d S^{cd}$. In the lab frame, in which the PN expansion is computed, we set $u^i = v^i$ with $u^0 = 1$, and $\sigma = t$, such that we obtain

$$\mathcal{L} = -mc^2 + \frac{1}{2} S_{ab} \Omega^{ab} + \frac{c_{\Omega,a}}{I} S_{ab} \frac{a^a u^b}{u^2} - \frac{1}{4I} S_{ab} S^{ab}, \tag{3.44}$$

with the expected acceleration correction in [41] when setting $c_{\Omega,a} = I$.

Since $u^a \Lambda_a{}^i = 0$, the tensors, $\nabla \alpha^{ab}$ and S^{ab}, are orthogonal to the four velocity. Therefore, we can obtain a constraint on the angular velocity,

$$u_a \nabla \alpha^{ab} = u^\mu \nabla_\mu u^b + u_a \Omega^{ab} = 0, \tag{3.45}$$

as well as on the spin,

$$u_a S^{ab} = \sqrt{u^2} S^{0b} + u_i S^{ib} = 0. \tag{3.46}$$

The latter, known as the spin supplementary condition, is equivalent to the relativistic Price-Newton-Wigner spin supplementary condition [89, 41], while the former is the constraint on the angular velocity derived in [46].

With all of our derived invariant operators, we write down the effective action of a charged spinning point particle in the particle's rest frame,

$$\mathcal{S} = \int \mathrm{d}\tau \left\{ -mc^2 + q u^a A_b + \frac{I}{4} \Omega_{ab} \Omega^{ab} + I \Omega_{ab} a^a \frac{u^b u_0}{u^2} + \dots \right\}. \tag{3.47}$$

Size Effects

Size effects in the EFT for extended objects was introduced in [29], which can be systematically taken into account by building invariant operators made up of the Weyl curvature tensor, W_{abcd}, that is obtained from the Riemann tensor, R_{abcd}, by subtracting out various traces. By defining the transformation [1]

$$R \equiv g_L \, \tilde{R}, \tag{3.48}$$

with, g_L, the Lorentz part of the parametrization eq. (3.16), the Riemann tensor transforms linearly under Lorentz transformations as expected. The explicit transformation reads

$$R_{abcd} = \Lambda_a{}^e \Lambda_b{}^f \Lambda_c{}^g \Lambda_d{}^h \tilde{R}_{efgh}, \tag{3.49}$$

with, $\tilde{R}_{abcd}$, the Riemann tensor in the local rest frame of the object. Having the correct transformations, we define the Weyl tensor as usual,

$$W_{abcd} = R_{abcd} + \frac{1}{2}(R_{ad}g_{bc} - R_{ac}g_{bd} + R_{bc}g_{ad} - R_{bd}g_{ac}) + \frac{1}{6}R(g_{ac}g_{bd} - g_{ad}g_{bc}), \quad (3.50)$$

which have the physical content [29]. The Weyl tensor measures the curvature of the spacetime and contains the tidal force exerted on an extended particle that is moving along the worldline, taking into account for how the shape of the body is distorted. It transforms as eq. (3.49).

Furthermore, we can also use the electromagnetic tensor to build invariant operators that take into account for the polarizability of the object. Following the above discussion, we define its transformation rule,

$$F \equiv g_L \, \tilde{F}. \quad (3.51)$$

Having defined the correct transformation rules for the Riemman and the electromagnetic tensor, we can now proceed to form rotationally invariant objects.

We form all leading order invariant operators that contribute to the dynamics, by combining all of our covariant quantities: W^{abcd}, F^{ab}, $\nabla\alpha^{ab}$ and u^a, in all possible ways allowed by the symmetries. In particular, for the electromagnetic and Weyl tensor, the building blocks are the electric like parity tensors, $E_a = F_{ab}u^b$, and $E_{ab} = W_{acbd}u^c u^d$, respectively [30]. By considering the electromagnetic dipolar and gravitational quadrupolar moments, we build the following leading order relevant operators for finite-size effects:

$$\tilde{\mathcal{O}}(u^a, \Omega^a, E^{ab}, E^a) = \begin{cases} E^{ab}E_{ab} & \text{Gravity}, \\ \Omega^a\Omega^b E_{ab} & \text{Spin} - \text{gravity}, \\ E^a E_a & \text{Electromagnetic}, \\ \Omega^a E_a & \text{Spin} - \text{electro}. \end{cases} \quad (3.52)$$

One can consider the magnetic parity operators as well, $B_{ab} = (1/2)\epsilon_{cdea}W^{cd}{}_{fb}u^e u^f$ and $B_a = \epsilon_{abcd}F^{bc}u^d$ [30], for the gravitational and electromagnetic case respectively, which are subleading with respect to the electric parity terms (at least for the gravitational case), therefore restricting our discussion to the electric parity action. The leading order magnetic parity operators can be build in analog to (3.52) i.e. $B^{ab}B_{ab}$, $B^a B_a$, etc.

Higher order terms to the ones shown in eqs. (3.52), can be built from the derived building blocks and the covariant derivatives, eqs. (3.6) and (3.7), i.e. $\nabla^g_c E_{ab}$ and $\nabla^q_b E_a$. Furthermore, it is worth noting that size effects can be seen as encoded in a composite operator Q^{ab}, which we comment below.

Dissipative Effects

Dissipation, due to the internal structure of an extended object, was introduced in EFT description in [30], where the existence of gapless modes that are localized on the worldline of the particle take into account for the energy and momentum loss from the interaction with external sources. Dissipative effects for slowly spinning objects were considered in [50, 46], and for maximally spinning in [42]. These large number of degrees of freedom can be encoded in operators allowed by the symmetries of the object. For a compact object, the allowed operators due to its symmetries gives rise to the invariant operators [30, 42]:

$$\text{Dissipative operators} = \begin{cases} \mathcal{P}^a(\sigma) F_{ab} u^b & \text{Electro,} \\ \mathcal{D}^{ab}(\sigma) W_{acbd} u^c u^d & \text{Gravity,} \end{cases} \tag{3.53}$$

with $\mathcal{P}(\tau)$ and $\mathcal{D}(\tau)$, composite operators corresponding to the electric parity of the electromagnetic dipole and the gravitational quadrupole moment respectively, encoding the dissipative degrees of freedom.

For a non-spinning BH, dissipation takes into account for the absorption of electromagnetic and gravitational waves, while for a non-spinning NS, dissipative effects take into account for the energy loss during the interaction with an external source given the internal equation of state of matter. On spinning objects, the spin has a time dependence between the object and its environment which generates dissipative effects. The operators in eq. (3.53), take into account for the spin dissipative effects as well. The coefficients do not appear explicitly in the Lagrangian, but they are encoded in the dynamical moments, $\mathcal{P}$ and $\mathcal{D}$, which are dependent on the internal degrees of freedom of the compact object in an unspecified way, but which explicit form is not necessary to obtain the dynamics [30, 42]. The dynamics of the system containing the dissipative degrees of freedom can be obtained using the in-in closed time path [90], a formalism that allows us to treat dissipative effects in a time asymmetric approach [30].

The expectation values of these operators, $\langle \mathcal{P}^a(\tau) \rangle$, $\langle \mathcal{D}^{ab}(\tau) \rangle$, are defined through the in-in path integral, which is the expectation value in the initial state of the internal degrees of freedom, and which in general is a functional of the building blocks, E^a and E^{ab}, respectively [42]. In the gravitational case, by considering the linear response in a weak external field, the in-in expectation values implies the form of the expectation value [42]

$$\langle \mathcal{D}^{ab}(\tau) \rangle = \int \mathrm{d}\tau' G_R^{ab,cd}(\tau - \tau') E_{cd}(\tau') + O\left(E^2\right), \tag{3.54}$$

where the expectation values of the retarded Green's function,

$$G_R^{ab,cd}(\tau - \tau') = i\theta(\tau - \tau') \left\langle [\mathcal{D}^{ab}(\tau), \mathcal{D}^{cd}(\tau')] \right\rangle, \tag{3.55}$$

are obtained at the initial state of the interaction where the external field is zero. By considering low frequencies, from which we assume that the degrees of freedom from the operator, $\mathcal{D}^{ab}$, are near equilibrium, the time ordered two point correlation function imply that the Fourier transform G_R must be an odd, analytic function of the frequency, $\omega > 0$ [30]. Therefore, the retarded correlation function, $\tilde{G}_R$, reads

$$G_R^{ab,cd}(\omega) \simeq i c_g \omega \left(\delta^{ac}\delta^{bd} + \delta^{ad}\delta^{cb} - \frac{2}{3}\delta^{ab}\delta^{cd} \right), \tag{3.56}$$

with the coefficient for dissipative effects, $c_g \geq 0$. Note that, in contrast to [30], we have absorbed the $1/2$ factor appearing in front of (3.80) into the dissipative coefficient.

By considering the response of the interaction to be nearly instantaneous, the operator due to gravitational dissipative effects takes the form [30, 42]

$$\langle \mathcal{D}_{ab}(\tau) \rangle \simeq i c_g \frac{\mathrm{d}}{\mathrm{d}\tau} E_{ab} + \ldots \tag{3.57}$$

In general, one can use the dynamical composite operator, $Q_{ab}(\tau)$, to account for the tidal response function, for which the above reasoning leads to [30, 42]

$$\langle Q_{ab}(\tau) \rangle \simeq n_g E_{ab} + i c_g \frac{\mathrm{d}}{\mathrm{d}\tau} E_{ab} + n_g^{'} \frac{\mathrm{d}^2}{\mathrm{d}\tau^2} E_{ab} + \ldots \tag{3.58}$$

The first term in last equation is the static quadrupolar tidal effect considered above, while the third term is a dynamical tidal effect in the quasi-static limit. The second term, which is the imaginary part of the response function, takes into account for the dissipative degrees of freedom. In our work we consider the static tidal response only, and use the operator, $\mathcal{D}_{ab}$, to contain only the dissipative degrees of freedom. Although in the numerical simulations for NSs we use dynamical oscillations in the quasi-static limit to study its effects, the state of the art modeling of dynamical oscillations is done in a different fashion [17], which is beyond the scope of this work.

On the electromagnetic side, an analog procedure can be taken, for which retarded correlation function reads [30]

$$G_R^{ab}(\omega) \simeq i c_q \delta^{ab} \omega, \tag{3.59}$$

with the coefficient, $c_q \geq 0$. Therefore, the operator for electromagnetic dissipative effects reads

$$\langle P_a(\tau) \rangle \simeq i c_q \frac{\mathrm{d}}{\mathrm{d}\tau} E_a + \ldots \tag{3.60}$$

3.1.3 Effective Action

Gathering all our results, we construct the most general, leading order and electric like parity, effective action for a compact object in the theory of General Relativity,

$$\begin{aligned} \mathcal{S}_{eff} = \int \mathrm{d}\tau \Big\{ & -mc^2 + q u^a A_a + \frac{I}{4} \Omega_{ab} \Omega^{ab} + I \Omega_{ab} a^b \frac{u^a u_0}{u^2} \\ & + n_{q,\Omega} \Omega^a E_a + n_{g,\Omega} \Omega^a \Omega^b E_{ab} + n_q E^a E_a \\ & + n_g E^{ab} E_{ab} + \mathcal{P}^a E_a + \mathcal{D}^{ab} E_{ab} + \ldots \Big\} + \mathcal{S}_0, \end{aligned} \tag{3.61}$$

with the electric parity tensor, $E_{ab} = W_{acbd} u^c u^d$, and $E_a = F_{ab} u^b$, that corresponds to the gravitational quadrupole and electromagnetic dipole moment respectively. The interaction action,

$$\mathcal{S}_0 = \int \det e \, \mathrm{d}^4 x \left\{ -\frac{1}{4\mu_0} F_{ab} F^{ab} + \frac{1}{16\pi G} R + \ldots \right\}, \tag{3.62}$$

is the Einstein-Maxwell action. The action describing the charged spinning compact object lives in the worldline, while $\mathcal{S}_0$ lives in the bulk.

Coefficients of the Effective Theory

The coefficients of the effective theory encode the microphysics of the compact objects, which are determined through a matching procedure to the full known theory, and ultimately from GW observations. We identify them from the results in literature, without the need to do the explicit calculations here. We already have pointed out the coefficients appearing in the action describing a charged spinning point particle with corrections due to its acceleration in eq. (3.47). The coefficient of the point particle term [29], $c_E = mc^2$, the coefficients in the spin corrections, $c_\Omega = I/2$ and $c_{\Omega,u} = I$ [43, 41], and the coefficient from the correction due to electromagnetic charge, $c_A = q$ [29, 63]. Now, we proceed to point out the rest of the coefficients due to the internal structure of the compact object.

We start with the coefficient due to static tidal effects, n_g, which is a coefficient that depends on the internal structure of the star through a parameter known as the Love number. Any stellar object that can be described by an equation of state of matter, can be described approximately in terms of its Love numbers. In the case of BHs, it has been found that their Love numbers vanishes $n_g = 0$ [91], and for spinning BHs $n_{g,\Omega} = 1$ [19, 92]. Furthermore, it has been shown that for non-spinning [93] and spinning BHs [92], the coefficients due to the polarizability vanishes as well, $n_q = 0$ and $n_{q,\Omega} = 0$.

On NSs, the leading order quadrupolar Love coefficient has the form [13]

$$n_g = \frac{2\ell^5 k_2}{3G}, \tag{3.63}$$

with k_2, the quadrupolar dimensionless Love number, and ℓ the radius of the star.[1] The Love numbers are dimensionless parameters that measure the rigidity and tidal deformability of the compact object, and varies given different equations of state of matter [48]. This number is related to other parameters of the star from the relativistic I-Love-Q relations [48, 47], which relates the moment of inertia, I, the tidal deformability parameter, or Love number, k_2, and the quadrupole moment. These relations, which are empirically found to hold for a wide range of equations of state of matter, are only approximate relations and are not exact first principles relations.

On the coefficient due to the coupling of spin-gravity size effects for spinning NSs, in the slow rotation limit, the relativistic coefficient, $n_{g,\Omega}$, is obtained through the Love-Q part of the I-Love-Q relations [47]. The latter coefficient in the Newtonian limit is the same as the one for static tides, $n_{g,\Omega} = n_g$ [47]. On the charge-gravity, and charge-spin size effects, given that charge in compact objects has been mostly neglected, the rest of the coefficients, $n_{q,\Omega}$, n_q and $n_{q,g}$, are unknown, and are to be derived by analytical and numerical means.

Moving on into dissipative effects, although their coefficients are not explicitly shown in the action, they are encoded in the operators, $\mathcal{P}$ and $\mathcal{D}$, as shown above. We point out the known coefficients for dissipative effects in BH interactions from the existing literature. The operator $\mathcal{D}^{ab}$, for non-spinning BHs, contains the coefficient, c_g, which encodes the capacity of the BH to absorb GWs, and which can be read off from the response function derived in [30],

$$c_g = \frac{16}{90}\frac{G^5 M^6}{c^{13}} = \frac{\ell_s^6}{360Gc}, \tag{3.64}$$

[1] We have chosen to denote the radius of the object with ℓ as in [46, 45], rather than with R as commonly used, given that we use R for the Ricci scalar.

with M the mass of the BH, and ℓ_s its radius. The coefficient in eq. (3.64), include the factor of $1/2$ from eq. (3.80) [30]. In the same way, we can obtain the coefficient for electromagnetic dissipative effects from the composite operator, $\mathcal{P}(\tau)$ [30],

$$c_q = \frac{2\pi\ell_s^4}{3\mu_0 c}, \tag{3.65}$$

which encodes the capacity of the BH to absorb electromagnetic waves.

On the dissipative effects of rotating BHs, these effects have been considered for the slow [46, 50] and maximally spinning [42] cases. The coefficients can be obtained from the response function derived in [19] using the Teukolsky equation, for both non-spinning and spinning case. We start by reading off the coefficient for the non-spinning BH from the response function, which in the notation of [19], reads

$$\frac{1}{2}N_2\ell_S^5\mathcal{F}_{2m_s}^{Sch} = i\frac{\ell_S^5 M}{90c^3}\omega + \mathcal{O}(\omega^3) \simeq i\frac{\ell_S^6}{360Gc}\omega, \tag{3.66}$$

where we have used the leading order mode, $l = 2$, of the angular momentum number, such that $N_2 = 1/3$, and with m_s, the azimuthal number, and ℓ_S, the Schwarzschild radius. To obtain eq. (3.66) as eq. (3.64), we have substituted the mass of the BH in terms of the Schwarzschild radius, $M = \ell_S c^2/2G$, and considered the extra factor of $1/2$, as for eq. (3.64).

Now we move into the spinning case, for which the response function reads [19]

$$\begin{aligned}\mathcal{F}_{2m_a}^{I,Kerr} &= -\frac{i}{30Gc}\frac{ism_s}{(\ell_+ - \ell_-)} + \frac{i}{15c^3}\frac{\ell_+ M}{(\ell_+ - \ell_-)}\omega + \mathcal{O}(\omega^3) \\ &\simeq -\frac{i}{30Gc}\frac{Im_s}{Mc(\ell_+ - \ell_-)}\Omega + \frac{i}{15c^3}\frac{\ell_+ M}{(\ell_+ - \ell_-)}\omega,\end{aligned} \tag{3.67}$$

with $s = J/Mc = I\Omega/Mc$, with $J = I\Omega$, the scalar value of the angular momentum, and ℓ_+ and ℓ_-, the outer and inner radius of the Kerr BH.[2] The moment of inertia of a BH is $I = 4GM^2/c^4$. The, the response function with its normalization constant, reads

$$\frac{1}{2}N_2\ell_+^5\mathcal{F}_{2m_s}^{I,Kerr} \simeq -\frac{i}{180}\frac{Im_s\ell_+^5}{MGc(\ell_+ - \ell_-)}\Omega + \frac{i}{90c^3}\frac{\ell_+^6 M}{(\ell_+ - \ell_-)}\omega. \tag{3.68}$$

Therefore, we have obtained a response function for the dissipative effects of the form, $\langle\mathcal{D}_{ab}(\tau,\Omega)\rangle \propto i(c_{g,\Omega}\Omega + c_g \mathrm{d}/\mathrm{d}\tau)E_{ab}$. We can identify that, for a rotating extended object, tidal dissipation arises due to two separate contributions. The first term of eq. (3.68), for which is nonzero even in the case of $\omega = 0$, arises given that the spin of the body has a time dependence between the object and its tidal environment. This can be seen, from the object perspective in its proper frame, as the external environment rotating with the frequency of the spin of the object.

Furthermore, now we have an expression which is explicit on the azimuthal numbers, m_s. For the dominant perturbation mode, $l = 2$, then, $m_s = [-2, -1, 0, 1, 2]$.

[2] To make the reading of the coefficients accessible, we have written the response function as in [19], and then converted it to our notation. Therefore, in this case, do not confuse, a, with the acceleration defined in the previous section

Nevertheless, we can not identify a specific value of m_s to be dominant. Therefore, it is necessary to sum over all possible values of m_s. This can be done by considering the size effects operators in terms of the electric and magnetic tidal moments. For instance, consider schematically the electric tidal moment, E_{lm_s}, for which leading order is E_{2m_s}. Then, we can proceed to identify the different elements of E_{2m_s}, given the possible values of m_s, to then couple each response function with its electric tidal moment. For instance, we would couple schematically, $Q_{2m_s} \propto \mathcal{D}_{2-2}E_{2-2} + \mathcal{D}_{2-1}E_{2-1} + \mathcal{D}_{20}E_{20} + \mathcal{D}_{21}E_{21} + \mathcal{D}_{22}E_{22}$. The same reasoning applies for the magnetic parity like tidal moments. On the dissipative effects for charged spinning BHs, the coefficient, $c_{q,\Omega}$, is still unknown.

The coefficients of NSs for dissipative effects are still unknown, and must be determined from hydrodynamical simulations, analytical computations, and ultimately from observations. Nevertheless, it is worth commenting that for a stellar object that is described by an equation of state of matter, there exists the weak friction model [94], which might be applicable for NSs. For the latter, the coefficient, $c_g = \Theta n_g$ [94], with Θ, being the time lag, which accounts for the tidal bulge formed in the NSs during the interaction with another compact object.

More on the Properties of Compact Objects

Neutron Stars

For a non-spinning NS, the spacetime outside it is described by the Schwarzschild metric, which leads to the inner most circular orbit distance or Last Stable Orbit LSO distance $d_{LSO} = 6Gm/c^2$, with m the mass of the star. For the case of a spinning NS, if the orbiting object is in prograde motion, to first order in χ, the LSO is $d_{LSO,\Omega} = 6Gm/c^2(1 - 0.54433\chi)$ [95], with χ being the dimensionless spin parameter defined below. The moment of inertia for a NS, can be approximated as [96]

$$I = 0.21\frac{m\ell^2}{1 - 2Gm/\ell c^2}, \tag{3.69}$$

where ℓ is the radius of the NS. We take the speed of sound inside the star $c_s \lesssim c/\sqrt{3}$ [97].

For the dynamical component of the tidal effects, the dimensionless dynamical Love number k', related to n'_g, is obtained from the response function of the NS in terms of the frequency ω_f, and dimensionful overlap integral, $\mathcal{I}_f$, of the fundamental mode of the star [49], which describes to which extent an external field excites the mode. $\mathcal{I}_f$ corresponds to $\mathcal{I}_{02}$ in [49], where the subscript indicates the fundamental mode, $l = 0$, and the quadrupolar moment, $k = k_2$. The response function in fourier space reads [49]

$$\mathcal{F}(Q^{ab}) = \frac{1}{2}\frac{\ell^5}{G}\frac{q_f^2}{\ell^2(\omega_f^2 - \omega^2)/c^2}\mathcal{F}(E^{ab}) = \frac{1}{2}\frac{\ell^5}{G}\frac{q_f^2}{\ell^2\omega_f^2/c^2}\left(1 + \frac{\omega^2}{\omega_f^2} + \dots\right)\mathcal{F}(E^{ab}), \tag{3.70}$$

where we have expanded over ω/ω_f, and q_f, is the dimensionless overlap integral which is related to the $\mathcal{I}_f$ through $q_f^2 = G\mathcal{I}_f^2/\ell^3$. The combination, $\ell\omega_f/c$, is dimensionless as well.

We identify the Love coefficient

$$n_g = \frac{1}{2}\frac{\ell^5}{G}\frac{q_f^2}{\ell^2\omega_f^2/c^2}, \tag{3.71}$$

and comparing to the Newtonian tidal Love number, $n_g = 2k\ell^5/3G$, we identify the dimensionless Love number k

$$k = \frac{3}{4}\frac{q_f^2}{\ell^2\omega_f^2/c^2}, \tag{3.72}$$

from which we find agreement with k obtained using the Clairaut-Radau equation [98]. From the above expansion of the response function, we can extract the term n_g'

$$n_g' = \frac{1}{2}\frac{\ell^7}{Gc^2}\frac{q_f^2}{\ell^4\omega_f^4/c^4} = \frac{1}{2}\frac{\ell^7}{Gc^2}k', \tag{3.73}$$

for a limit in which $\omega/\omega_f \ll 1$.

For all the considered NS simulations, we consider the mass and radius defined above, even when considering different equations of state. From the considered speed of sound inside the NS, and its radius, we can safely add spin, $\chi \leq 0.2$, without breaking down the theory.

Black Holes

The radius of a Schwarzschild BH is $\ell_S = 2GM/c^2$. The LSO distance for a nonspinning BH is $d_{LSO} = 6Gm/c^2$. For a spinning BH, the LSO is $d_{LSO} = 6Gm/c^2 - 2\sqrt{\frac{2}{3}}\Omega_J$ [99], with Ω_J the angular velocity projected into the angular momentum of the BH. The moment of inertia of a BH is

$$I = 4\frac{m^3G^2}{c^3}. \tag{3.74}$$

3.1.4 Slowly Spinning Objects

As previously mentioned, our theory is valid as long as, $\Omega\ell \ll c_s$ holds, which can be tested once we specify the properties of the objects. First, it is important to note that instead of specifying values of the angular velocity, one works with the dimensionless spin, $\vec{\chi}$,

$$\chi = \frac{cJ}{GM^2} = \frac{cI\Omega}{GM^2}, \tag{3.75}$$

where, $J = I\Omega$, is the scalar value of the angular momentum of the star. In order for our theory to work appropriately, we need χ, to be slow $\chi \ll 1$, to not break down the theory. Plugging in the values for a compact object we find that compact objects with the characteristic of the so far detected compact objects, will rotate slowly.

3.2 Newtonian Dynamics of Compact Objects

The action we have derived, taking into account the stellar structure and neglecting charge, has the schematic form

$$\mathcal{S} = \mathcal{S}_{PP} + \mathcal{S}_{\Omega} + \mathcal{S}_{Q} + \mathcal{S}_{\mathcal{D}}, \tag{3.76}$$

where, $\mathcal{S}_{PP}$, is the action for a spinning point particle, $\mathcal{S}_\Omega$, gravitational corrections due to spin, $\mathcal{S}_Q$, dynamical tides and $\mathcal{S}_\mathcal{D}$, dissipative effects. We consider each of the leading order terms for these effects in turn, to obtain their Newtonian limit. Thus, the effective action reads

$$\mathcal{S} = \int \mathrm{d}\tau \left\{ -mc^2 + \frac{I}{2}\Omega_{ij}\Omega^{ij} + n_{g,\Omega}\Omega^i\Omega^j W_{0i0j} + Q^{ij}W_{0i0j} + \mathcal{D}^{ij}W_{0i0j} + \dots \right\}, \quad (3.77)$$

where t is the proper time. The indices $i, j, k, ...$, denote spatial components of the Lorentz indices and the tildes indicates quantities in the comoving frame. This action is Lorentz invariant.

The first two terms in equation (3.77) describes the leading order corrections for a relativistic spinning particle with mass, m, moment of inertia, I, and angular velocity, $\Omega_{ij} = \Lambda_i{}^k D_\tau \Lambda_{kj}$, and $\Omega_{ij} = \epsilon_{ijk}\Omega^k$. The third term is a spin correction due to gravity, with W_{0i0j}, the traceless Weyl tensor. The fourth term accounts for dynamical quadrupolar tidal effects with, $Q = F(\tau)W_{0i0j}$ and $F(\tau)$, a dynamical response function whose Fourier transformation can be Taylor expanding around small frequencies, ω, we have $\mathcal{F}(F) \propto n_g + n'_g\omega^2$.[3] [49] The coefficient, n_g, is the dimensionful Love number for static tides [49], or simply Love coefficient, which is related to the dimensionless Love number k, via $n_g = 2k\ell^5/3G$ [13, 91], with ℓ, the radius of the star. Furthermore the coefficient, n'_g, is the dynamical Love coefficient. These quadrupolar effects encode the fact that the object has finite size. Finally, the last term contains dissipative effects due to the internal structure of the stellar object, with $\mathcal{D}^{ij}$ a composite operator that represents these leading order additional degrees of freedom in a model independent way [30]. The ellipsis represents the tower of higher order operators not taken into account.

We can ensure that our theory will be predictive by expanding our action in small parameters v/c, ℓ/r and Ω/Ω_0 to the desired accuracy. The scales, ℓ, the radius of the object and Ω_0, the typical frequency, do not appear explicitly in the action but determine the characteristic size of the dimensionful coupling constants. The tower of higher order spin terms is under control as long as the rotational velocity is much less than the speed of sound c_s of the material in the star, i.e. $\Omega\ell \ll c_s$ [1]. For a star, this rotational frequency would be such that the body would undergo large non-linear stresses and order one distortions, breaking down the theory.

Newtonian Limit

We perform a Lorentz transformation from the frame embedded in the rigid body to the lab frame. We then take the Newtonian limit of our effective action, which is contained in the lowest order PN expansion of each of the terms. Therefore, in the lab frame, $\sigma = t$, $\tilde{W}_{0i0j} \approx \partial_i\partial_j\Phi$, with Φ the Newtonian potential, and $\tilde{\Omega}^i = \frac{1}{2}\epsilon^{ijk}\mathcal{R}_{jl}\partial_t\mathcal{R}_k{}^l$, with $\mathcal{R}(\theta^i)$ a rotation matrix, where the θ's are the Euler angles describing the orientation of the rigid body [46].

The action then reads,

[3] We have explicitly separated dissipative effects from the response function in the action compared to [49].

$$\begin{aligned}\mathcal{S} = \int \mathrm{d}t \Bigg\{ & \frac{mv^2}{2} - m\Phi + \frac{I}{2}\tilde{\Omega}_{ij}\tilde{\Omega}^{ij} + \frac{n_\Omega}{2}\tilde{\Omega}^i\tilde{\Omega}^j\partial_i\partial_j\Phi \\ & + \frac{n_E}{4}\partial^i\partial^j\Phi\partial_i\partial_j\Phi + \frac{n'_E}{4}\partial^i\partial^j\dot{\Phi}\partial_i\partial_j\dot{\Phi} + \frac{1}{2}\partial_i\partial_j\Phi\mathcal{R}^i{}_k\mathcal{R}^j{}_l\mathcal{D}_g^{kl} + \dots \Bigg\}.\end{aligned} \tag{3.78}$$

Each term in the action has a simple physical interpretation as described in [46]. The first three terms describe a non-relativistic spinning point particle coupled to gravity. The fourth term describes the coupling between gravity and the ensuing quadrupole. By expanding the gravitational potential around some background value $\bar{\Phi}$, this term can be seen as a deformation of the inertia tensor of the form $\delta I \propto n_{g,\Omega}\partial^2\bar{\Phi}$. The first term in the second line describes the coupling of the induced quadrupole $\delta Q \propto n_g\partial^2\bar{\Phi}$, and the second term its dynamical part. The last term contains dissipative effects, which are encoded in the composite operator $\mathcal{D}_g^{ij}$.

As we are not interested in explicitly keeping the degrees of freedom encoded in $\mathcal{D}_g^{ij}$, it is necessary to average over them in a systematic way using the in-in formalism [90] for this context [29, 46], which for dissipative systems, leads to obtainment of the equations of motion from a modified variation [100],

$$\delta\mathcal{S} + i\int \mathrm{d}t\mathrm{d}t'\delta J_{ij}(t)\tilde{G}_R^{ijkl}(t-t')J_{kl}(t') = 0, \tag{3.79}$$

where $J_{kl} = \frac{1}{2}\partial_i\partial_j\Phi\mathcal{R}^i{}_k\mathcal{R}^j{}_l$, and $\tilde{G}_R$ is the retarded correlation function of the operators $\mathcal{D}_g^{ij}$ [46]. Then, by considering low frequencies, from which we assume that the degrees of freedom from $\mathcal{D}_g^{ij}$ are near equilibrium, the time ordered two point correlation function imply that the Fourier transform $\tilde{G}_R$ must be an odd, analytic function of the frequency $\omega > 0$ [30]. Thus, the retarded correlation function $\tilde{G}_R$ reads

$$\tilde{G}_R^{ijkl}(\omega) \simeq c_g\omega\left(\delta^{ik}\delta^{jl} + \delta^{il}\delta^{kj} - \frac{2}{3}\delta^{ij}\delta^{kl}\right), \tag{3.80}$$

with the coefficient for dissipative effects, $c_g \geq 0$.

Then, by combining eq. (3.80) with the modified variation eq. (4.98), and varying it with respect to x^i and θ^i, the equation of motion reads

$$\begin{aligned}m\dot{v}_i = & -m\partial_i\Phi + \frac{n_\Omega}{2}\tilde{\Omega}^k\tilde{\Omega}^j\partial_i\partial_j\partial_k\Phi \\ & + \frac{n_g}{2}\partial_i\partial_j\partial_k\Phi\partial^j\partial^k\Phi + \frac{n'_g}{2}\partial_i\partial_j\partial_k\dot{\Phi}\partial^j\partial^k\dot{\Phi} \\ & - \frac{c_g}{2}\partial_i\partial_j\partial_k\Phi(\partial^j\partial^k\dot{\Phi} + 2\partial^j\partial_l\Phi\epsilon^{klm}\tilde{\Omega}_m),\end{aligned} \tag{3.81}$$

for the acceleration of the compact object, and

$$\begin{aligned}\partial_t(I\Omega_i + n_{g,\Omega}\tilde{\Omega}^j\partial_i\partial_j\Phi) = & -n_{g,\Omega}\epsilon_{ijk}\tilde{\Omega}^k\tilde{\Omega}^l\partial^j\partial_l\Phi \\ & + c_g\partial^j\partial^k\Phi(3\partial_i\partial_j\Phi\tilde{\Omega}_k - 2\partial_j\partial_k\Phi\tilde{\Omega}_i + \epsilon_{ikl}\partial^l\partial_j\dot{\Phi}),\end{aligned} \tag{3.82}$$

for the change of rotational angular momentum with contributions from $n_{g,\Omega}$ and c_g. These equations of motion were originally obtained in [46], with the exception of

the dynamical tides term with coefficient n'_g, which we have derived.

By substituting the Newtonian potential, Φ, and restricting the spin, $\tilde{\Omega}^i$, to be aligned with the angular momentum of the binary, we obtain

$$\begin{aligned} m_1\dot{\vec{v}} = &-\frac{Gm_1m_2\hat{r}}{r^2} - \frac{3n_{g,\Omega}Gm_2\tilde{\Omega}^2\hat{r}}{2r^4} - \frac{9n_gG^2m_2^2\hat{r}}{r^7} \\ &- \frac{9c_gG^2m_2^2}{r^8}(\vec{r}\times\vec{\tilde{\Omega}} + \vec{v} + 2\hat{r}(\hat{r}\cdot\vec{v})) \\ &- \frac{18n'_gG^2m_2^2}{r^9}\left(2v^2\hat{r} + 5(\hat{r}\cdot\vec{v})^2\hat{r} - \vec{v}(\hat{r}\cdot\vec{v})\right), \end{aligned} \tag{3.83}$$

and

$$\left(I + \frac{Gm_2n_{g,\Omega}}{r^3}\right)\partial_t\vec{\tilde{\Omega}} = \frac{3Gm_2n_{g,\Omega}(\hat{r}\cdot\vec{v})\vec{\tilde{\Omega}}}{r^4} + \frac{9c_gG^2m_2^2}{r^7}\left(\hat{r}\times\vec{v} - r\vec{\tilde{\Omega}}\right). \tag{3.84}$$

Although we have restricted the spin to be aligned for simplicity, in principle any spin can be considered. Furthermore, these equations of motion are valid for any stellar object that can be described by an equation of state of matter, with the only difference on the values that the coefficients will take for different stellar types.

Chapter 4

The Binary Inspiral

4.1 The Effective Theory of Compact Objects

Using the coset construction [35, 86] in the framework of the EFT for extended objects [29, 30, 1], in the last chapter we have built the leading order effective action for charged spinning compact objects, taking into account for the stellar structure, such as polarizability, tides and dissipation. The key idea in modelling compact objects as an EFT is that we can treat them as point particles, with the properties and internal structure encoded in higher order operators allowed by the symmetries of the compact object.

In the proper frame, this is represented by the effective action

$$\mathcal{S}_{CO} = \int \mathrm{d}\tau \left\{ -mc^2 + \sum_n c_n \tilde{\mathcal{O}}_n \right\}, \tag{4.1}$$

with τ, the proper time, and where the first term describes a relativistic point particle with mass, m, and the second term, the sum over all possible higher order corrections. The tildes represents that the operators are in the proper frame The coefficients, c_n, are the Wilson coefficients of the effective theory that are to be matched from the full known theory, and ultimately from GW observations. The invariant operators, $\tilde{\mathcal{O}}_n$, are the higher order corrections that are allowed by the symmetries. These operators can be built from the covariant building blocks that are derived from the coset construction, by identifying the symmetry breaking pattern of a compact object. The sum is in principle infinite, and can be cut-off to the desired accuracy.

The effective action in eq. (4.1), is the one particle EFT in which the scale of the single compact object, determined by its radius, ℓ, has been removed. All the UV physics are encoded in the coefficients, $c_n = c_n(\ell)$, while the operators, $\tilde{\mathcal{O}} = \tilde{\mathcal{O}}(r)$, depend only on the orbital scale of the binary, r. Therefore, the terms in the effective action scale as powers of, ℓ/r, and in the non-relativistic limit, as powers of, v/c, with v, the relative velocity of the binary, from which we can obtain the PN order at which each of the terms enters into the dynamics. In last chapter, we have identified the coefficients from the literature [29, 30, 43, 41, 14, 63], which are used to obtain predictive results. Throughout this chapter we set $c = 1$, and when relevant we recover the c factor to stress the PN order.

4.1.1 The Effective Action

The effective action for charged spinning compact objects in eq. (3.61), has been constructed in the proper frame, for which the transformation rules to change to

the lab frame, have been derived as well. For the purpose of computing the PN expansion and expanding over the velocity, v, the action in the lab frame is needed. Therefore we start by pointing out the covariant building blocks and basic ingredients of the theory in the proper frame, and then transform to the lab frame.

The Proper Frame

In the proper frame of the particle, the effective action for the most general compact object allowed in an effective theory of gravity as general relativity with electrodynamics, from eq. (3.61), reads

$$\mathcal{S}_{eff} = \mathcal{S}_{CO} + \mathcal{S}_0, \tag{4.2}$$

with S_0, the interaction Einstein-Maxwell action,

$$\mathcal{S}_0 = \int \sqrt{-g}\, \mathrm{d}^4x \left\{ -\frac{1}{4\mu_0} F_{\mu\nu}F^{\mu\nu} + \frac{1}{16\pi G} R + \dots \right\}, \tag{4.3}$$

where $F_{\mu\nu} = \partial_\mu A_\nu - \partial_\nu A_\mu$, is the electromagnetic field tensor, and R, the Ricci scalar.

The worldline point particle for the compact object, S_{CO}, reads

$$\begin{aligned} \mathcal{S}_{CO} = \int \mathrm{d}\tau \Big\{ & -mc^2 + q\tilde{u}^a \tilde{A}_a + \frac{I}{4}\tilde{\Omega}_{ab}\tilde{\Omega}^{ab} + I\tilde{\Omega}_{ab}\tilde{a}^a \frac{\tilde{u}^b \tilde{u}_0}{\tilde{u}^2} \\ & + n_{q,\Omega}\tilde{\Omega}^a \tilde{E}_a + n_{g,\Omega}\tilde{\Omega}^a\tilde{\Omega}^b\tilde{E}_{ab} + n_q \tilde{E}^a \tilde{E}_a \\ & + n_g \tilde{E}^{ab}\tilde{E}_{ab} + \tilde{\mathcal{P}}^a \tilde{E}_a + \tilde{\mathcal{D}}^{ab}\tilde{E}_{ab} + \dots \Big\}, \end{aligned} \tag{4.4}$$

with, $\tilde{u}^a$, the velocity of the object, $\tilde{\Omega}_{ab}$, the relativistic angular velocity, and $\tilde{A}_a$, the gauge field of electromagnetism. The electric like parity tensors, $\tilde{E}_a$ and $\tilde{E}_{ab}$, correspond to the electromagnetic dipolar and gravitational quadrupolar moment respectively. The composite operators, $\tilde{\mathcal{P}}^a$ and $\tilde{\mathcal{D}}^{ab}$, encode the dissipative degrees of freedom. The action describing the compact object, lives in the worldline, while the underlying theory, eq. (4.3), lives in the bulk.

The first three terms of eq. (4.4) describes the LO correction of a charged spinning point particle, with mass, m, charge, q, moment of inertia I, and angular velocity, $\tilde{\Omega}^{ab}$. The fourth term is a higher order correction to the spin which is necessary for a correct description of the dynamics at the order that we consider. The first term in the second line is a spin correction due to the electromagnetic coupling, while the second term is a spin correction due to gravity. The last term of the second line corresponds to the coupling between electromagnetism and the ensuing dipole, while the first term in the last line corresponds to the coupling between gravity and the ensuing quadrupole. The last two terms couple the degrees of freedom which are responsible for the electromagnetic and gravitational dissipation during an interaction.

All the terms from the second and third line, encode the fact that a compact object is not truly a point particle, and therefore are finite-size corrections [29, 30]. We refer to the size effects due to gravity as tidal effects, while for the ones due to electromagnetism, we refer as polarization effects. The internal structure of the compact object is encoded in the coefficients of the theory, n_q, n_g, $n_{q,\Omega}$ and $n_{g,\Omega}$, and the coefficients, c_q and c_g, which come from the operators that encode the dissipative

effects. The explicit expressions of the operators due to dissipative effects can be obtained using the in-in formalism [90]. These coefficients, as well as the ones from the corrections from the first line, $n_\Omega = I/4$ and $n_{\Omega,a} = I$, have been identified in Chapter 3.

The explicit expressions of the covariant building blocks included in the effective action reads

$$\tilde{u}^a = \partial_\tau x^a, \tag{4.5}$$
$$\tilde{A}^a = \Lambda_b{}^a A^b = \Lambda_b{}^a e_\mu{}^b A^\mu, \tag{4.6}$$
$$\tilde{a}^a = \partial_\tau \tilde{u}^a + \tilde{u}^\mu \omega_\mu{}^{ab} \tilde{u}_b \tag{4.7}$$
$$\tilde{\Omega}^{ab} = \Lambda_c{}^a (\eta^{cd}\partial_\tau + \tilde{u}^\mu \omega_\mu{}^{cd}) \Lambda_d{}^b, \tag{4.8}$$
$$\tilde{E}^a = \tilde{F}^{ab}\tilde{u}_b, \tag{4.9}$$
$$\tilde{E}^{ab} = \tilde{W}^{acbd}\tilde{u}_c\tilde{u}_d, \tag{4.10}$$
$$\tilde{P}^a = ic_q \dot{\tilde{E}}^a, \tag{4.11}$$
$$\tilde{\mathcal{D}}^{ab} = ic_g \dot{\tilde{E}}^{ab}, \tag{4.12}$$

with A_μ, being invariant under the gauge transformation, $A_\mu \to A_\mu + \partial_\mu \xi$, and $\tilde{\Omega}^{0i} = \tilde{a}^i = 0$, by definition. The relativistic angular velocity can be expressed in terms of the epsilon tensor, $\tilde{\Omega}_{ab} = \epsilon_{abc}\tilde{\Omega}^c$. The Lorentz matrices, $\Lambda_a{}^b = B_a{}^c(\beta^i)\mathcal{R}_c{}^b(\theta^i)$, are parameterized by the product of a boost and a rotation matrix, with β^i, the velocity as a function of the rapidity, and θ^i, the Euler angles that describe the orientation of the compact object [1].

The field, e^a_μ, is the vierbein from the tetrad formalism, which defines the metric as, $g_{\mu\nu} = \eta_{ab}e^a_\mu e^b_\nu$, and used to change from the local to the general orthogonal frame, i.e. $V_\mu = e_\mu{}^b V_b$, and vice versa. The spin connection, ω^{ab}_μ, is defined in terms of the vierbein field [1],

$$\omega^{ab}_\mu(e) = \frac{1}{2}\left\{e^{\nu a}(\partial_\mu e_\nu{}^b - \partial_\nu e_\mu{}^b) + e_{\mu c}e^{\nu a}e^{\lambda b}\partial_\lambda e_\nu{}^c - (a \leftrightarrow b)\right\}, \tag{4.13}$$

for the theory of General Relativity. The Christoffel symbol in terms of the vierbein and the spin connection is identified,

$$\Gamma^a_{\mu\nu} = \partial_\mu e_\nu{}^a + e_{\mu b}\omega_\nu^{ab}, \tag{4.14}$$

from which one can recover the space-time Christoffel symbol, $\Gamma^\sigma_{\mu\nu} = e^\sigma_a \Gamma^a_{\mu\nu}$, or obtain the spin connection in terms of the Christoffel symbol.

The electric parity tensors in the proper frame, $\tilde{E}_a$ and $\tilde{E}_{ab}$, for the electromagnetic and gravitational case, depend on the electromagnetic strength field tensor $\tilde{F}_{ab}$, and on the Weyl tensor, $\tilde{W}_{abcd}$, respectively. The dissipative operators in eqs. (4.11) and (4.12), are the in-in expectation values at the initial state of the internal degrees of freedom, which are defined through the in-in path integral [90], and which are in general a function of the building blocks, $\tilde{E}^a$ and $\tilde{E}^{ab}$, respectively [30, 42]. The dot denotes derivative with respect to τ. The dissipative degrees of freedom are encoded in the imaginary part of the action.

The Lab Frame

In our effective theory, the position of the particle, x^μ, is not affected by the local Poincaré group, but it is transformed under diffeomorphisms [1]. To transform the rest of the building blocks from the proper frame to the lab frame, we use the Lorentz matrices, $\Lambda^a{}_b = B^a{}_c(\beta^i)\mathcal{R}^c{}_b(\theta^i)$. The covariant building blocks in the lab frame are given by

$$
\begin{aligned}
v^a &= \partial_t x^a, && (4.15)\\
A^a &= \Lambda^a{}_b \tilde{A}^b, && (4.16)\\
a^a &= \Lambda^a{}_b \tilde{a}^b = (\partial_\tau v^a + v^\mu \omega_\mu{}^{ab} v_b) && (4.17)\\
\Omega^{ab} &= \Lambda^a{}_c \Lambda^b{}_d \tilde{\Omega}^{cd} = \Lambda_c{}^a \partial_t \Lambda^{cb} + v^\mu \omega_\mu{}^{ab}, && (4.18)\\
E^a &= \Lambda^a{}_b \tilde{E}^b = F^{ac} v_c, && (4.19)\\
E^{ab} &= \Lambda^a{}_c \Lambda^b{}_d \tilde{E}^{cd} = W^{acbd} v_c v_d, && (4.20)\\
\mathcal{P}^a &= \Lambda^a{}_b \tilde{\mathcal{P}}^b, && (4.21)\\
\mathcal{D}^{ab} &= \Lambda^a{}_c \Lambda^b{}_d \tilde{\mathcal{D}}^{cd}, && (4.22)\\
& && (4.23)
\end{aligned}
$$

with t, the time measured by the observer, and the dot denotes derivative with respect to t. Given the usual notation of the PN expansion, we have denoted the velocity, $\dot{x}^a = v^a$, with $v^0 = 1$. Having transformed the covariant quantities, the worldline action that describes the compact object in the lab frame now reads,

$$
\begin{aligned}
\mathcal{S}_{CO} = \int \mathrm{d}t \Big\{ & -m + q A_a v^a + \frac{I}{4}\Omega_{ab}\Omega^{ab} + I\Omega_{ab}\frac{a^a v^b}{v^2} \\
& + n_{q,\Omega}\Omega_a E^a + n_{g,\Omega}\Omega_a\Omega_b E^{ab} + n_q E_a E^a \\
& + n_g E_{ab} E^{ab} + E_a \Lambda^a{}_b \tilde{\mathcal{P}}^b + E_{ab}\Lambda^a{}_c\Lambda^b{}_d\tilde{\mathcal{D}}^{cd} + \ldots \Big\}.
\end{aligned} \tag{4.24}
$$

To reproduce the well known results in the current literature on the PN expansion for spinning objects, it is necessary to introduce the relativistic spin degree of freedom [43, 41, 17],

$$
S^{ab} = 2\frac{\partial \mathcal{L}}{\partial \Omega_{ab}}, \tag{4.25}
$$

which is the conjugate variable of the angular velocity. Then, by Legendre transforming the Lagrangian that describes the compact object, we obtain

$$
\mathcal{L}_{CO} = -m + \frac{1}{2}S_{ab}\Omega^{ab} + \ldots = -m + \frac{I}{2}S_{ab}(\Lambda^a{}_c \partial_\tau \Lambda^{cb} + \partial_t x^\mu \omega_\mu^{ab}), \tag{4.26}
$$

where we have inserted the explicit expression of the angular velocity, eq. (4.18). This is the minimal spin coupling, and the ellipses denote the rest of the terms, which are taken into account when obtaining the PN expansion. The spin minimal coupling correction, eq. (4.26), is equivalent to the one in [41, 80].

4.2 Binary Inspiral

The effective action, eq. (4.24), describes the EFT of a single compact object, with their coefficients, $n(\ell)$, encoding the internal structure. For a compact object, $\ell \sim Gm$. To describe a binary system, we construct the effective action

$$\mathcal{S}_{eff} = \mathcal{S}_0 + \sum_{n=1}^{2} \mathcal{S}_{CO}, \tag{4.27}$$

where the first term, $\mathcal{S}_0 = \mathcal{S}_g + \mathcal{S}_q$, is the Einstein-Maxwell action in eq. (4.3), and the second term is the action describing each of the compact objects that form the binary system, with $\mathcal{S}_{CO}$ the worldline point particle action, eq. (4.24). The operators that appear in $\mathcal{S}_{CO}$, depend only on the scale of the binary, r, the orbital separation between the two compact objects. At the scale of the inspiraling binary, which is bound gravitationally, the virial theorem holds, $Gm/r \sim v^2$ [29]. Therefore, we encounter the first hierarchy of scales, $\ell \ll r$.

The gravitationally bound system composed of compact objects, will shrink its orbit due to the loss of energy and momentum through gravitational wave radiation, whose frequency is fixed by the orbital frequency of the binary, ω_s. The emitted radiation is ultimately observed by our GW detectors, which implies that these radiation modes are on shell, satisfying the momentum relation, $k_0 = |\vec{k}|$, for its four momentum vector, $k = (k_0, \vec{k})$. This is in contrast to the modes that mediate the gravitational interaction, which are off-shell and therefore its momentum, $k_0 \neq |\vec{k}|$. Therefore, we can establish the next hierarchy, $r \ll \lambda$, with λ the wavelength of radiation, scaling as $\lambda \sim 1/\omega_s \sim r/v$. Thus, an inspiraling binary made up of compact objects, satisfies the hierarchy of scales [29],

$$\ell \ll r \ll \lambda. \tag{4.28}$$

Given this hierarchy, we expand the gravitational field around flat spacetime [29],

$$g_{\mu\nu} = \eta_{\mu\nu} + H_{\mu\nu} + h_{\mu\nu}, \tag{4.29}$$

where $H_{\mu\nu}$, are the potential modes that mediate the interaction between the two objects, and $h_{\mu\nu}$, the radiation modes, which are finally observed by the GW detectors. The latter modes are on-shell, while the former ones are off-shell, which imply that its components scale as [29]

$$\partial_t H_{\mu\nu} \sim \frac{v}{r} H_{\mu\nu}, \qquad \partial_i H_{\mu\nu} \sim \frac{1}{r} H_{\mu\nu}, \tag{4.30}$$

$$h_{\mu\nu} \sim \frac{v}{r} h_{\mu\nu}. \tag{4.31}$$

To obtain the conservative dynamics of the binary system, we are interested in integrating out the orbital modes.

The photon field, A_μ, is decomposed analogously to the gravitational field. It is separated into [63]

$$A_\mu = \mathbf{A}_\mu + \bar{A}_\mu, \tag{4.32}$$

with $\bar{A}_\mu$, the radiation modes, and $\mathbf{A}_\mu$, the potential modes that mediate the interaction. Their scaling is equivalent to the ones in eq. (4.30) and (4.31), for each mode respectively,

$$\partial_t \mathbf{A}_\mu \sim \frac{v}{r}\mathbf{A}_\mu, \qquad \partial_i \mathbf{A}_\mu \sim \frac{1}{r}\mathbf{A}_\mu, \tag{4.33}$$

$$\bar{A}_\mu \sim \frac{v}{r}\bar{A}_\mu. \tag{4.34}$$

Therefore, the conservative dynamics of the interaction of a binary composed of charged spinning compact objects, is obtained in a diagrammatic approach by integrating out the potential modes of the gravitational and electromagnetic field, which removes the orbital scale of the binary. The procedure of integrating out the orbital scale, is defined by the functional integral

$$e^{i\mathcal{S}_{bin}} = \int DH_{\mu\nu} D\mathbf{A}_\mu e^{i\mathcal{S}_{eff}}, \tag{4.35}$$

with, $\mathcal{S}_{eff}$, the action defined in eq. (4.27). The action, $\mathcal{S}_{bin}$, describes the conservative dynamics of the binary system. In this interaction, only tree diagrams contribute to the dynamics, given that these objects are described classically, and that any quantum effects [101, 102], at least during the inspiral, can be neglected. After integrating out the orbital modes, the effective theory of the binary system will be given by the action,

$$\mathcal{S}_{bin} = \mathcal{S}_0(\eta_{\mu\nu} + h_{\mu\nu}, \bar{A}_\mu) + \sum_{n=1}^{2} \mathcal{S}_{CO}(\eta_{\mu\nu} + h_{\mu\nu}, \bar{A}_\mu). \tag{4.36}$$

4.3 The Post-Newtonian Expansion

In this thesis, rather than obtaining high order PN corrections, we show the predictivity of the theory by recovering well known results. We derive new results on the finite-size structure of charged spinning compact objects. The computation of higher order PN corrections for such objects will be approached elsewhere.

In this section we will be as explicit as possible on the derivation of the Feynman rules and the computation of the Feynman diagrams, to provide a step-by-step description of a binary system composed of compact objects. For a thorough review on the PN expansion we refer the reader to [80, 81]. The code EFTofPNG package [103] for computing the post-Newtonian expansion, was extensively used to cross check results.

4.3.1 Non-relativistic General Relativity

In the non-relativistic regime of gravity [29], the time dimension can be regarded as compact in comparison to the spatial dimensions [62]. Thus, we switch to a Kaluza-Klein (KK) parameterization, with the metric [62],

$$g_{\mu\nu}\mathrm{d}x^\mu \mathrm{d}x^\nu \equiv -e^{2\phi}(\mathrm{d}t - \mathcal{A}_i \mathrm{d}x^i)^2 + e^{-2\phi}\gamma_{ij}\mathrm{d}x^i\mathrm{d}x^j, \tag{4.37}$$

which defines the KK or non-relativistic fields: ϕ, the Newtonian scalar, $\mathcal{A}_i$, the gravitomagnetic vector of the KK parameterization, and $\gamma_{ij} \equiv \delta_{ij} + \sigma_{ij}$, the tensor field with, $\gamma^{ij}\gamma_{jk} \equiv \delta^i_k$ and $\mathcal{A}^i \equiv \gamma^{ij}\mathcal{A}_j$. The matrix form of the metric is given by,

$$g_{\mu\nu} = \begin{pmatrix} -e^{2\phi} & e^{2\phi}\mathcal{A}_j \\ e^{2\phi}\mathcal{A}_i & e^{-2\phi}\gamma_{ij} - e^{2\phi}\mathcal{A}_i\mathcal{A}_j \end{pmatrix}. \tag{4.38}$$

From eq. (4.38), the vierbein in the KK parameterization can be read off. As pointed out in [41], the vierbein can be gauge fixed using the time gauge of Schwinger [104], which fixes the time axes of the local coordinate system to the one of the general coordinate frame. In equations, we fix e^a_0, and choose a local frame in which their spatial components are zero,

$$e^i_0 = 0. \tag{4.39}$$

Using this constraint, altogether with eq. (4.38), and $g_{\mu\nu} = \eta_{ab}e^a_\mu e^b_\nu$, the vierbein reads [41]

$$e^{\ a}_{\mu} = \begin{pmatrix} e^{\phi} & -e^{\phi}\mathcal{A}_i \\ 0 & e^{-\phi}\sqrt{\gamma}_{ij} \end{pmatrix}, \tag{4.40}$$

which completely fixes the redundant degrees of freedom.

To extract the Feynman rules and obtain the propagators of the theory, we need to fix the gauge of the interaction action, $\mathcal{S}_0$, to remove the physically equivalent field configurations. For the gravitational action, $\mathcal{S}_g$, we choose the harmonic gauge [29]

$$\mathcal{S}_g = \mathcal{S}_{EH} + \mathcal{S}_{GF,g} = \frac{1}{16\pi}\int \mathrm{d}^4x\sqrt{-g}R - \frac{1}{32\pi G}\int \mathrm{d}^4x\sqrt{-g}g_{\mu\nu}\Gamma^\mu\Gamma^\nu, \tag{4.41}$$

with $\Gamma^\mu \equiv \Gamma^\mu_{\rho\sigma}g^{\rho\sigma}$. Then, by parametrizing $\mathcal{S}_g$ in a KK fashion, the gravitational action can be cast as [62]

$$\mathcal{S}_g = \frac{1}{16\pi G}\int \mathrm{d}t\mathrm{d}^3x\sqrt{\gamma}\left(R[\gamma] - 2\partial_i\phi\partial^i\phi + \frac{1}{4}e^{4\phi}\mathcal{F}^2\right), \tag{4.42}$$

with $\partial_i\partial^i\phi = \gamma^{ij}\partial_i\phi\partial_j\phi$, and where we have defined the analog of the field strength tensor, F_{ab}, but in terms of the KK gravitomagnetic tensor, $\mathcal{A}_i$, such that, $\mathcal{F}_{ij} = \partial_i\mathcal{A}_j - \partial_j\mathcal{A}_i$.

On the action for the photon field,

$$\mathcal{S}_q = \mathcal{S}_M + \mathcal{S}_{GF,q} = -\frac{1}{\mu_0}\int \mathrm{d}^4x\sqrt{-g}\left(\frac{1}{4}F^2 + \frac{1}{2\xi}(\partial_\mu A^\mu)^2\right), \tag{4.43}$$

we choose the Feynman-'tHooft gauge, which implies $\xi = 1$.

4.3.2 The Feynman Rules

We start by extracting the propagators of the effective theory. From the gravitational action in the KK decomposition, eq. (4.42), the propagators can be read off from the terms that are quadratic in the fields. The non-relativistic field propagators in the harmonic gauge reads [62]

$$\text{———} = \langle \phi(x_1)\phi(x_2)\rangle = 4\pi G\,\delta(t_1-t_2)\int \frac{\mathrm{d}^3\vec{k}}{(2\pi)^3}\frac{e^{i\vec{k}\cdot\vec{r}}}{\vec{k}^2}, \tag{4.44}$$

$$\text{- - - - - - - -} = \langle \mathcal{A}_i(x_1)\mathcal{A}_j(x_2)\rangle = -16\pi G\,\delta(t_1-t_2)\int \frac{\mathrm{d}^3\vec{k}}{(2\pi)^3}\frac{e^{i\vec{k}\cdot\vec{r}}}{\vec{k}^2}\delta_{ij}, \tag{4.45}$$

$$\text{═══} = \langle \sigma_{ij}(x_1)\sigma_{kl}(x_2)\rangle = 32\pi G\,\delta(t_1-t_2)\int \frac{\mathrm{d}^3\vec{k}}{(2\pi)^3}\frac{e^{i\vec{k}\cdot\vec{r}}}{\vec{k}^2}P_{ij;kl}, \tag{4.46}$$

with $P_{ij;kl} = \frac{1}{2}(\delta_{ik}\delta_{jl}+\delta_{il}\delta_{jk}-2\delta_{ij}\delta_{kl})$. We have used the scaling of the orbital modes, $k_0 \simeq v/r$ and $|\vec{k}| \simeq 1/r$, and expanded over, $k_0^2/\vec{k}^2 \sim v^2$, such that

$$\int \frac{\mathrm{d}^4k}{(2\pi)^4}e^{-i\vec{k}\cdot\vec{r}}\frac{1}{k^2} = \int \frac{\mathrm{d}k_0}{2\pi}\frac{\mathrm{d}^3\vec{k}}{(2\pi)^3}e^{-ik_0}\frac{e^{i\vec{k}\cdot\vec{r}}}{\vec{k}^2}\left(1+\frac{k_0^2}{\vec{k}^2}+\ldots\right) = \delta(t)\int \frac{\mathrm{d}^3k}{(2\pi)^3}\frac{e^{i\vec{k}\cdot\vec{r}}}{\vec{k}^2}+\ldots, \tag{4.47}$$

and therefore the propagator is instantaneous, with the relativistic time corrections to the propagator being considered as quadratic perturbations [29].

The propagators obtained in the KK parameterization have a simple form, in which the fields, ϕ and $\mathcal{A}_i$, dominates the interaction. The time relativistic corrections can be read from eq. (4.44) and (4.47),

$$\text{———}\times\text{———} = 4\pi G\,\frac{\mathrm{d}}{\mathrm{d}t_1\mathrm{d}t_2}\delta(t_1-t_2)\int \frac{\mathrm{d}^3\vec{k}}{(2\pi)^3}\frac{e^{i\vec{k}\cdot\vec{r}}}{\vec{k}^4}. \tag{4.48}$$

From the electromagnetic interaction action in a non-relativistic parameterization, the propagators can be read off from the quadratic terms as well. We separate the time dimension of the photon field from the spatial ones, such that the propagators reads

$$= \langle A_0(x_1)A_0(x_2)\rangle = -\mu_0\,\delta(t_1-t_2)\int \frac{\mathrm{d}^3\vec{k}}{(2\pi)^3}\frac{e^{i\vec{k}\cdot\vec{r}}}{\vec{k}^2}, \tag{4.49}$$

$$= \langle A_i(x_1)A_j(x_2)\rangle = \mu_0\,\delta(t_1-t_2)\int \frac{\mathrm{d}^3\vec{k}}{(2\pi)^3}\frac{e^{i\vec{k}\cdot\vec{r}}}{\vec{k}^2}\delta_{ij}. \tag{4.50}$$

The time relativistic correction,

$$= -\mu_0\,\frac{\mathrm{d}}{\mathrm{d}t_1\mathrm{d}t_2}\delta(t_1-t_2)\int \frac{\mathrm{d}^3\vec{k}}{(2\pi)^3}\frac{e^{i\vec{k}\cdot\vec{r}}}{\vec{k}^4}. \tag{4.51}$$

Having derived the relevant propagators, we express the worldline action of the binary system in terms of the non-relativistic fields, from which we can read off the vertices. We do so by considering term by term from the action in eq. (4.24).

Point Particles

We start by expressing the mass coupling, from the worldline point particle in eq. (4.24), in terms of the non-relativistic fields [62]

$$\mathcal{S}_{pp} = -m\int \mathrm{d}t\sqrt{-g_{\mu\nu}\frac{\mathrm{d}x^\mu}{\mathrm{d}t}\frac{\mathrm{d}x^\nu}{\mathrm{d}t}} = -m\int \mathrm{d}t\left\{e^{\phi}\sqrt{-(1-\mathcal{A}_i v^i)^2 + e^{-4\phi}\gamma_{ij}v^i v^j}\right\}, \tag{4.52}$$

which is then expanded in the velocity and the KK fields,

$$\mathcal{S}_{pp} = -m\int \mathrm{d}t\left(1-\frac{1}{2}v^2+\phi-\mathcal{A}_i v^i-\frac{1}{8}v^4+\frac{3}{2}\phi v^2+\frac{1}{2}\phi^2-\frac{1}{2}v^i v^j\sigma_{ij}+\ldots\right). \tag{4.53}$$

The ellipses denotes higher order corrections.

From the last expression we can extract the vertex for the one graviton coupling to the worldline mass,

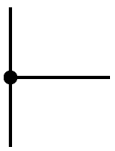

$$= -m\int \mathrm{d}t\phi\left\{1+\frac{3}{2}v^2+O(v^4)\right\}, \tag{4.54}$$

(4.55)

where the bold vertical line represents the worldline of the compact object, the black dot represents the mass coupling and the horizontal line the scalar propagator.

Higher order corrections are obtained from the mass coupling vertex with the vector propagator,

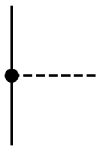

$$= m \int \mathrm{d}t \mathcal{A}_i v^i \left(1 + O(v^2)\right). \tag{4.56}$$

The mass coupling vertex containing the tensor propagator, σ_{ij}, can be read from eq. (4.53) as well, $\propto v^i v^j \sigma_{ij}$, but will not be necessary for the computations of this work. Then we extract the two graviton exchange,

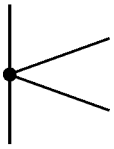

$$= -\frac{1}{2} m \int \mathrm{d}t \phi^2 \left(1 + O(v^2)\right). \tag{4.57}$$

We have extracted the necessary pieces only required for the computations of this work. Nevertheless, higher order PN corrections to the point mass coupling can be obtained by extracting higher order corrections from the worldline point particle action.

Spinning Particles

We have cast the minimal spin coupling Lagrangian in a suitable form for the PN expansion in eq. (4.26). In order to extract the correct vertices, it is necessary to take into account the higher order spin correction, $\propto S_{ab} v^a a^b$ [41]. This term arises by Legendre transforming eq. (4.24), to express it in terms of the spin, such that the relevant corrections reads

$$\mathcal{L}_S = \frac{1}{2} S_{ab} \left(\Omega^{ab} + \frac{a^a v^b}{v^2} \right) = \frac{I}{2} S_{ab} \left(v^\mu \omega_\mu^{\ ab} + 2(\partial_\tau v^a + v^\mu \omega_\mu^{\ ac} v_c) \frac{v^b}{v^2} \right), \tag{4.58}$$

where we have neglected the term, $\propto \Omega \Lambda \partial_t \Lambda$, given that it does not contribute to the dynamics.

Before parametrizing the spin Lagrangian in terms of the KK fields, we recall the spin condition of our effective theory,

$$\sqrt{v^2} S^{0b} + v_i S^{ib} = 0, \tag{4.59}$$

which implies the expansion [71]

$$S^{0i} = \frac{1}{2} S^{ji} v_j + \frac{1}{4} \Omega^{ji} \mathcal{A}_j + O(v^4), \tag{4.60}$$

suppressing the temporal spin components with respect to the spatial ones by at least an order of v.

The vertices can be obtained by expressing the spin connection in eq. (4.58), in terms of the vierbein and the Christoffel symbol using eq. (4.14). Then, by implementing the spin condition, eq. (4.60), one obtains the expected spin couplings [81]

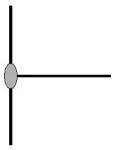

$$= \int \mathrm{d}t \epsilon_{ijk} S^k v^i \left(2\partial^j \phi + v^2 \partial^j \phi + \dots\right), \tag{4.61}$$

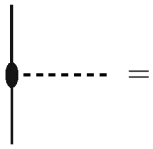

$$= \int \mathrm{d}t \epsilon_{ijk} S^k \left(\frac{1}{2}\partial^i \mathcal{A}^j + \frac{3}{4} v^i v^l (\partial_l \mathcal{A}^j - \mathcal{A}^j \partial_l) + v^i \partial_t \mathcal{A}^j + \dots\right), \tag{4.62}$$

as well as for the spin coupling with tensor propagator, which we do not show here.

Size Effects

There are two gravitational, electric parity, leading order corrections to consider due to the finite-size structure of a spinning compact object, one of which is induced by the spin, and the other which is a contribution for any extended object, even if it is not rotating. The vertices encoding the finite size effects, can be extracted from

$$\mathcal{L}_W = n_{g,\Omega} S^a S^b E_{ab} + n_g E^{ab} E_{ab}. \tag{4.63}$$

Therefore, by parametrizing eq. (4.63) in a KK parameterization, we extract the spin-size coupling

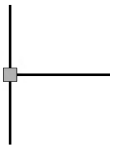

$$= \int \mathrm{d}t \frac{n_{g,\Omega}}{2} S^i S^j \partial_i \partial_j \phi + \dots, \tag{4.64}$$

and the two scalar size coupling,

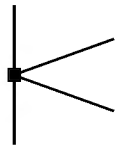

$$= \int \mathrm{d}t \frac{n_g}{4} \partial^i \partial^j \phi \partial_i \partial_j \phi + \dots. \tag{4.65}$$

The coefficients, $n_{g,\Omega}$ and n_g, encode the internal structure of the object.

Charged Particles

From the worldline action,

$$\mathcal{S}_q = \int \mathrm{d}t q v^a A_a = -\int \mathrm{d}t q A_0 + \int \mathrm{d}t q v^i A_i, \tag{4.66}$$

parameterized in the non-relativistic parameterization, the vertices for the photon coupling to the worldline charge can be extracted,

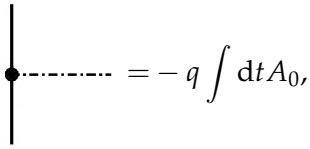

$$= -q \int \mathrm{d}t A_0, \tag{4.67}$$

and

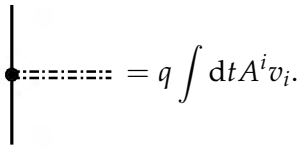

$$= q \int \mathrm{d}t A^i v_i. \tag{4.68}$$

Polarizability

An external electromagnetic field in an extended object generates size effects as well, which we will refer as the polarization. The polarizability is encoded in the terms of the worldline action that are made up of the the electromagnetic tensor,

$$\mathcal{L}_F = n_{q,\Omega} S^a B_a + n_q E^a E_a + \ldots, \tag{4.69}$$

which are invariant under time reversibility. There is a term $\propto B^a B_a$ in the ellipses, but we have neglected to keep the discussion short. We obtain the scalar spin-polarization coupling

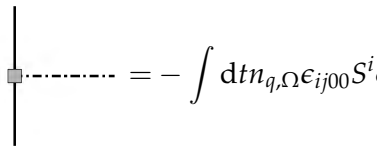

$$= -\int \mathrm{d}t n_{q,\Omega} \epsilon_{ij00} S^i \partial^j A^0, \tag{4.70}$$

while the two scalar polarization vertex,

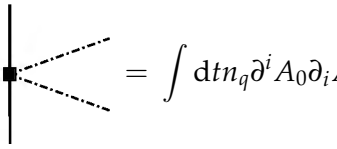

$$= \int \mathrm{d}t n_q \partial^i A_0 \partial_i A^0. \tag{4.71}$$

Just as in the gravitational case, the coefficients $n_{q,\Omega}$ and n_q, encode the internal structure of the compact object.

Dissipation

The vertices encoding the dissipative effects, can be obtained from the Lagrangian,

$$\mathcal{L}_{\mathcal{P},\mathcal{D}} = E_a \Lambda^a{}_b \tilde{\mathcal{P}}^b + E_{ab} \Lambda^a{}_c \Lambda^b{}_d \tilde{\mathcal{D}}^{cd} = i c_q E_a \frac{\mathrm{d}}{\mathrm{d}t} \Lambda^a{}_b \tilde{E}^b + i c_g E_{ab} \frac{\mathrm{d}}{\mathrm{d}t} \Lambda^a{}_c \Lambda^b{}_d \tilde{E}^{cd}. \quad (4.72)$$

With the purpose of recovering the LO known results for a slowly rotating object [46], we promote the partial derivative in eq. (4.72) to be covariant, such that

$$\frac{\mathrm{D}}{\mathrm{D}t} \Lambda_c{}^a \Lambda_d{}^b \tilde{E}^{cd} = \left(2 \Lambda_c{}^a \frac{\mathrm{D}}{\mathrm{D}t} \Lambda_d{}^b \tilde{E}^{cd} + \Lambda_c{}^a \Lambda_d{}^b \frac{\mathrm{D}}{\mathrm{D}t} \tilde{E}^{ab} \right) \quad (4.73)$$

$$= \left(2 E^a{}_c \epsilon^{bcd} \Omega_d + \dot{E}^{ab} + \ldots \right). \quad (4.74)$$

Therefore, for the gravitational case, there are two LO vertices contributing to the dynamics, the two scalar vertex due to dissipation,

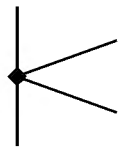

$$= i \frac{c_g}{4} \int \mathrm{d}t \partial_i \partial_j \phi \partial^i \partial^j \dot{\phi}, \quad (4.75)$$

and the two scalar spin dissipative coupling,

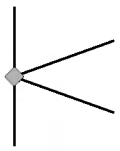

$$= i \frac{c_{g,\Omega}}{2} \int \mathrm{d}t \partial_i \partial_j \phi \partial^i \partial_k \phi \epsilon^{jkl} S_l. \quad (4.76)$$

On the electromagnetic side, a spin dissipative part is not generated in the LO correction. Therefore, the only vertex to be considered, reads

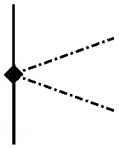

$$= i c_q \int \mathrm{d}t \partial_i A_0 \partial^i \dot{A}_0. \quad (4.77)$$

4.3.3 Dynamics of Compact Objects

In this section we show the computation of the Feynman diagrams relevant to obtain some of the very well known results for the PN expansion, and to derive new LO PN corrections on charged spinning compact objects. The higher order PN expansion is left for a future work. Although throughout most of the work we have worked with units $c = 1$, when showing the final Lagrangian or diagram due to each effect, we will include the c, in order to stress the PN order at which the effect enters into the dynamics. Finally, we point out that in the computation of the diagrams, we connect two vertices with a, $\times$ symbol, i.e.

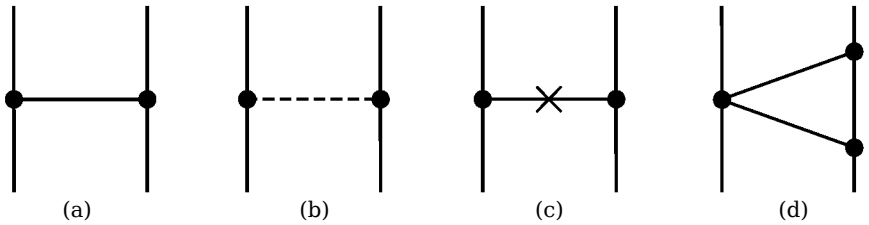

FIGURE 4.1: Feynman diagrams to obtain the 0 and 1 PN corrections to the dynamics, from which the Newtonian and the Einstein-Infeld-Hoffman Lagrangian are derived.

$$\int \mathrm{d}t_1 \overbrace{\phi(x_1) \times \int \mathrm{d}t_2 \phi(x_2)} = 4\pi G \int \mathrm{d}t_1 \mathrm{d}t_2 \delta(t_1 - t_2) \int \frac{\mathrm{d}^3\vec{k}}{(2\pi)^3} \frac{e^{i\vec{k}\cdot\vec{r}}}{\vec{k}^2},$$

meaning that the relevant propagator is to be inserted. The time relativistic propagator is denoted as $\times|_t$.

The Newtonian Potential

The simplest example is the Newtonian potential, which is contained in the diagram (a) of figure 4.1, by neglecting the corrections due to velocity in eq. (4.55). Therefore the diagram reads

$$\begin{aligned} \text{Figure } 4.1(\text{a}) &= m_1 \int \mathrm{d}t_1 \phi(x_1) \times m_2 \int \mathrm{d}t_2 \phi(x_2) \\ &= 4\pi G m_1 m_2 \int \mathrm{d}t_1 \mathrm{d}t_2 \delta(t_1 - t_2) \int \frac{\mathrm{d}\vec{k}^3}{(2\pi)^3} \frac{e^{i\vec{k}\cdot\vec{r}}}{\vec{k}^2} = \int \mathrm{d}t \frac{G m_1 m_2}{r}, \end{aligned} \tag{4.78}$$

with $r = |\vec{x}_1 - \vec{x}_2|$, and where we have used

$$\int \frac{\mathrm{d}\vec{k}^3}{(2\pi)^3} \frac{e^{i\vec{k}\cdot\vec{r}}}{\vec{k}^2} = \frac{1}{4\pi} \frac{1}{r}. \tag{4.79}$$

The Newtonian correction, eq. (4.78), is a 0 PN correction.

The Einstein-Infeld-Hoffman Correction

The 1 PN correction, known as the Einstein-Infeld-Hoffman correction [67], in the KK parameterization is encoded in the diagrams of figure 4.1. For the diagram (a), by considering the velocity corrections in eq. (4.55), up to order v^2, the diagram reads

$$\begin{aligned}\text{Figure } 4.1(\text{a}) &= m_1 \int \mathrm{d}t_1 \phi(x_1) \left(1 + \frac{3}{2} v_1^2\right) \times m_2 \int \mathrm{d}t_2 \phi(x_2) \left(1 + \frac{3}{2} v_2^2\right) \\ &= 4\pi G m_1 m_2 \int \mathrm{d}t_1 \mathrm{d}t_2 \delta(t_1 - t_2) \int_{\vec{k}} \frac{e^{i\vec{k}\cdot\vec{r}}}{\vec{k}^2} \left(1 + \frac{3}{2}(v_1^2 + v_2^2) + \ \ldots\right) \\ &= \int \mathrm{d}t \frac{G m_1 m_2}{r} \left(1 + \frac{3}{2}(v_1^2 + v_2^2)\right).\end{aligned} \tag{4.80}$$

The next diagram with the dotted propagator, yields

$$\begin{aligned}\text{Figure } 4.1(\text{b}) &= m_1 \int \mathrm{d}t_1 \mathcal{A}_i(x_1) v_1^i \times m_2 \int \mathrm{d}t_2 \mathcal{A}_j(x_2) v_2^j \\ &= -\int \mathrm{d}t \frac{4 G m_1 m_2}{r} \delta_{ij} v_1^i v_2^j = -\int \mathrm{d}t \frac{4 G m_1 m_2}{r} (\vec{v}_1 \cdot \vec{v}_2).\end{aligned} \tag{4.81}$$

Then, we obtain the diagram with the time relativistic correction

$$\begin{aligned}\text{Figure } 4.1(\text{c}) &= m_1 \int \mathrm{d}t_1 \phi(x_1) \times |_t \, m_2 \int \mathrm{d}t_2 \phi(x_2) \\ &= 4\pi G m_1 m_2 \int \mathrm{d}t_1 \int \mathrm{d}t_2 \frac{\mathrm{d}}{\mathrm{d}t_1 \mathrm{d}t_2} \delta(t_1 - t_2) \int \frac{\mathrm{d}\vec{k}^3}{(2\pi)^3} \frac{e^{\vec{k}\cdot\vec{r}}}{(k^2)^2} \\ &= \int \mathrm{d}t \frac{1}{2} \frac{G m_1 m_2}{r} \left(\vec{v}_1 \cdot \vec{v}_2 - \frac{(\vec{v}_1 \cdot \vec{r})(\vec{v}_2 \cdot \vec{r})}{r^2}\right),\end{aligned} \tag{4.82}$$

where we have used [80]

$$\int \frac{\mathrm{d}\vec{k}^3}{(2\pi)^3} \frac{k^i k^j}{\vec{k}^4} e^{i\vec{k}\cdot\vec{r}} = \frac{1}{8\pi r^3} \left(r^2 \delta^{ij} - r^i r^j\right). \tag{4.83}$$

Finally, we compute the last diagram which is a non-linear static contribution,

$$\begin{aligned}\text{Figure } 4.1(\text{d}) &= -\frac{1}{2} m_1 \int \mathrm{d}t_1 \phi_1^2 \times m_2^2 \int \mathrm{d}t_2 \phi_2 \phi_2 \\ &= -\int \mathrm{d}t \frac{1}{2} \frac{G^2 m_1 m_2^2}{r^2}.\end{aligned} \tag{4.84}$$

By obtaining the mirror image of 4.1(d), and gathering all of our results, we obtain the 1 PN, Einstein-Infeld-Hoffman Lagrangian,

$$\begin{aligned}\mathcal{L}_{EIH} =& \frac{1}{c^2} \left(\frac{1}{8} \sum_{1,2} m v^4 + \frac{3}{2} \frac{G m_1 m_2}{r} \left(v_1^2 + v_2^2\right) - \frac{7}{2} \frac{G m_1 m_2}{r} (\vec{v}_1 \cdot \vec{v}_2) \right. \\ & \left. - \frac{1}{2} \frac{G m_1 m_2}{r} \frac{(\vec{v}_1 \cdot \vec{r})(\vec{v}_2 \cdot \vec{r})}{r^2} - \frac{1}{2} \frac{G^2 m_1 m_2 (m_1 + m_2)}{r^2} \right),\end{aligned} \tag{4.85}$$

where the higher order kinetic term has been obtained from the worldline point particle in eq. (4.53).

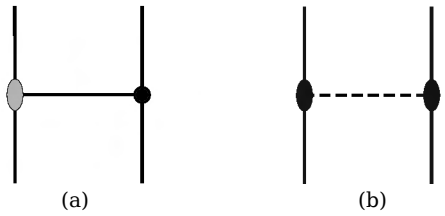

FIGURE 4.2: The LO PN correction from the spin-orbit coupling, which is encoded in (a), and the LO PN correction from the spin-spin coupling, encoded in (b).

Spinning Objects

For spinning objects, two effects come into play in the dynamics from the spin-orbit and the spin-spin coupling. The LO terms are contained in the diagrams of fig. 4.2. We start by considering fig. 4.2(a), which yields the well known LO spin orbit contribution,

$$\begin{aligned}\text{Figure 4.2(a)} &= -\int \mathrm{d}t_1 2\epsilon_{ijk} S_1^k v_1^i \partial^j \phi(x_1) \times \int \mathrm{d}t_2 m_2 \phi(x_2) \\ &= -\int \mathrm{d}t G m_2 2\epsilon_{ijk} S_1^k v_1^i \partial^j \frac{1}{r} \\ &= \int \mathrm{d}t \frac{2}{c^3} \frac{G m_2}{r^2} \vec{S}_1 \cdot (\vec{v}_1 \times \hat{r}),\end{aligned} \tag{4.86}$$

with $\hat{r}$, the unit radial vector, and where we have used, $\epsilon_{ijk} a^i b^j c^k = a \cdot (b \times c)$. To obtain the dynamics of the binary, the mirror image of the last diagram is needed as well.

The next LO correction, from the spin-spin coupling, is encoded in fig. 4.2(b). This diagram yields

$$\begin{aligned}\text{Figure 4.2(b)} &= \int \mathrm{d}t_1 \frac{1}{2} \epsilon_{ijk} S_1^k \partial^i A^j(x_1) \times \int \mathrm{d}t_2 \frac{1}{2} \epsilon_{lmn} S_2^n \partial^l A^m(x_2) \\ &= -\int \mathrm{d}t G \epsilon_{ijk} S_1^k \delta^{jm} \partial^i \partial^l \left(\frac{1}{r}\right) \epsilon_{lmn} S_2^n \\ &= -\int \mathrm{d}t \frac{1}{c^4} \frac{G}{r^3} \left(\vec{S}_1 \cdot \vec{S}_2 - 3\left(\vec{S}_1 \cdot \hat{r}\right)\left(\vec{S}_2 \cdot \hat{r}\right)\right),\end{aligned} \tag{4.87}$$

as expected [41]. Therefore, the LO spin-orbit contribution, eq. (4.86), enters at order 1.5 PN, while the LO spin-spin contribution, (4.87), enters at 2 PN, for a maximally spinning compact object. If the star is slowly spinning, then these effects will enter into the dynamics at a higher order.

Size Effects

The LO size effects due to gravity are contained in the diagrams of fig. 4.3. The correction from the spin-gravity coupling, reads

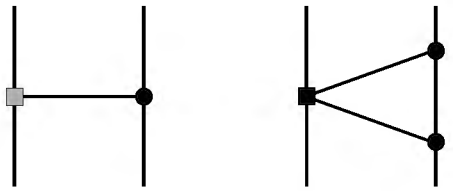

FIGURE 4.3: Corrections due to size effects. In (a), the LO spin-size correction, while (b), the LO static size correction.

$$\begin{aligned}\text{Figure } 4.3\text{(a)} &= \int \mathrm{d}t_1 \frac{n_{\Omega,g}}{2} S_1^i S_1^j \partial_i \partial_j \phi(x_1) \times \int \mathrm{d}t_2 m_2 \phi(x_2) \\ &= \int \mathrm{d}t \frac{n_{\Omega,g}}{2} \frac{G m_2}{r^3} \left(-\vec{S}_1^2 + 3 \left(\vec{S}_1 \cdot \hat{r} \right)^2 \right).\end{aligned} \tag{4.88}$$

The second diagram encodes the size effects of an extended object, even if it is not rotating. We obtain,

$$\begin{aligned}\text{Figure } 4.3\text{(b)} &= \int \mathrm{d}t_1 \frac{n_g}{4} \partial^i \partial^j \phi(x_1) \partial_i \partial_j \phi(x_1) \times \int \mathrm{d}t_2 m_2 \phi(x_2) m_2 \phi(x_2) \\ &= \int \mathrm{d}t 3 n_g \frac{G^2 m_2^2}{r^6}.\end{aligned} \tag{4.89}$$

Both of the size corrections agree with the literature [41, 46]. The mirror image of both diagrams are needed for a complete description of the system.

For the correction in eq. (4.89), due to static tides, it is commonly said that it enters into the dynamics at 5 PN order. This is because the coefficient, $n_g \propto \ell^5/G$, with ℓ the radius of the object. For a compact object, $\ell \sim Gm$, for which altogether with the virial theorem, $v^2 \sim Gm/r$, implies the parameter expansion, $\ell/r \sim v^2$. Therefore, one can identify that eq. (4.89), will be of order v^{10}, which according to the PN counting, it is equivalent to a 5 PN. Nevertheless, this is not strictly speaking a 5 PN correction, although it helps us to understand the order at which this effect will play a role in the dynamics.

A similar analysis can be done for eq. (4.88). For instance, for a NS, the coefficient $n_{\Omega,g} \sim n_g$ [47], and therefore one can conclude that the spin-size effects roughly enters at 2 PN order. The magnitude of the spin and the radius of the star will change the order at which this effect enters into the PN expansion.

Charge

Moving into the dynamics of the electromagnetic interaction, the 0 and 1 PN corrections are encoded in fig. 4.4. We start with the diagram (a), which yields

$$\begin{aligned}\text{Figure } 4.4\text{(a)} &= \int \mathrm{d}t_1 q_1 A_0(x_1) \times \int \mathrm{d}t_2 q_2 A_0(x_2) \\ &= -\int \mathrm{d}t \frac{\mu_0}{4\pi} \frac{q_1 q_2}{r},\end{aligned} \tag{4.90}$$

the Coulomb potential, which is 0 PN order.

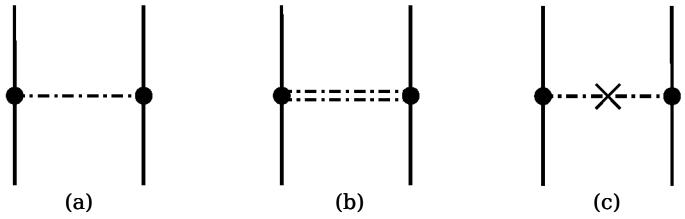

FIGURE 4.4: Corrections due to charge. The Coulomb interaction, which is 0 PN order, is encoded in (a), while the 1 PN correction is encoded in the last two diagrams.

Then, we obtain the diagram (b),

$$\begin{aligned}\text{Figure } 4.4(\text{b}) =& \int \mathrm{d}t_1 q_1 A^i(x_1) v_{1i} \times \int \mathrm{d}t_2 q_2 A^j(x_2) v_{2j} \\ =& \frac{\mu_0}{4\pi}\frac{q_1 q_2}{r}\left(\vec{v}_1 \cdot \vec{v}_2\right).\end{aligned} \tag{4.91}$$

The diagram (c), with the time relativistic correction, yields

$$\begin{aligned}\text{Figure } 4.4(\text{c}) =& \int \mathrm{d}t_1 q_1 A_0(x_1) \times |_t \int \mathrm{d}t_2 q_2 A_0(x_2) \\ =& -\mu_0 q_1 q_2 \int \mathrm{d}t_1 \int \mathrm{d}t_2 \frac{\mathrm{d}}{\mathrm{d}t_1 \mathrm{d}t_2}\delta(t_1 - t_2) \int \frac{\mathrm{d}\vec{k}^3}{(2\pi)^3}\frac{e^{\vec{k}\cdot\vec{r}}}{(k^2)^2} \\ =& -\int \mathrm{d}t \frac{\mu_0}{2}\frac{q_1 q_2}{4\pi}\frac{1}{r}\left(\vec{v}_1 \cdot \vec{v}_2 - \frac{(\vec{v}_1 \cdot \vec{r})(\vec{v}_2 \cdot \vec{r})}{r^2}\right),\end{aligned} \tag{4.92}$$

where we used eq. (4.83).

Gathering our results, we obtain the 1 PN correction of the electromagnetic interaction [63]

$$\mathcal{L}_{q,1\text{PN}} = \frac{1}{c^2}\left\{\frac{\mu_0}{2}\frac{q_1 q_2}{4\pi}\frac{1}{r}\left(\left(\vec{v}_1 \cdot \vec{v}_2\right) + \frac{(\vec{v}_1 \cdot \vec{r})(\vec{v}_2 \cdot \vec{r})}{r^2}\right)\right\}. \tag{4.93}$$

Polarizability

The polarization induced by an electromagnetic field is encoded in the diagrams of fig 4.5. For an object that is spinning, the LO correction is given by

$$\begin{aligned}\text{Figure } 4.5(\text{a}) =& \int \mathrm{d}t_1 n_{q_1,\Omega_1}\epsilon_{ij00} S_1^i \partial^j A_0(x_1) \times \int \mathrm{d}t_2 q_2 A_0(x_2) \\ =& \int \mathrm{d}t \frac{\mu_0}{4\pi}\frac{q_2 n_{q_1,\Omega_1}}{r^3}\epsilon_{ij00} S_1^i r^j,\end{aligned} \tag{4.94}$$

The LO polarization correction when an object is not rotating, reads

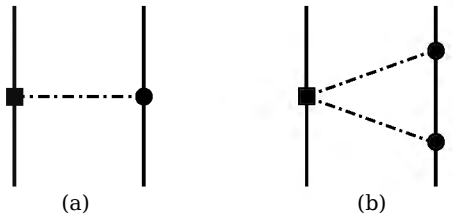

FIGURE 4.5: The LO correction due to the polarization for a spinning compact object in diagram (a), and for a non-spinning in diagram (b).

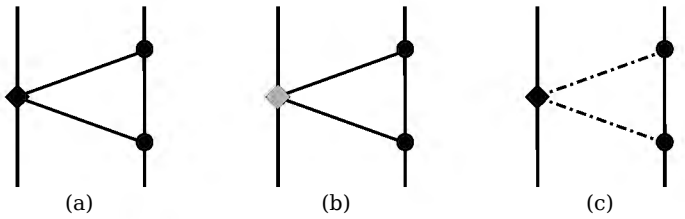

FIGURE 4.6: The LO corrections due to dissipative effects. For the gravitational case, the LO correction receives two contributions, (a) and (b), the first one due to the gravitational interaction, and the second one due to spin. For the LO dissipative correction in the electromagnetic case, the spin part does not contribute, thus having only the diagram (c).

$$\begin{aligned}\text{Figure 4.5(b)} &= \int \mathrm{d}t_1 n_{q_1} \partial^i A_0(x_1) \partial_i A_0(x_1) \times \int \mathrm{d}t_2 q_2^2 A_0(x_2) A_0(x_2) \\ &= \int \mathrm{d}t n_{q_1} \left(\frac{\mu_0 q_2}{4\pi}\right)^2 \frac{1}{r^4},\end{aligned} \tag{4.95}$$

Both diagrams show that an extended object, even without charge, will be polarized if the companion is charged and the coefficients are different from zero, $n_{q_{...}} \neq 0$. The coefficients, n_q and $n_{q,\Omega}$ for a BH are zero. [93, 92], while for a NS are unknown. By dimensional analysis we find that, $n_{q,\Omega} \propto n_q \propto \ell^3$, which implies that, eq. (4.94) and eq. (4.95), enter roughly at 1 PN and 3 PN respectively. The magnitude of the charge and the spin will change the order at which these effects enter into the dynamics.

Dissipative Effects

We consider both electromagnetic and gravitational dissipative effects. For a non-spinning BH, dissipation takes into account for the absorption of electromagnetic and gravitational waves. For a non-spinning NS, we can think of this effect as the energy loss due to its equation of state of the matter during an electromagnetic or gravitational interaction. Dissipation on spinning objects, arises given that the spin of the body has a time dependence between the object and its tidal environment.

The dissipative correction for the gravitational case, even if the object is not rotating, reads

$$\begin{aligned}\text{Figure 4.6(a)} &= \int \mathrm{d}t_1 \frac{ic_{g_1}}{4}\partial_i\partial_j\phi(x_1)\partial^i\partial^j\dot{\phi}(x_1) \times m_2^2 \int \mathrm{d}t_2\phi^2(x_2) \\ &= \int \mathrm{d}t \frac{ic_{g_1}}{4}\partial_i\partial_j\left(\frac{Gm_2}{r}\right)\partial^i\partial^j\partial^t\left(\frac{Gm_2}{r}\right) \\ &= \int \mathrm{d}t i 9 c_{g_1} G^2 m_2^2 \frac{(\vec{r}\cdot\vec{v})}{r^8}.\end{aligned} \tag{4.96}$$

For a BH, the coefficient, $c_g \propto \ell_s^6/G$, due to the absorption of GWs [30], and therefore its dissipative effects enter at 6.5 PN order. For a stellar object that is described by an equation of state of matter, in the weak friction model, the coefficient $c_g = \Theta n_g$, with Θ, being the time lag [94]. Thus, by using the Love coefficient, for which $n_g \propto \ell^5/G$, we conclude that if a NS is described by the weak friction approximation, its dissipative effects will play a role at $\sim$ 5.5 PN order. The intermediate line of eq. (4.96), is used to obtain the equations of motion below.

If the object is spinning, the dissipative correction yields

$$\begin{aligned}\text{Figure 4.6 (b)} &= \int \mathrm{d}t_1 \frac{ic_{g_1,\Omega_1}}{2}\partial_i\partial_j\phi(x_1)\partial^i\partial_k\phi(x_1)\epsilon^{jkl}S_l \times m_2 \int \mathrm{d}t_2\phi(x_2) \\ &= \int \mathrm{d}t \frac{ic_{g_1,\Omega_1}}{2}\partial_i\partial_j\left(\frac{Gm_2}{r}\right)\partial^i\partial_k\left(\frac{Gm_2}{r}\right)\epsilon^{jkl}S_l \\ &= \int \mathrm{d}t \frac{ic_{g_1,\Omega_1}}{2} G^2 m_2^2 \left(\frac{\delta_{jk}}{r^6} + 3\frac{r_j r_k}{r^8}\right)\epsilon^{jkl}S_l.\end{aligned} \tag{4.97}$$

For a spinning BH, $n_{g,\Omega} \propto GM^2\ell_+^5/c^5(\ell_+ - \ell_-)$, depends on both of its radi, ℓ_+ and ℓ_-[19]. A careful analysis shows that this effect scales as a 5 PN order effect, with two prefactors, Ω/c and $\ell_+/(\ell_+ - \ell_-)$, and where we have considered, $\ell_+/r \sim v^2$. For a NS this coefficient is unknown.

In what follows, we derive the equations of motion due to the dissipative effects. The equations of motion due to the gravitational dissipative effects were derived in the Newtonian limit of a spinning star [46], and therefore our LO corrections for dissipative effects should reproduce the results as well. For a dissipative system, the equations of motion can be obtained from the modified variation [100],

$$\delta\mathcal{S} + i\int \mathrm{d}t\mathrm{d}t'\delta J_{ab}(t)\tilde{G}_R^{ab,cd}(t-t')J_{cd}(t') = 0, \tag{4.98}$$

where $J_{cd} = \Lambda^e{}_c\Lambda^f{}_d E_{ef}$, and $\tilde{G}_R$, the retarded correlation function of the operators $\tilde{\mathcal{D}}^{ab}$ [30].

Then, using eq. (4.96) and (4.97) in the modified variation, (4.98), and varying with respect to x^i, one obtains the expected equations of motion due to dissipation for a gravitationally interacting spinning star [46],

$$m_1\dot{v}_{1i}\Big|_{\mathcal{D}} = -\frac{c_{g_1}}{2}\partial_i\partial_j\partial_k\Phi_1\partial^i\partial_j\dot{\Phi}_1 - c_{g_1,\Omega_1}\partial_i\partial_j\partial_k\Phi_1\partial^i\partial_k\Phi_1\epsilon^{jkl}S_l \tag{4.99}$$

with $\Phi_1 = Gm_2/r$, the Newtonian potential. The mirror image of the last two diagrams is needed for the complete description of the binary.

Moving into the electromagnetic case, the LO dissipative contribution reads

$$\begin{aligned}\text{Figure 4.6(c)} &= \int \mathrm{d}t_1 i c_{q_1} \partial_i A_0(x_1) \partial^i \dot{A}_0(x_1) \times \int \mathrm{d}t_2 q_2^2 A_0^2(x_2) \\ &= \int \mathrm{d}t\, i c_{q_1} \left(\frac{\mu_0 q_2}{4\pi}\right)^2 \partial_i \left(\frac{1}{r}\right) \partial^i \partial^t \left(\frac{1}{r}\right).\end{aligned} \tag{4.100}$$

For a BH, the coefficient due to the absorption of electromagnetic waves, $c_q \propto \ell_s^4$ [30], and therefore enters roughly at 4.5 PN order. Of course this order will change depending on the charge of the object. The equations of motion from the modified variation leads to,

$$m_1 \vec{v}_1^i \Big|_{\mathcal{P}} = c_{q_1} \left(\frac{\mu_0 q_2}{4\pi}\right)^2 \left(\frac{v^i}{r^6} + \frac{3(\vec{r}\cdot\vec{v})r^i}{r^8}\right). \tag{4.101}$$

4.4 Gravitational Radiation

From the EFT perspective, we can obtain the PN corrections to each of the terms in the action, eq. (4.24). The PN expansion to the point mass can be expanded in a series as

$$\vec{a}_{PN} = \vec{a}_{PP} + c^{-2}\vec{a}_2 + c^{-4}\vec{a}_4 + c^{-5}\vec{a}_5 + O(c^{-6}), \tag{4.102}$$

where, $\vec{a}_{PP} = \vec{a}_N$, is the point particle acceleration or Newtonian term. The terms $\vec{a}_2$ and $\vec{a}_4$ are the first and second order PN contributions of the conservative sector which accounts for, i.e. the periastron shift. The leading order term that accounts for radiation of energy and momentum through GW radiation is the 2.5 PN term, $\vec{a}_5$, which we denote as, $\vec{a}_{GW} = \vec{a}_5$.

To obtain the leading order GW radiation correction in the EFT, one needs to integrate out the radiation modes of the gravitational field as well [65]. This computation is beyond the scope of this work, but it is extracted for completeness. Nevertheless, we can extract this correction from the literature, which reads [65, 51]

$$\vec{a}_{GW} = \frac{4}{5}\frac{G^2 m_1 m_2}{r^3}\left[\left(\frac{2Gm_1}{r} - \frac{8Gm_2}{r} - v^2\right)\vec{v} + (\hat{r}\cdot\vec{v})\left(\frac{52Gm_2}{3r} - \frac{6Gm_1}{r} + 3v^2\right)\hat{r}\right]. \tag{4.103}$$

For the numerical experiments in the late inspiral, we will make use of the modified acceleration, $\vec{a} = \vec{a}_\star + c^{-5}\vec{a}_{GW}$, where $a_\star$, is the acceleration which includes the Newtonian term and the properties and stellar structure of the star that we have taken into account in eq. (3.83). We neglect the PN contribution from the conservative sector given that it does not contribute to the decay of the binary. The GW decay due to the 2.5 PN term is shown in Fig. 1.1 for an equal mass BBH.

Chapter 5

Compact Object Evolution

5.1 Numerical Simulations

We implement a 4th order Hermite integrator [82, 105] which can solve the dynamics of point-like particles numerically. We briefly review the basics to evolve a system of point particles numerically and then solve for the dynamics of the compact objects in a binary system.

5.1.1 Point Particle Simulations

Position, Velocity and Acceleration

In the point particle approximation, the predicted values of the position, velocity and acceleration for the next step are obtained from

$$\begin{aligned}
\vec{r}_{i+1} &= \vec{r}_i + \vec{v}_i \Delta t + \frac{1}{2!}\vec{a}_i \Delta t^2 + \frac{1}{3!}\vec{j}_i \Delta t^3 + \ldots, \\
\vec{v}_{i+1} &= \vec{v}_i + \vec{a}_i \Delta t + \frac{1}{2!}\vec{j}_i \Delta t^2 + \ldots, \\
\vec{a}_{i+1} &= \vec{a}_i + \vec{j}_i \Delta t + \ldots,
\end{aligned} \tag{5.1}$$

where $\vec{j} = \dot{\vec{a}}$. The force calculation is computed as

$$\begin{aligned}
\vec{a}_i &= \frac{G m_2 \hat{r}}{r^2} + \ldots, \\
\vec{j}_i &= \frac{G m_2}{r^3}\{\vec{v} - 3(\vec{v}\cdot\hat{r})\hat{r}\} + \ldots,
\end{aligned} \tag{5.2}$$

with the position and velocity from the previous step. The ellipses denote all other effects we have taken into account: GW radiation, spin size corrections, dynamical tides and dissipation. The force calculation, $\vec{a}_{i+1}$ and $\vec{j}_{i+1}$, is done using the predicted values, $\vec{r}_{i+1}$ and $\vec{v}_{i+1}$, to get the corrected position, velocity and acceleration

$$\begin{aligned}
\vec{r}_{i+1,c} &= \vec{r}_i + \frac{1}{2}(\vec{v}_i + \vec{v}_{i+1})\Delta t + \frac{1}{12}(a_i - \vec{a}_{i+1})\Delta t^2, \\
\vec{v}_{i+1,c} &= \vec{v}_i + \frac{1}{2}(\vec{a}_i + \vec{a}_{i+1})\Delta t + \frac{1}{12}(\vec{j}_i - \vec{j}_{i+1})\Delta t^2, \\
\vec{a}_{i+1,c} &= \vec{a}_i + \frac{1}{2}(\vec{j}_i + \vec{j}_{i+1})\Delta t,
\end{aligned} \tag{5.3}$$

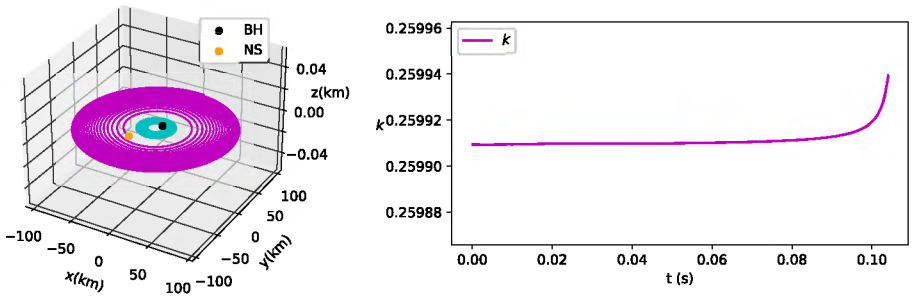

FIGURE 5.1: Simulation of the coalescence of a BH-NS binary and the measurement of the dimensionless static tidal number k of the NS during the interaction. The binary is composed of a BH of mass $m_\bullet = 5M_\odot$, and a NS of mass $m_\star = 1.2\,M_\odot$ and radius $\ell_\star = 8.89$ km. The simulation has an initial orbital distance of $d = 8\,\ell_\bullet$. The figure on the left illustrates the trajectories followed by the binary until the LSO orbit is reached. The purple and cyan line represents the trajectory followed by the NS and the BH respectively. On the right figure the coefficient k is measured at each fixed time-step in the simulation. The theoretical value of the coefficient for the NS used in this case is $k = 2.59909$, which can be measured with high accuracy with an appropriate time step, dt. For this simulation, $dt = 0.1$ in code units.

up to the jerk correction. With this very simple framework we are capable of numerically evolving the equations of motion of the effective theory, obtaining the desired accuracy by using a specific time-step Δt.

Spin Evolution

We solve for the angular velocity, $\vec{\Omega}$, in a similar fashion as above. We define $\vec{b} = \partial_t \vec{\Omega}$ and correct the angular velocity as follows

$$\vec{\Omega}_{i+1,c} = \vec{\Omega}_i + \frac{1}{2}(\vec{b}_i + \vec{b}_{i+1})\Delta t + \frac{1}{12}(\dot{\vec{b}}_i - \dot{\vec{b}}_{i+1})\Delta t^2. \tag{5.4}$$

5.1.2 Numerical Tests and the Matching of Coefficients

Many Newtonian and PN codes have been implemented to do numerical experiments. Testing the Newtonian limit is straightforward. To test the PN corrections we use the GW time decay eq. (5.18). In figure 5.4, we show that our implementation reproduces the leading order waveform as a function of the coalescence time t_c.

To test the rest of the effects we can match the coefficients of the theory from the corrected position, velocity and acceleration at each time-step, which serves as an internal test of the implementation and shows the accuracy of the simulation. From an EFT perspective, we can follow the energy hierarchy to measure different coefficients. Consider for instance a BH-NS binary without any spin, and neglect for a moment the GW radiation effects. The dynamics of the NS will change due to the static tidal effects, and the matching of the dimensionless coefficient reads

$$k = \frac{1}{6}\frac{m_1}{m_2}\left(\frac{r}{\ell}\right)^5 \left(\frac{a_{\star,j}}{a_{N,j}} - 1\right), \tag{5.5}$$

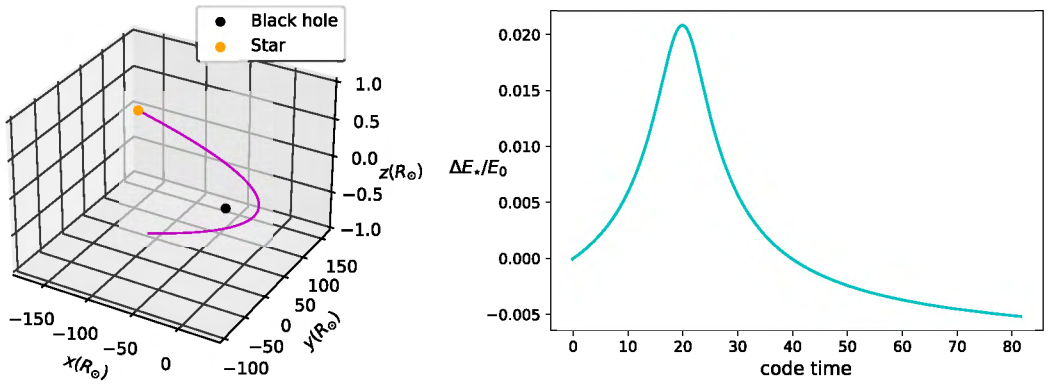

FIGURE 5.2: Simulation of the parabolic encounter of a giant with a BH using hydrodynamical code [106]. On the left figure the trajectories of the parabolic encounter of the star with a BH. On the right figure we have the energy deposition or energy lost during the encounter due to the internal structure of the star.

where $a_{N,j}$ is one of the spatial components of the Newtonian term ($j = \{x, y, z\}$) without any other effect, and $a_{\star,j} = a_{N,j} + a_{T,j}$ is the total acceleration of the star, with $a_{T,j}$ being the acceleration due to static tides. Thus, if we solve our system in the $x - y$ plane with these coordinates, we are to match to coefficient for each spatial component. Then we add GW radiation effects and measure the coefficient as

$$k = \frac{1}{6}\frac{m_1}{m_2}\left(\frac{r}{\ell}\right)^5 \left(\frac{a_{\star,j}}{a_{N,j}} - \frac{a_{GW,j}}{a_{N,j}} - 1\right). \tag{5.6}$$

Figure 5.1 shows the time evolution measurement of the dimensionless static Love number, k, from a BH-NS coalescence. The matching of coefficients from static tidal effects is the simplest, but we can add all other effects and go order by order in the energy hierarchy to measure the coefficients and test the implementation.

Although it might seem trivial to match the coefficients within the simulation, the matching of coefficients from simulations can be done to compare, i.e. our state of the art hydrodynamics or numerical relativity codes to the EFT for compact objects, a first step towards matching the coefficients from GW observations.

5.2 Phenomenology of the Internal Structure

The action for the stellar objects without spin and without charge in gravity has the schematic form

$$\mathcal{S} = \mathcal{S}_{PP} + \mathcal{S}_T + \mathcal{S}_{\mathcal{D}}, \tag{5.7}$$

where, $\mathcal{S}_{PP}$, is the action for a massive point particle, $\mathcal{S}_T$, the action describing static tides and $\mathcal{S}_{\mathcal{D}}$, dissipative effects. We consider each of the leading order terms for these effects in turn, to study their overall role during a parabolic encounter. Therefore, the effective action in the Newtonian limit reads

$$m_1\dot{\vec{v}} = -\frac{Gm_1m_2\hat{r}}{r^2} - \frac{9n_EG^2m_2^2\hat{r}}{r^7} - \frac{9\eta_EG^2m_2^2}{r^8}\left(\vec{v} + 2\hat{r}(\hat{r}\cdot\vec{v})\right). \tag{5.8}$$

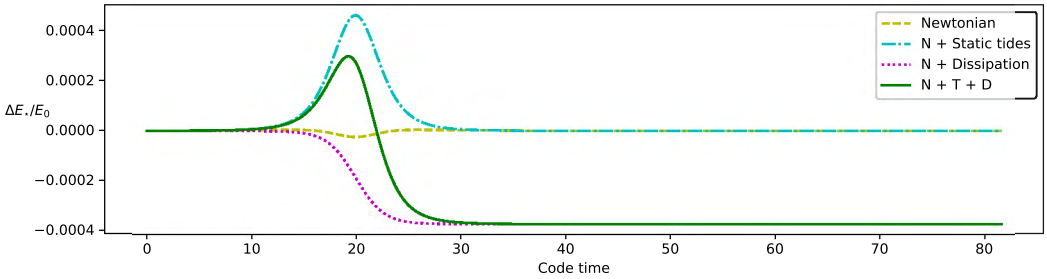

FIGURE 5.3: In this figure, the green line shows the total energy deposition during a parabolic interaction including all the effects due to the stellar structure, and the rest of the lines are each of the different isolated effects. The yellow line is the energy change due by considering only the Newtonian term. The cyan line is the energy change by adding static tidal effects to the Newtonian term, while the magenta represent dissipation.

To better understand the role of each effect, we compared our simulations to the state of the art hydrodynamical simulations. Therefore, we show the role of the different effects due to the internal structure of the stellar object. We start by showing numerical results from a hydrodynamical simulation, of the change of orbital energy during a parabolic interaction of a giant star, determined by an equation of state of matter with polytropic index $n = 1.5$, mass $m = 1M_\odot$ and radius $\ell = 1R_\odot$, with a BH of mass $M = 1000M_\odot$.

The tidal radius distance for the star due to the presence of the BH is $d_\tau \simeq 10R_\odot$. The interaction starts with an initial distance of $d_i = 100R_\odot$, and have a pericenter distance or distance of closest approach of $d_p = 30R_\odot \simeq 3d_\tau$. In fig. 5.3, we show the energy loss during the parabolic encounter, ΔE, due to dynamical tidal effects from the data given of a simulation of the above initial conditions using the numerical code Cholla [106]. The energy loss is measured as

$$\Delta E = -\frac{E_{\rm orb} - E_{{\rm orb},i}}{E_0}, \tag{5.9}$$

with

$$E_{\rm orb} = -\frac{GMm}{r} + \frac{1}{2}\frac{Mm}{(M+m)}v^2, \tag{5.10}$$

and

$$E_0 = \frac{(-3+n)m^2}{(-5+n)\ell}, \tag{5.11}$$

.

with n, the polytropic index. Thus, our purpose is to reproduce the energy deposition with our framework.

5.2.1 EFT Simulations

We do a simple but illustrative study of each effect individually. Figure 5.3 shows the role of each effect, where we have considered a constant value of $c_g = n_g/3$, and $n_g = 2\ell^5 k/3G$, with $k = 0.143279$, which corresponds to the polytropic index, $n = 1.5$. We have chosen the coefficient c_g given the weak friction model [94] for dissipative effects due to the formation of a tilda bulge.

In figure 5.3. The yellow line shows the change of energy by considering only the Newtonian term in the equations of motion, eq. (5.8). The cyan line is the energy change with the inclusion of static tides, which as we can observe, the second term of eq. (5.8) generates the positive bump. The magenta line is due to dissipative effects, the third term in eq. (5.8), which generates energy loss during the interaction as expected. Nevertheless, although we have obtained a similar plot to the one in 5.2, we struggle to reproduce the peak due to tidal effects as in the hydrodynamical simulations, as one can see by comparing fig. 5.2 and fig. 5.3, for which our results are two order of magnitude below. This might be because we need to consider dynamical tides as in [17], but this implementation into our framework is left for a future work. And also because the simulated star with hydrodynamical simulations is used for non-compact objects, and a comparison to numerically general relativistic simulations needs to be carried out. But for now, we proceed to implement the EFT framework numerically.

5.3 Waveforms and Observational Signatures

5.3.1 Waveform Extraction

Gravitational radiation is produced at lowest order by the time varying mass quadrupole moment. An analytical expression for the quadrupole gravitational waveform from the inspiral of a binary can be obtained in the setting of flat background spacetime with linearized gravity. One can solve the linearized Einstein's equations in the presence of the binary as a matter source and obtain a solution for the amplitude, project it into the tranverse-traceless gauge, and expand it as a multipole expansion. The solution is the amplitude for each polarization mode, h_+ and $h_\times$ [107].

Binaries whose orbital distance is large enough, such that changes in the orbital distance due to GW radiation over several periods are small, can be considered as binaries with fixed orbits. In this scenario, the quadrupolar, + polarized, GW amplitude for an inspiral binary in a circular fixed orbit reads [107]

$$h_+(\omega_s, t) = \frac{2}{r_o}\frac{G^{5/3}}{c^4}\frac{m_1 m_2}{m^{1/3}}\omega_s^{2/3}\cos(2\omega_s t) = \frac{2G\mu x}{c^2 r_o}\cos(2\omega_s t), \tag{5.12}$$

where r_o, is the distance from the observer to the binary, μ, the reduced mass, m, the total mass of the binary, and ω_s, the orbital frequency. We have introduced the dimensionless variable, $x \equiv \left(Gm\omega_s/c^3\right)^{2/3}$. Furthermore, we have chosen the inclination angle, $\iota = \pi/2$, such that, the $\times$ polarized amplitude, $h_\times$, vanishes.

For the late inspiral regime, where the changes in the orbital distance and frequency are relevant, it is necessary to take into account for the orbital decay in the waveform. This can be done by obtaining the radiated power, the amount of energy radiated through GWs per unit time, and relating it to the change of energy of the system, $\dot{E}_{orb}$, as $P = -\dot{E}_{orb}$. From the latter equality, an expression for the change of

the orbital frequency in time, $\dot{\omega}_s$, is obtained in terms of ω_s. By integrating it over the coalescence time measured by an observer, $t_c = T_c - t$, with T_c, the time that the binary takes to merge, one obtains the relation between orbital frequency and the time of coalescence,

$$\omega_s(t_c) = \frac{1}{8}\left(\frac{5c^5}{G^{5/3}}\frac{m^{1/3}}{m_1 m_2}\right)^{3/8} t_c^{-3/8}. \tag{5.13}$$

Then, in eq. (5.12), one replaces the phase, $2\omega_s t \rightarrow \varphi(t)$, with the accumulated orbital phase,

$$\varphi(t) = 2\int_t \mathrm{d}t\, \omega_s(t) = -2\int_{t_c} \mathrm{d}t_c\, \omega_s(t_c), \tag{5.14}$$

where we have used $\mathrm{d}t = -\mathrm{d}t_c$. By substituting eq. (5.13) into last equation, solving the integral for the time of coalescence, and expressing it in terms of the orbital frequency, one obtains the accumulated orbital phase,

$$\varphi(x) = -\frac{1}{32}\frac{m^2}{m_1 m_2}x^{-5/2} + \varphi_0 = -\frac{1}{32}\frac{m^2}{m_1 m_2}x^{-5/2} - \frac{2Gm\omega_s}{c^3}\log\left(\frac{\omega_s}{\omega_0}\right), \tag{5.15}$$

where φ_0 has been fixed from [51], and with ω_0, a constant frequency that is chosen as the frequency at which the binary enters into the detectability band.

Thus, the gravitational waveform that takes into account for the GW decay, reads

$$h_+(x(\omega_s)) = \frac{2G\mu x}{c^2 r_o}\cos 2\varphi(x). \tag{5.16}$$

with μ, the reduced mass. We simply denote, $h_+(x(\omega_s)) = h_+(\omega_s)$. This expression is the lowest order or $0-$PN waveform in the PN approximation. By writing $x = ((Gm/r)(r\omega_s/c^3))^{2/3}$, we find its scaling given that, $Gm/r \sim v^2$, and $r\omega_s \sim v$. Thus, every x scales as $x = O\left(v^2/c^2\right)$, meaning that corrections in powers of v/c can be expressed in powers of $x^{1/2}$. The PN expansion of the $+$ polarized waveform in powers of x, reads [51]

$$h_+(x) = \frac{2G\mu x}{c^2 r_0}\left(H_+^0 + x^{1/2}H_+^{(1/2)} + xH_+^{(1)} + x^{3/2}H_+^{(3/2)} + x^2 H_+^{(2)} + \mathcal{O}(c^{-5})\right), \tag{5.17}$$

with $H_+^0 = \cos 2\varphi$. The last expression shows the program to extract high order PN waveforms that matches observations. Nevertheless, for the purpose of this work we consider only the amplitude in eq. (5.16).

5.3.2 Comparison to Known Results

Working with the amplitude formula as a function of the orbital frequency, ω_s, we need to generate the input numerically by solving the equations of motion as shown in the numerical section. This is in contrast to the amplitude as a function of the time of coalescence, t_c measured by the observer, which can be obtained via

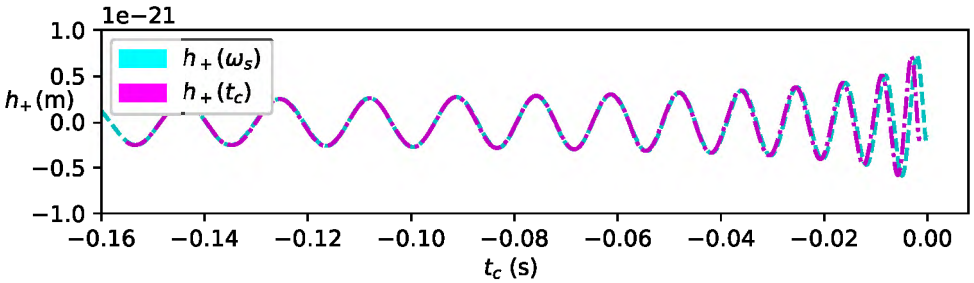

FIGURE 5.4: Comparison of the leading order gravitational waveform as a function of the time of coalescence, t_c, and of the orbital frequency, ω_s. Using the same equal mass BBH as in figure 1.1, we extract the orbital frequency and time of coalescence to obtain the waveforms. The cyan line is the waveform as a function of ω_s, input generated with our numerical simulations. The magenta line is the waveform as a function of t_c, which is obtained from using eq. (5.18) as the only input.

eq. (5.13) in eq. (5.16). In this case, the waveform can be simply extracted if the coalescence time is known. The analytical formula for the time of coalescence for two point masses orbiting each other in a circular orbit, which approximates very well to a binary black hole, reads [108]

$$T_c(d) = \frac{5}{256}\frac{d^4c^5}{G^3 m_1 m_2 (m_1+m_2)}, \tag{5.18}$$

with d, the orbital distance of the binary. Nevertheless, the stellar structure changes the merger time, and deriving analytical expressions becomes a hard task. Thus, to measure the imprints of the stellar structure in the late inspiral of the binary, it makes sense to extract the waveform as a function of the orbital frequency, ω_s.

To compare our methodology to known methodologies, we show the extraction of the orbital frequency from the decay of a binary from the simulations. Consider a binary with masses m_1 and m_2, and relative distance, $\vec{r} = \vec{r}_2 - \vec{r}_1$, in some inertial frame. Then, considering only Newtonian gravity, the relative motion, $\vec{a}_N = \vec{a}_2 - \vec{a}_1$, reads

$$\vec{a}_N = -G\frac{m}{r^2}\hat{r}. \tag{5.19}$$

with $m = m_1 + m_2$. The Newtonian orbital frequency, ω_N, is simply obtained from Kepler's law, by equating the centripetal to the Newtonian relative acceleration. The centripetal acceleration, $a_c = v^2/r$, is a radial force that has the opposite direction to the gravitational radial acceleration. Furthermore, the relative velocity, v, is related to the orbital frequency as $v = \omega r$. Thus, the Newtonian orbital frequency is simply given by

$$\omega_N = \sqrt{\frac{Gm}{r^3}}. \tag{5.20}$$

Using the above reasoning, we proceed to obtain the orbital frequency with the GW effects included. This can be done by equating the total radial acceleration,

including the radial term in (4.103), to the orbital frequency, ω_s. Thus, the orbital frequency taking into account gravitational radiation, reads

$$\omega_s = \omega_{N+GW} = \sqrt{\frac{Gm}{r^3} - \frac{4}{5}\frac{G^2 m_1 m_2}{r^4}(\hat{r}\cdot\vec{v})\left(\frac{52Gm}{3r} - \frac{6Gm}{r} + 6v^2\right)}. \tag{5.21}$$

In figure 5.4, we show the comparison of our method for GW extraction dependent on the orbital frequency using eq. (5.16) and eq. (5.21), to the leading order amplitude as a function of the coalescence time, t_c [107].

Given the initial distance, $d = 10\ell_s$, of an equal mass binary BH, with $m_\bullet = 20M_\odot$, we can obtain the coalescence time and extract the waveform, $h_+(t_c)$ [107]. To extract the waveform as a function of the orbital frequency, $h_+(\omega_s)$, we generate eq. (5.21) numerically with our code described below, and then evaluate it in eq. (5.16). Both waveforms matches on most of the inspiral, with some discrepancies near the coalescence time, which is due to the lack of the rest of the PN corrections. Recall that we are only using the leading order GW radiation correction, or 2.5 PN term, which is the lowest order term that drives the decay. With these results, we can safely proceed to study, to leading order, the effects due to the stellar structure in compact object interactions.

5.3.3 Observational Signatures

There are observable consequences due to the internal properties of the star that can be quantified. The effective potential changes the acceleration on each object, making the frequency and amplitude of the GW to shift. To obtain the frequency shift, we include the stellar structure and derive the orbital frequency in the same way as for the GW decay. We only show the static tidal effects for simplicity, but all other effects are incorporated in the same manner. The contribution from static tidal effects is purely radial, such that the orbital frequency now reads

$$\omega_{N+GW+T} = \sqrt{\frac{Gm}{r^3} - \frac{4}{5}\frac{G^2 m_1 m_2}{r^4}(\hat{r}\cdot\vec{v})\left(\frac{52Gm}{3r} - \frac{6Gm}{r} + 6v^2\right) + \frac{9n_E G^2(m_1^2+m_2^2)}{r^8}}, \tag{5.22}$$

where the subindex, T, in this example, is referring to static tidal effects.

To quantify the phase shift, $\Delta\varphi$, generated in the waveform (5.16), we compare simulations of binaries including different effects, but same initial conditions. For instance, consider the orbital frequency from two binaries, one with GW radiation only, ω_{N+GW}, and the other with GW radiation and static tidal effects, ω_{N+GW+T}. From equation (5.16), we find the change in the phase shift due to the additional effects,

$$\Delta\varphi = (\varphi_{N+GW+T} - \varphi_{N+GW}). \tag{5.23}$$

The phase shift is to be measured at each time step of the simulation. In general, the phase shift due to the contribution of an additional effect is measured as

$$\Delta\varphi = (\varphi_b - \varphi_a), \tag{5.24}$$

where the a and b refer to different effects in the simulations to be compared.

5.4 The Late Inspiral

5.4.1 Numerical Experiments and Observations

The LIGO-Virgo observatories detect gravitational waves from distant astrophysical sources in the frequency range, $f_{GW} \sim [10, 10000]$ Hz [109], with $f_{GW} = \omega_{GW}/2\pi = \omega_s/\pi$ as in [107], and ω_s the orbital frequency. Thus, for the purpose of waveform extraction and measurement of the different effects, we run illustrative simulations of the coalescence of various systems with initial and final frequency inside the LIGO-Virgo band. We systematically add the stellar structure effects and extract the lowest order gravitational waveform for different systems, (5.16). We choose an arbitrary distance to the system, r_o, that makes the system detectable in the LIGO-Virgo band.

Each binary system is set in a circular orbit, with initial conditions generated by a simulation with twice the distance of the shown examples. This is done with the purpose of avoiding numerical errors that can be generated in the first orbits of the system.

Neutron Star - Black Hole Interactions

In this interaction, all the effects we have considered play a role in the dynamics: static and dynamical tides in the NS and dissipation in the BH. Although in principle dissipative effects can play a role in NSs as well, given that the corresponding coefficient is unknown, we do not include such effect. We divide the BH-NS simulations into two sets, one set to show the role of each effect due to the internal structure of the objects, and the other set to compare the role of different static Love coefficients by considering different equations of state of matter for the NS. In each simulation, we have the same initial conditions of a NS-BH binary, with the mass of the BH, $m_\bullet = 5\,M_\odot$, and the mass and radius of the NS, $m_\star = 1.2\,M_\odot$ and $\ell_\star = 8.89$ km. The simulations start at an initial distance of $d = 25\,\ell_\bullet$ and initial frequency of $f_{GW} = 40$ Hz. The simulations are finished when the NS reaches the d_{LSO} of the BH. Furthermore, we have included slow spin to the NS, $\Omega = [0.1, 0.2]$, aligned to the orbital momentum of the binary.

First we consider the BH-NS system without any spin. In Fig. 5.5, we compare the phase evolution in the waveforms and quantify the phase shifts from the binaries with different effects: GWs, GWs + static tides, GWs + dynamical tides, and GWs + dissipation. The effects due to the internal structure are small, as one can not distinguish a difference by eye in the waveforms of the upper plot of fig 5.5. In the lower plot of fig. 5.5, we measure the difference of the accumulated orbital phase, $\Delta\varphi$, due to the different effects. As expected from eq. (3.81), the major contribution comes from the static tides term, having a final phase shift, $\Delta\varphi_{ST} \simeq 0.2$ radians, in our simulations, which is depicted with cyan color. The addition of dynamical tides contributes, $\Delta\varphi_{DT} \simeq 0.009$ rad, with respect to the static tides, which is shown by the green line. Finally, the effects of dissipation from the BH contributes the least, shifting the waveform by $\Delta\varphi_{Diss} \simeq 0.0018$ rad.

Then we add the dimensionless spin, $\chi = [0.1, 0.2]$, to the NS in the same BH-NS system. This is a restricted case in which the spins are aligned to the orbital angular momentum. From the definition in eq. (3.75), we obtain the angular velocity of the NS, Ω_1 and Ω_2, for each taken value of χ. On the top figure of fig. 5.6, we show the extracted gravitational waveform from simulations containing the different effects.

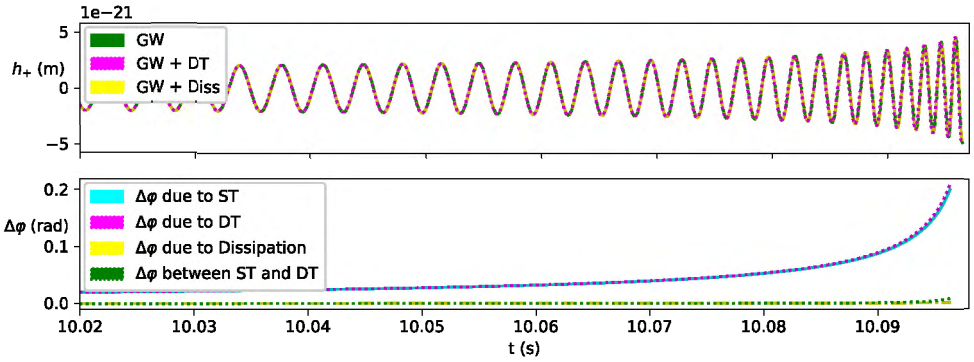

FIGURE 5.5: Gravitational waveforms and phase shifts from the late inspiral of a BH-NS coalescence with $m_\bullet = 5M_\odot$, $m_\star = 1.2\,M_\odot$ and $\ell_\star = 8.89$ km, at an initial distance of $d = 12\,\ell_\bullet$. The time to the LSO is $T_c \approx 10.096$ sec. We show the very last part of the simulation. On the top figure, each waveform color is extracted from simulations with different effects. The green waveform includes only GWs, the magenta GWs + dynamical tides (which includes the static part), and the yellow GWs + dissipation. On the plot below, the phase shift is measured. The cyan line is the wave shift generated by including static tidal effects to the GWs, the magenta line by taking into account static and dynamical tides, the yellow line by dissipation, and the green line is the phase shift that dynamical tides generate with respect to the static part.

The green waveform contains GWs + dynamical tides (DT), the cyan GWs + DT + Ω_1, and the magenta GWs + DT + Ω_2. On the plot below, the phase shift is measured. The green line is the wave shift generated by DT, the cyan line is the wave shift generated by the angular velocity Ω_1, while the magenta line is the wave shift due to Ω_2. The wave shift generated by dynamical tides is the same as before. The spin, Ω_1, generates a wave shift of $\Delta\varphi \simeq 0.45$ rad, while Ω_2, generates a wave shift of $\Delta\varphi \simeq 1.8$ rad. Therefore, the corrections due to spin-size effects, can be the leading order contribution from the stellar structure. The spin evolution is negligible, having the same final value as the initial, which is expected from the aligned spin case.

Finally, by considering static effects, as well as spin-size effects, in figure 5.7, we show the role of different Love coefficients in the waveform by measuring the phase shifts from the late inspiral of the same BH-NS interaction described in figure 5.5 and 5.6, but with different dimensionless Love numbers, with corresponding polytropic index, n [14]. In all the figures, the line color refers to different polytropic indices for the NSs. The cyan line for $n = 0.5$, the magenta for $n = 0.7$ and the yellow for $n = 1$. On the top figure we show the different phase shift generated by considering only static tides given different equations of state, without any spin. The phase shift generated, $\Delta\varphi \simeq [0.346, 0.278, 0.200]$ rad, for each $q = [0.5, 0.7, 1]$, respectively. The middle plot is the phase shift with respect to the top figure due to the inclusion of spin/size effects, for which we have added Ω_1. On the plot below we show the phase difference from the top plot and the inclusion of Ω_2. The effects of Ω_1 generates a wave shift of $\Delta\varphi \simeq [0.808, 0.649, 0.458]$ rad, while Ω_2 generates a wave shift of $\Delta\varphi \simeq [3.136, 2.555, 1.851]$ rad, for each $n = [0.5, 0.7, 1]$. As it is expected, our results shows that the smaller the value of n, the more compact the star, leading to stronger signatures in the signal.

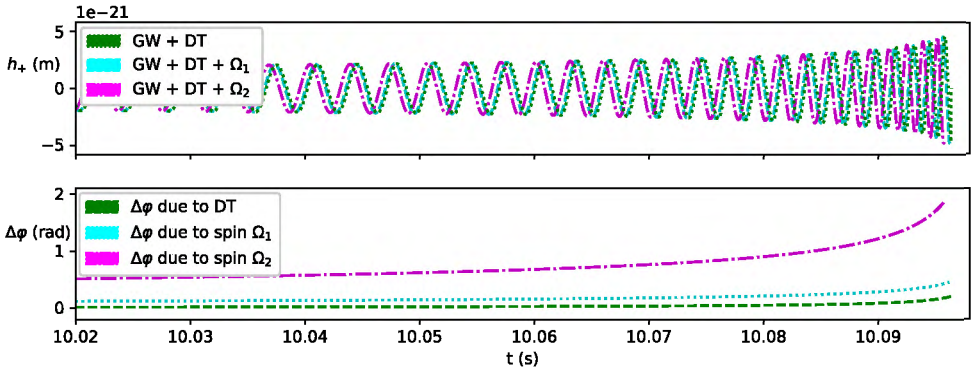

FIGURE 5.6: Gravitational waveforms and phase shifts from the late inspiral of the same BH-NS interaction described in figure 5.5, but with dimensionless spin $\chi = [0.1, 0.2]$ on the NS. On the top figure, each waveform color is extracted from simulations with different effects. The green waveform is GWs + DT, the cyan is GWs + DT + Ω_1 , and the magenta is GWs + DT + Ω_2. On the plot below, the phase shift is measured. The green line is the wave shift generated by dynamical tides, cyan line is the wave shift generated by the spin Ω_1, while the magenta line is the wave shift by Ω_2.

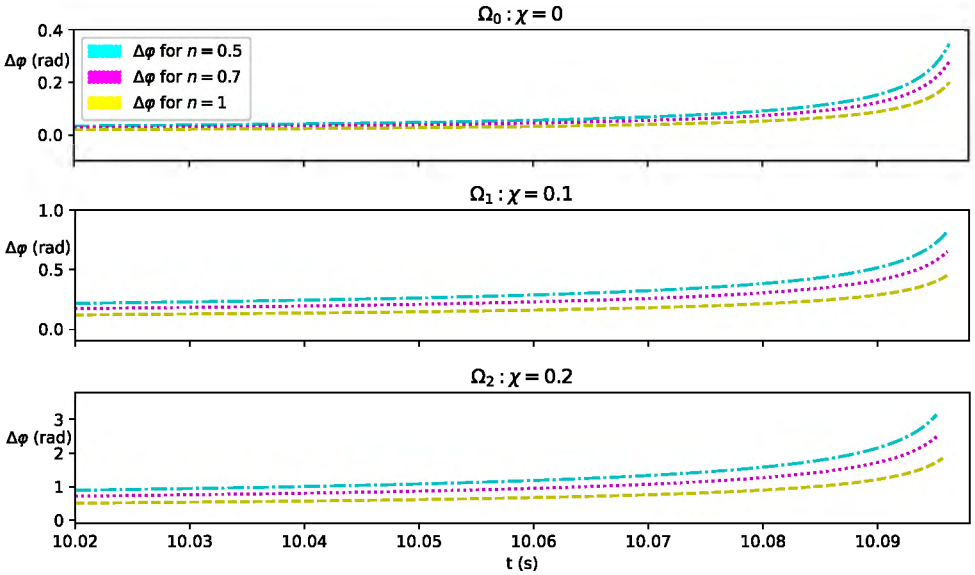

FIGURE 5.7: Phase shifts from the late inspiral of the same BH-NS interaction described in figure 5.5 and 5.6, but with different dimensionless Love numbers, with corresponding polytropic index $n = [0.5, 0.7, 1]$. In all the figures, the line color refers to different polytropic indices for the NSs. On the top figure we show the different phase shift generated by static tides given different equations of state. The middle plot is the phase shift with respect to the top figure due to the inclusion of spin/size effects, for which we have included the angular velocity Ω_1, to the NS, with $\chi_1 = 0.1$. On the plot below we show the phase difference from the top plot and the inclusion of the angular velocity Ω_2, with $\chi_2 = 0.2$.

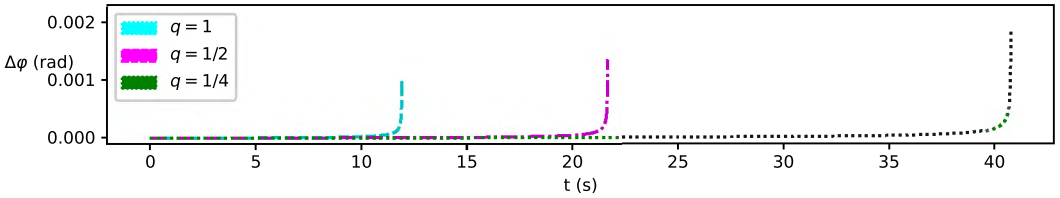

FIGURE 5.8: The phase shift of the gravitational waveform from the late inspiral of three different BBHs that contains dissipative effects due to GW absoprtion. We have performed three different simulations, each of them starting with initial $f_{gw} = 10$ Hz, but differing in the mass ratio, $q = m_2/m_1$, of the binary. The cyan line is for an equal mass case, $q = 1$, with $m_1 = 20M_\odot$. The magenta line is for the unequal mass case, $q = 1/2$, and the green line for $q = 1/4$, both with $m_1 = 20M_\odot$.

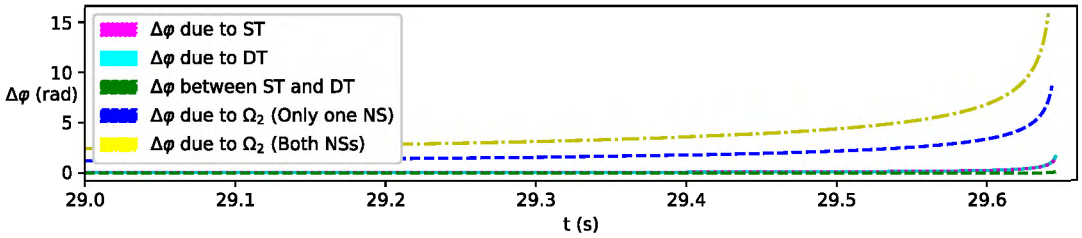

FIGURE 5.9: Phase shifts from simulations of a NS-NS coalescence with an initial frequency of $f_{gw} = 40$ Hz. We add GWs, DT and then spin to the NSs, first only to one member and then to both. The magenta color is the phase shift due to static tides, the cyan for dynamical tides, and the green the difference between both. The blue line is the phase shift due to one spinning star with $\chi = 0.2$, and the orange line for the case in which both stars are spinning with same magnitude and direction (aligned spins).

Binary Black Hole Coalescence

We have performed simulations for three different nonspinning BBHs to study the effects of dissipation due to GW absoprtion in the waveform, which differ in the mass ratio of the binary, $q = m_2/m_1$. All of the simulations are set with an initial gravitational wave frequency, $f_{gw} = 10$ Hz. The cyan line is for an equal mass case, $q = 1$, with $m_1 = 20M_\odot$. The magenta line is for the unequal mass case, $q = 1/2$, and the green line for $q = 1/4$, both with $m_1 = 20M_\odot$. The phase shift due to dissipative effects is, $\Delta\varphi \simeq [0.0009, 0.0013, 0.0018]$, for each $q = [1, 1/2, 1/4]$ respectively. Our results shows that the effect of dissipation can increases for more unequal cases, but this also depends on the mass ratios taken into account. For instance, a simulation of the first detected binary black hole merger, GW150914, shows that dissipative effects makes a phase shift of $\Delta\varphi \simeq 0.0004$, which is the smallest phase shift of all. The study of spin in BH interactions is left for a future study.

Neutron Star Binaries

We set an equal mass NS-NS binary with initial frequency of $f_{gw} = 40$ Hz. In order to illustrate different scenarios, we run four different simulations that includes GWs, DT and aligned spin, $\chi = 0.2$, to the NSs, first only to one member and then to both. In figure 5.9, we show that for tidal effects, the contribution to the wave

shift due to the static term is of $\Delta\varphi \simeq 1$ radians, while the dynamic part contributes to the latter by $\Delta\varphi \simeq 0.1$ rad. By comparing to the wave shift of the BH-NS case, we find that tidal effects in a NS-NS binary have a stronger effect on modifying the waveform. The role of spin-size effects is also enhanced in the NS-NS binary case, for which the waveform is shifted by, $\Delta\varphi \simeq 8$ rad, with only one spinning star, and $\Delta\varphi \simeq 15$ rad, from both spinning NS with same Ω_2 aligned to the orbital momentum of the binary. Each NS contributes the same phase shift, and just like in the BH-NS system, the spin evolution is negligible, having the same final value as the initial one.

Chapter 6

Summary and Outlook

6.1 Summary

In this thesis, we have reviewed and extended the model for spinning extended objects introduced in [1], which is derived using the coset construction [36, 86], a very powerful method that allows us to construct an effective theory from the symmetry breaking pattern as the only input. In this approach, a spinning extended object whose ground state breaks space-time symmetries, is coupled to a gravitational theory formulated as a gauge theory with local Poincaré symmetry and translations being non-linearly realized. We have included the internal structure [29, 30, 46] and electromagnetic charge [30, 63], such that we describe charged spinning extended objects, the most general extended object allowed in a theory of gravity such as general relativity with electrodynamics.

We have derived the covariant building blocks of the effective theory, to build up invariant operators and form an action. We built the underlying theory and matched the coefficients to the full known theory, to obtain the Einstein-Maxwell action in the vierbein formalism. Then, by recognizing the symmetry breaking pattern of a charged spinning extended object, we have built the leading order invariant operators that are allowed by the symmetries, to describe it as a worldline point particle with its properties and internal structure encoded in higher order corrections in the action. Such corrections take into account for the basic necessary ingredients to completely describe an extended object in the developed EFT. By matching the coefficients of the effective action from the literature, we have described charged spinning compact objects, such as BHs and NSs.

Although this effective theory for spinning extended objects [1] by construction is a low energy description of the dynamics, we have shown that spinning compact objects, which are described classically, fit into the description of "slowly" spinning. We have shown the equivalence of our effective theory to the ones currently used to obtain state of the art perturbative results of the binary dynamics [43, 41], with the advantage that the covariant building blocks to construct the tower of invariant operators to all orders have been derived. Therefore, our work complements the aforementioned theories for spinning extended objects, and lays on the foundations for a full description of the possible compact objects that can exists, including modified theories of gravity.

The most direct application of the derived action is on the PN expansion. By matching the coefficients from the currently used effective theories for extended objects [29, 30], which can be spinning [43, 41] and charged [63], our theory reproduces the well known results. In fact, we have shown that the EFT for spinning extended objects in [1], is equivalent to the one in [41], when considering higher order corrections of the bosons, from which the spin-acceleration correction arises. Therefore, our work serves as a bridge between the different effective theories, to provide a

better understanding of the description of compact objects. Nonetheless, this equivalence is only for a special case of the theory developed from the coset, and the vierbein formalism can be exploited for a deeper understanding of the problem.

Moreover, the development of the EFT allowed us to obtain new results on the dynamics of charged spinning compact objects as NSs. Particularly on the conservative and non-conservative polarization effects, due to the presence of an electromagnetic field and spin. These results are essential to probe whether or not charged BHs can exists in nature, and to describe appropriately NSs, or any other extended object that could possibly exists in nature within the current known laws of physics. Given that from the coset construction one derives the basic covariant building blocks, it gives the possibility to construct the tower of higher order invariant operators to all orders. Therefore, this works sets the basis to obtain the state of the art PN results for charged spinning compact objects.

On the numerical side, in this work we have implemented the numerical evolution of the late inspiral of compact objects within the EFT framework using a high accuracy 4th order Hermite integrator for point particle simulations. We have successfully included in the dynamics, leading order spin corrections due to gravity, dynamical tidal and dissipative effects, and the 2.5 PN correction due to GW radiation. We have tested our implementation with analytical results, and matched the coefficients of the effective theory at each time step from the numerical simulations as an internal test. We have extracted the leading order gravitational waveform as a function of the orbital frequency of the binary, and showed the role of the coefficients of the theory by studying the overall phase evolution of the waveform due to the different effects.

Although our current implementation is inaccurate for reproducing high order PN waveforms, what can be learned from our numerical experiments is the order at which the effects of the stellar structure arise in the gravitational waveform. For instance, we have found that in the BH-NS case, the coefficients due to static tides can be measured if LIGO-Virgo observatories, and future detectors, are sensitive enough to measure a shift in the waveform of, $\Delta\varphi \simeq O(10^{-1})$ radians, which will allow us to constrain between different Love coefficients. Furthermore, the stellar structure of spinning NS plays a role on shifting the waveform at order, $\Delta\varphi \simeq O(1)$ radians, which suggest that the spin-size effects, with coefficient n_Ω, can be the leading order effect due to the stellar structure, depending on the value of the spin. On the other hand, to detect dynamical tides (quasi-static) and better constrain the EOS of matter in the NS-BH case, it is necessary to measure, $\Delta\varphi \simeq O(10^{-3})$ radians, same as for dissipative effects due to the GW absorption of the BH.

In the case of the NS-NS binary, the wave shift due to tidal effects is enhanced, with the static tidal effects generating a shift on the wave of, $\Delta\varphi \simeq O(1)$ radians, while the dynamical tides, $\Delta\varphi \simeq O(10^{-1})$ radians, from the contribution of both stars. Just as in the case of the BH-NS, the gravitational spin correction is leading order, and could generate a wave shift of $\Delta\varphi \simeq O(10)$ radians. Nevertheless, the dynamics of nonaligned spins with different magnitudes may complicate this task, as well as binaries with members described by different equations of state. Finally, from the BBH simulations including dissipation, we have shown that their effects generate a shift in the waveform at order, $\Delta\varphi \simeq O(10^{-3})$ radians.

Thus, we conclude that the first coefficient to match, given the order at which it contributes and which requires the least sensitivity, is the coefficient, n_Ω, from the spin-size effects of spinning NSs, both in BH-NS and NS-NS binaries. Then the static tidal coefficient in BH-NS binaries, and the dynamical tides coefficient in NS-NS binaries. Finally dynamical tides in BH-NS interactions, and dissipative effects

in both BH-NS and BBH, which play a role roughly at the same order, and which requires the most sensitivity for the observatories to measure. We argue that the sensitivity required for the LIGO-Virgo and future GWs observatories to constrain the stellar structure of the compact objects with high precision, needs to measure wave shifts with an accuracy of at least, $\Delta\varphi \simeq O(10^{-4})$ radians.

6.2 Outlook

This master's thesis is an exploration for extracting accurate GWs within the EFT framework for a wide class of astrophysical objects, in the region in which the dynamics can be described by the post-Newtonian expansion. In this sense, this framework can allows us to create a rich template bank of waveforms for different classes of systems, such as the ones described in this work, and many others that can be detected by ground and space based GW detectors. There is plenty of room for improvement on our implementation and gravitational wave extraction, and this will be pursued in future work.

On the development of the EFT for compact objects, the special case that we considered here to obtain the PN expansion, was only to show the predictability of the theory. Nonetheless, at the time this work is being finally submitted, we have further developed the EFT to introduce a new methodology that does nos introduce new additional degrees of freedom, like conjugate variables, and which is based solely on the construction used in this work. We are currently obtaining state of the art post-Newtonian and post-Minkowskian results, showing their connection, and performing an exploration to use the developed EFT in the Effective One Body as an input.

Bibliography

[1] Luca V. Delacrétaz et al. "(Re-)Inventing the Relativistic Wheel: Gravity, Cosets, and Spinning Objects". In: *JHEP* 11 (2014), p. 008. DOI: 10.1007/JHEP11(2014)008. arXiv: 1405.7384 [hep-th].

[2] B.P. Abbott et al. "Observation of Gravitational Waves from a Binary Black Hole Merger". In: *Phys. Rev. Lett.* 116.6 (2016), p. 061102. DOI: 10.1103/PhysRevLett.116.061102. arXiv: 1602.03837 [gr-qc].

[3] B.P. Abbott et al. "GW170817: Observation of Gravitational Waves from a Binary Neutron Star Inspiral". In: *Phys. Rev. Lett.* 119.16 (2017), p. 161101. DOI: 10.1103/PhysRevLett.119.161101. arXiv: 1710.05832 [gr-qc].

[4] B. P. Abbott et al. "Multi-messenger Observations of a Binary Neutron Star Merger". In: *Astrophys. J. Lett.* 848.2 (2017), p. L12. DOI: 10.3847/2041-8213/aa91c9. arXiv: 1710.05833 [astro-ph.HE].

[5] B. P. Abbott et al. "Gravitational Waves and Gamma-rays from a Binary Neutron Star Merger: GW170817 and GRB 170817A". In: *Astrophys. J. Lett.* 848.2 (2017), p. L13. DOI: 10.3847/2041-8213/aa920c. arXiv: 1710.05834 [astro-ph.HE].

[6] R. Abbott et al. "Observation of Gravitational Waves from Two Neutron Star–Black Hole Coalescences". In: *Astrophys. J. Lett.* 915.1 (2021), p. L5. DOI: 10.3847/2041-8213/ac082e. arXiv: 2106.15163 [astro-ph.HE].

[7] B. P. Abbott et al. "GWTC-1: A Gravitational-Wave Transient Catalog of Compact Binary Mergers Observed by LIGO and Virgo during the First and Second Observing Runs". In: *Phys. Rev. X* 9.3 (2019), p. 031040. DOI: 10.1103/PhysRevX.9.031040. arXiv: 1811.12907 [astro-ph.HE].

[8] R. Abbott et al. "Population Properties of Compact Objects from the Second LIGO-Virgo Gravitational-Wave Transient Catalog". In: (Oct. 2020). arXiv: 2010.14533 [astro-ph.HE].

[9] A. Buikema et al. "Sensitivity and performance of the Advanced LIGO detectors in the third observing run". In: *Physical Review D* 102.6 (). ISSN: 2470-0029. DOI: 10.1103/physrevd.102.062003. URL: http://dx.doi.org/10.1103/PhysRevD.102.062003.

[10] M. Punturo et al. "The Einstein Telescope: A third-generation gravitational wave observatory". In: *Class. Quant. Grav.* 27 (2010). Ed. by Fulvio Ricci, p. 194002. DOI: 10.1088/0264-9381/27/19/194002.

[11] Michele Maggiore et al. "Science Case for the Einstein Telescope". In: *JCAP* 03 (2020), p. 050. DOI: 10.1088/1475-7516/2020/03/050. arXiv: 1912.02622 [astro-ph.CO].

[12] Enrico Barausse et al. "Prospects for Fundamental Physics with LISA". In: *Gen. Rel. Grav.* 52.8 (2020), p. 81. DOI: 10.1007/s10714-020-02691-1. arXiv: 2001.09793 [gr-qc].

[13] Eanna E. Flanagan and Tanja Hinderer. "Constraining neutron star tidal Love numbers with gravitational wave detectors". In: *Phys. Rev. D* 77 (2008), p. 021502. DOI: 10.1103/PhysRevD.77.021502. arXiv: 0709.1915 [astro-ph].

[14] Tanja Hinderer. "Tidal Love numbers of neutron stars". In: *Astrophys. J.* 677 (2008), pp. 1216–1220. DOI: 10.1086/533487. arXiv: 0711.2420 [astro-ph].

[15] Kent Yagi and Nicolas Yunes. "I-Love-Q Relations in Neutron Stars and their Applications to Astrophysics, Gravitational Waves and Fundamental Physics". In: *Phys. Rev. D* 88.2 (2013), p. 023009. DOI: 10.1103/PhysRevD.88.023009. arXiv: 1303.1528 [gr-qc].

[16] Tanja Hinderer et al. "Effects of neutron-star dynamic tides on gravitational waveforms within the effective-one-body approach". In: *Phys. Rev. Lett.* 116.18 (2016), p. 181101. DOI: 10.1103/PhysRevLett.116.181101. arXiv: 1602.00599 [gr-qc].

[17] Jan Steinhoff et al. "Spin effects on neutron star fundamental-mode dynamical tides: Phenomenology and comparison to numerical simulations". In: *Phys. Rev. Res.* 3.3 (2021), p. 033129. DOI: 10.1103/PhysRevResearch.3.033129. arXiv: 2103.06100 [gr-qc].

[18] Eric Poisson. "Absorption of mass and angular momentum by a black hole: Time-domain formalisms for gravitational perturbations, and the small-hole / slow-motion approximation". In: *Phys. Rev. D* 70 (2004), p. 084044. DOI: 10.1103/PhysRevD.70.084044. arXiv: gr-qc/0407050.

[19] Horng Sheng Chia. "Tidal deformation and dissipation of rotating black holes". In: *Phys. Rev. D* 104.2 (2021), p. 024013. DOI: 10.1103/PhysRevD.104.024013. arXiv: 2010.07300 [gr-qc].

[20] Lavinia Heisenberg. "A systematic approach to generalisations of General Relativity and their cosmological implications". In: *Phys. Rept.* 796 (2019), pp. 1–113. DOI: 10.1016/j.physrep.2018.11.006. arXiv: 1807.01725 [gr-qc].

[21] Steven B. Giddings, Seth Koren, and Gabriel Treviño. "Exploring strong-field deviations from general relativity via gravitational waves". In: *Phys. Rev. D* 100.4 (2019), p. 044005. DOI: 10.1103/PhysRevD.100.044005. arXiv: 1904.04258 [gr-qc].

[22] Vitor Cardoso et al. "Testing strong-field gravity with tidal Love numbers". In: *Phys. Rev. D* 95.8 (2017). [Addendum: Phys.Rev.D 95, 089901 (2017)], p. 084014. DOI: 10.1103/PhysRevD.95.084014. arXiv: 1701.01116 [gr-qc].

[23] Samir D. Mathur. "The Fuzzball proposal for black holes: An Elementary review". In: *Fortsch. Phys.* 53 (2005). Ed. by E. Kiritsis, pp. 793–827. DOI: 10.1002/prop.200410203. arXiv: hep-th/0502050.

[24] Pawel O. Mazur and Emil Mottola. "Gravitational condensate stars: An alternative to black holes". In: (Sept. 2001). arXiv: gr-qc/0109035.

[25] Thibault Damour and Sergey N. Solodukhin. "Wormholes as black hole foils". In: *Phys. Rev. D* 76 (2007), p. 024016. DOI: 10.1103/PhysRevD.76.024016. arXiv: 0704.2667 [gr-qc].

[26] Remo Ruffini and Silvano Bonazzola. "Systems of selfgravitating particles in general relativity and the concept of an equation of state". In: *Phys. Rev.* 187 (1969), pp. 1767–1783. DOI: 10.1103/PhysRev.187.1767.

[27] Daniel Baumann, Horng Sheng Chia, and Rafael A. Porto. "Probing Ultralight Bosons with Binary Black Holes". In: *Phys. Rev. D* 99.4 (2019), p. 044001. DOI: 10.1103/PhysRevD.99.044001. arXiv: 1804.03208 [gr-qc].

[28] Leong Khim Wong, Anne-Christine Davis, and Ruth Gregory. "Effective field theory for black holes with induced scalar charges". In: *Phys. Rev. D* 100.2 (2019), p. 024010. DOI: 10.1103/PhysRevD.100.024010. arXiv: 1903.07080 [hep-th].

[29] Walter D. Goldberger and Ira Z. Rothstein. "An Effective field theory of gravity for extended objects". In: *Phys. Rev. D* 73 (2006), p. 104029. DOI: 10.1103/PhysRevD.73.104029. arXiv: hep-th/0409156.

[30] Walter D. Goldberger and Ira Z. Rothstein. "Dissipative effects in the worldline approach to black hole dynamics". In: *Phys. Rev. D* 73 (2006), p. 104030. DOI: 10.1103/PhysRevD.73.104030. arXiv: hep-th/0511133.

[31] Nima Arkani-Hamed, Yu-tin Huang, and Donal O'Connell. "Kerr black holes as elementary particles". In: *JHEP* 01 (2020), p. 046. DOI: 10.1007/JHEP01(2020)046. arXiv: 1906.10100 [hep-th].

[32] Nathan Moynihan. "Kerr-Newman from Minimal Coupling". In: *JHEP* 01 (2020), p. 014. DOI: 10.1007/JHEP01(2020)014. arXiv: 1909.05217 [hep-th].

[33] Alfredo Guevara, Alexander Ochirov, and Justin Vines. "Scattering of Spinning Black Holes from Exponentiated Soft Factors". In: *JHEP* 09 (2019), p. 056. DOI: 10.1007/JHEP09(2019)056. arXiv: 1812.06895 [hep-th].

[34] Ming-Zhi Chung et al. "The simplest massive S-matrix: from minimal coupling to Black Holes". In: *JHEP* 04 (2019), p. 156. DOI: 10.1007/JHEP04(2019)156. arXiv: 1812.08752 [hep-th].

[35] S. Coleman, J. Wess, and Bruno Zumino. "Structure of Phenomenological Lagrangians. I". In: *Phys. Rev.* 177 (5 Jan. 1969), pp. 2239–2247. DOI: 10.1103/PhysRev.177.2239. URL: https://link.aps.org/doi/10.1103/PhysRev.177.2239.

[36] Curtis G. Callan Jr. et al. "Structure of phenomenological Lagrangians. 2." In: *Phys. Rev.* 177 (1969), pp. 2247–2250. DOI: 10.1103/PhysRev.177.2247.

[37] Dmitri V. Volkov. "Phenomenological Lagrangians". In: *Fiz. Elem. Chast. Atom. Yadra* 4 (1973), pp. 3–41.

[38] E. A. Ivanov and V. I. Ogievetsky. "The Inverse Higgs Phenomenon in Nonlinear Realizations". In: *Teor. Mat. Fiz.* 25 (1975), pp. 164–177. DOI: 10.1007/BF01028947.

[39] Riccardo Penco. "An Introduction to Effective Field Theories". In: (June 2020). arXiv: 2006.16285 [hep-th].

[40] J. Goldstone. "Field Theories with Superconductor Solutions". In: *Nuovo Cim.* 19 (1961), pp. 154–164. DOI: 10.1007/BF02812722.

[41] Michele Levi and Jan Steinhoff. "Spinning gravitating objects in the effective field theory in the post-Newtonian scheme". In: *JHEP* 09 (2015), p. 219. DOI: 10.1007/JHEP09(2015)219. arXiv: 1501.04956 [gr-qc].

[42] Walter D. Goldberger, Jingping Li, and Ira Z. Rothstein. "Non-conservative effects on spinning black holes from world-line effective field theory". In: *JHEP* 06 (2021), p. 053. DOI: 10.1007/JHEP06(2021)053. arXiv: 2012.14869 [hep-th].

[43] Rafael A. Porto. "Post-Newtonian corrections to the motion of spinning bodies in NRGR". In: *Phys. Rev. D* 73 (2006), p. 104031. DOI: 10.1103/PhysRevD.73.104031. arXiv: gr-qc/0511061.

[44] Michele Levi and Jan Steinhoff. "Leading order finite size effects with spins for inspiralling compact binaries". In: *JHEP* 06 (2015), p. 059. DOI: 10.1007/JHEP06(2015)059. arXiv: 1410.2601 [gr-qc].

[45] Irvin Martinez and Amanda Weltman. "Effective Field Theory for Compact Object Evolution in Non-Relativistic General Relativity". In: (Dec. 2020). DOI: 10.17605/OSF.IO/Q6AEH. arXiv: 2012.04140 [gr-qc].

[46] Solomon Endlich and Riccardo Penco. "Effective field theory approach to tidal dynamics of spinning astrophysical systems". In: *Phys. Rev. D* 93.6 (2016), p. 064021. DOI: 10.1103/PhysRevD.93.064021. arXiv: 1510.08889 [gr-qc].

[47] Kent Yagi and Nicolás Yunes. "Approximate Universal Relations for Neutron Stars and Quark Stars". In: *Phys. Rept.* 681 (2017), pp. 1–72. DOI: 10.1016/j.physrep.2017.03.002. arXiv: 1608.02582 [gr-qc].

[48] Kent Yagi and Nicolas Yunes. "I-Love-Q Relations: From Compact Stars to Black Holes". In: *Class. Quant. Grav.* 33.9 (2016), p. 095005. DOI: 10.1088/0264-9381/33/9/095005. arXiv: 1601.02171 [gr-qc].

[49] Sayan Chakrabarti, Térence Delsate, and Jan Steinhoff. "Effective action and linear response of compact objects in Newtonian gravity". In: *Phys. Rev. D* 88 (2013), p. 084038. DOI: 10.1103/PhysRevD.88.084038. arXiv: 1306.5820 [gr-qc].

[50] Rafael A. Porto. "Absorption effects due to spin in the worldline approach to black hole dynamics". In: *Phys. Rev. D* 77 (2008), p. 064026. DOI: 10.1103/PhysRevD.77.064026. arXiv: 0710.5150 [hep-th].

[51] Luc Blanchet. "Gravitational radiation from post-Newtonian sources and inspiralling compact binaries". In: *Living Rev. Rel.* 9 (2006), p. 4.

[52] Alessandra Buonanno and Thibault Damour. "Transition from inspiral to plunge in binary black hole coalescences". In: *Phys. Rev. D* 62 (2000), p. 064015. DOI: 10.1103/PhysRevD.62.064015. arXiv: gr-qc/0001013.

[53] Frans Pretorius. "Evolution of binary black hole spacetimes". In: *Phys. Rev. Lett.* 95 (2005), p. 121101. DOI: 10.1103/PhysRevLett.95.121101. arXiv: gr-qc/0507014.

[54] E. W. Leaver. "An Analytic representation for the quasi normal modes of Kerr black holes". In: *Proc. Roy. Soc. Lond. A* 402 (1985), pp. 285–298. DOI: 10.1098/rspa.1985.0119.

[55] A. Buonanno and T. Damour. "Effective one-body approach to general relativistic two-body dynamics". In: *Phys. Rev. D* 59 (1999), p. 084006. DOI: 10.1103/PhysRevD.59.084006. arXiv: gr-qc/9811091.

[56] Thibault Damour and Alessandro Nagar. "Effective One Body description of tidal effects in inspiralling compact binaries". In: *Phys. Rev. D* 81 (2010), p. 084016. DOI: 10.1103/PhysRevD.81.084016. arXiv: 0911.5041 [gr-qc].

[57] Sebastiano Bernuzzi, Alessandro Nagar, and Anil Zenginoglu. "Horizon-absorption effects in coalescing black-hole binaries: An effective-one-body study of the non-spinning case". In: *Phys. Rev. D* 86 (2012), p. 104038. DOI: 10.1103/PhysRevD.86.104038. arXiv: 1207.0769 [gr-qc].

[58] LIGO Scientific Collaboration. *LIGO Algorithm Library - LALSuite*. free software (GPL). 2018. DOI: 10.7935/GT1W-FZ16.

[59] John G. Baker et al. "Consistency of post-Newtonian waveforms with numerical relativity". In: *Phys. Rev. Lett.* 99 (2007), p. 181101. DOI: 10.1103/PhysRevLett.99.181101. arXiv: gr-qc/0612024.

[60] Michael Boyle et al. "High-accuracy comparison of numerical relativity simulations with post-Newtonian expansions". In: *Phys. Rev. D* 76 (2007), p. 124038. DOI: 10.1103/PhysRevD.76.124038. arXiv: 0710.0158 [gr-qc].

[61] Walter D. Goldberger and Ira Z. Rothstein. "Towers of Gravitational Theories". In: *Gen. Rel. Grav.* 38 (2006), pp. 1537–1546. DOI: 10.1142/S0218271806009698. arXiv: hep-th/0605238.

[62] Barak Kol and Michael Smolkin. "Non-Relativistic Gravitation: From Newton to Einstein and Back". In: *Class. Quant. Grav.* 25 (2008), p. 145011. DOI: 10.1088/0264-9381/25/14/145011. arXiv: 0712.4116 [hep-th].

[63] Raj Patil. "EFT approach to general relativity: correction to EIH Lagrangian due to electromagnetic charge". In: *Gen. Rel. Grav.* 52.9 (2020), p. 95. DOI: 10.1007/s10714-020-02748-1. arXiv: 2009.11107 [gr-qc].

[64] Irvin Martínez. "Effective actions for compact objects in an effective field theory of gravity". In: (Nov. 2021). arXiv: 2111.09070 [hep-th].

[65] Walter D. Goldberger and Andreas Ross. "Gravitational radiative corrections from effective field theory". In: *Phys. Rev. D* 81 (2010), p. 124015. DOI: 10.1103/PhysRevD.81.124015. arXiv: 0912.4254 [gr-qc].

[66] Michele Levi and Jan Steinhoff. "Complete conservative dynamics for inspiralling compact binaries with spins at the fourth post-Newtonian order". In: *JCAP* 09 (2021), p. 029. DOI: 10.1088/1475-7516/2021/09/029. arXiv: 1607.04252 [gr-qc].

[67] A. Einstein, L. Infeld, and B. Hoffmann. "The Gravitational Equations and the Problem of Motion". In: *Annals of Mathematics* 39.1 (1938), pp. 65–100. ISSN: 0003486X. URL: http://www.jstor.org/stable/1968714.

[68] Stefano Foffa and Riccardo Sturani. "Effective field theory calculation of conservative binary dynamics at third post-Newtonian order". In: *Phys. Rev. D* 84 (2011), p. 044031. DOI: 10.1103/PhysRevD.84.044031. arXiv: 1104.1122 [gr-qc].

[69] Stefano Foffa et al. "Conservative dynamics of binary systems to fourth Post-Newtonian order in the EFT approach II: Renormalized Lagrangian". In: *Phys. Rev. D* 100.2 (2019), p. 024048. DOI: 10.1103/PhysRevD.100.024048. arXiv: 1903.05118 [gr-qc].

[70] Stefano Foffa et al. "Static two-body potential at fifth post-Newtonian order". In: *Phys. Rev. Lett.* 122.24 (2019), p. 241605. DOI: 10.1103/PhysRevLett.122.241605. arXiv: 1902.10571 [gr-qc].

[71] Michele Levi. "Next to Leading Order gravitational Spin1-Spin2 coupling with Kaluza-Klein reduction". In: *Phys. Rev. D* 82 (2010), p. 064029. DOI: 10.1103/PhysRevD.82.064029. arXiv: 0802.1508 [gr-qc].

[72] Rafael A Porto and Ira Z. Rothstein. "Next to Leading Order Spin(1)Spin(1) Effects in the Motion of Inspiralling Compact Binaries". In: *Phys. Rev. D* 78 (2008). [Erratum: Phys.Rev.D 81, 029905 (2010)], p. 044013. DOI: 10.1103/PhysRevD.78.044013. arXiv: 0804.0260 [gr-qc].

[73] Rafael A. Porto and Ira Z. Rothstein. "Spin(1)Spin(2) Effects in the Motion of Inspiralling Compact Binaries at Third Order in the Post-Newtonian Expansion". In: *Phys. Rev. D* 78 (2008). [Erratum: Phys.Rev.D 81, 029904 (2010)], p. 044012. DOI: 10.1103/PhysRevD.78.044012. arXiv: 0802.0720 [gr-qc].

[74] Michele Levi. "Next to Leading Order gravitational Spin-Orbit coupling in an Effective Field Theory approach". In: *Phys. Rev. D* 82 (2010), p. 104004. DOI: 10.1103/PhysRevD.82.104004. arXiv: 1006.4139 [gr-qc].

[75] Rafael A. Porto. "Next to leading order spin-orbit effects in the motion of inspiralling compact binaries". In: *Class. Quant. Grav.* 27 (2010), p. 205001. DOI: 10.1088/0264-9381/27/20/205001. arXiv: 1005.5730 [gr-qc].

[76] Michèle Levi, Stavros Mougiakakos, and Mariana Vieira. "Gravitational cubic-in-spin interaction at the next-to-leading post-Newtonian order". In: *JHEP* 01 (2021), p. 036. DOI: 10.1007/JHEP01(2021)036. arXiv: 1912.06276 [hep-th].

[77] Michèle Levi and Fei Teng. "NLO gravitational quartic-in-spin interaction". In: *JHEP* 01 (2021), p. 066. DOI: 10.1007/JHEP01(2021)066. arXiv: 2008.12280 [hep-th].

[78] Michèle Levi, Andrew J. Mcleod, and Matthew Von Hippel. "N^{3}LO gravitational spin-orbit coupling at order G^4". In: *JHEP* 07 (2021), p. 115. DOI: 10.1007/JHEP07(2021)115. arXiv: 2003.02827 [hep-th].

[79] Michèle Levi, Andrew J. Mcleod, and Matthew Von Hippel. "N^{3}LO gravitational quadratic-in-spin interactions at G^4". In: *JHEP* 07 (2021), p. 116. DOI: 10.1007/JHEP07(2021)116. arXiv: 2003.07890 [hep-th].

[80] Rafael A. Porto. "The effective field theorist approach to gravitational dynamics". In: *Phys. Rept.* 633 (2016), pp. 1–104. DOI: 10.1016/j.physrep.2016.04.003. arXiv: 1601.04914 [hep-th].

[81] Michèle Levi. "Effective Field Theories of Post-Newtonian Gravity: A comprehensive review". In: *Rept. Prog. Phys.* 83.7 (2020), p. 075901. DOI: 10.1088/1361-6633/ab12bc. arXiv: 1807.01699 [hep-th].

[82] Piet Hut, Jun Makino, and Steve McMillan. "Building a better leapfrog". In: *Astrophys. J. Lett.* 443 (1995), p. L93. DOI: 10.1086/187844.

[83] Curt Cutler and Eanna E. Flanagan. "Gravitational waves from merging compact binaries: How accurately can one extract the binary's parameters from the inspiral wave form?" In: *Phys. Rev. D* 49 (1994), pp. 2658–2697. DOI: 10.1103/PhysRevD.49.2658. arXiv: gr-qc/9402014.

[84] Sidney R. Coleman and J. Mandula. "All Possible Symmetries of the S Matrix". In: *Phys. Rev.* 159 (1967). Ed. by A. Zichichi, pp. 1251–1256. DOI: 10.1103/PhysRev.159.1251.

[85] Michele Maggiore. *A Modern introduction to quantum field theory*. 2005.

[86] E. A. Ivanov and J. Niederle. "Gauge Formulation of Gravitation Theories. 1. The Poincare, De Sitter and Conformal Cases". In: *Phys. Rev. D* 25 (1982), p. 976. DOI: 10.1103/PhysRevD.25.976.

[87] Ian Low and Aneesh V. Manohar. "Spontaneously broken space-time symmetries and Goldstone's theorem". In: *Phys. Rev. Lett.* 88 (2002), p. 101602. DOI: 10.1103/PhysRevLett.88.101602. arXiv: hep-th/0110285.

[88] A.J Hanson and T Regge. "The relativistic spherical top". In: *Annals of Physics* 87.2 (1974), pp. 498–566. ISSN: 0003-4916. DOI: https://doi.org/10.1016/0003-4916(74)90046-3. URL: https://www.sciencedirect.com/science/article/pii/0003491674900463.

[89] Jan Steinhoff. "Spin gauge symmetry in the action principle for classical relativistic particles". In: (Jan. 2015). arXiv: 1501.04951 [gr-qc].

[90] R.D. Jordan. "Effective Field Equations for Expectation Values". In: *Phys. Rev. D* 33 (1986), pp. 444–454. DOI: 10.1103/PhysRevD.33.444.

[91] Taylor Binnington and Eric Poisson. "Relativistic theory of tidal Love numbers". In: *Phys. Rev. D* 80 (2009), p. 084018. DOI: 10.1103/PhysRevD.80.084018. arXiv: 0906.1366 [gr-qc].

[92] Panagiotis Charalambous, Sergei Dubovsky, and Mikhail M. Ivanov. "On the Vanishing of Love Numbers for Kerr Black Holes". In: *JHEP* 05 (2021), p. 038. DOI: 10.1007/JHEP05(2021)038. arXiv: 2102.08917 [hep-th].

[93] Lam Hui et al. "Ladder Symmetries of Black Holes: Implications for Love Numbers and No-Hair Theorems". In: (May 2021). arXiv: 2105.01069 [hep-th].

[94] P. Hut. "Tidal evolution in close binary systems." In: *aap* 99 (June 1981), pp. 126–140.

[95] M. Coleman Miller, Frederick K. Lamb, and Gregory B. Cook. "Effects of rapid stellar rotation on equation of state constraints derived from quasi-periodic brightness oscillations". In: *Astrophys. J.* 509 (1998), p. 793. DOI: 10.1086/306533. arXiv: astro-ph/9805007.

[96] D. G. Ravenhall and C. J. Pethick. "Neutron Star Moments of Inertia". In: *apj* 424 (Apr. 1994), p. 846. DOI: 10.1086/173935.

[97] Paulo Bedaque and Andrew W. Steiner. "Sound velocity bound and neutron stars". In: *Phys. Rev. Lett.* 114.3 (2015), p. 031103. DOI: 10.1103/PhysRevLett.114.031103. arXiv: 1408.5116 [nucl-th].

[98] E. Poisson and C.M. Will. *Gravity: Newtonian, Post-Newtonian, Relativistic*. Cambridge University Press, 2014. ISBN: 9781107032866. URL: https://books.google.com.mx/books?id=PZ5cAwAAQBAJ.

[99] Paul I. Jefremov, Oleg Yu. Tsupko, and Gennady S. Bisnovatyi-Kogan. "Innermost stable circular orbits of spinning test particles in Schwarzschild and Kerr space-times". In: *Phys. Rev. D* 91.12 (2015), p. 124030. DOI: 10.1103/PhysRevD.91.124030. arXiv: 1503.07060 [gr-qc].

[100] Chad R. Galley. "Classical Mechanics of Nonconservative Systems". In: *Phys. Rev. Lett.* 110.17 (2013), p. 174301. DOI: 10.1103/PhysRevLett.110.174301. arXiv: 1210.2745 [gr-qc].

[101] John F. Donoghue. "General relativity as an effective field theory: The leading quantum corrections". In: *Phys. Rev. D* 50 (1994), pp. 3874–3888. DOI: 10.1103/PhysRevD.50.3874. arXiv: gr-qc/9405057.

[102] N. E. J Bjerrum-Bohr, John F. Donoghue, and Barry R. Holstein. "Quantum gravitational corrections to the nonrelativistic scattering potential of two masses". In: *Phys. Rev. D* 67 (2003). [Erratum: Phys.Rev.D 71, 069903 (2005)], p. 084033. DOI: 10.1103/PhysRevD.71.069903. arXiv: hep-th/0211072.

[103] Michele Levi and Jan Steinhoff. "EFTofPNG: A package for high precision computation with the Effective Field Theory of Post-Newtonian Gravity". In: *Class. Quant. Grav.* 34.24 (2017), p. 244001. DOI: 10.1088/1361-6382/aa941e. arXiv: 1705.06309 [gr-qc].

[104] Julian S. Schwinger. "Quantized gravitational field". In: *Phys. Rev.* 130 (1963). Ed. by K. A. Milton, pp. 1253–1258. DOI: 10.1103/PhysRev.130.1253.

[105] Junichiro Makino et al. "GRAPE-4: A Massively Parallel Special-Purpose Computer for Collisional N-Body Simulations". In: 480.1 (May 1997), pp. 432–446. DOI: 10.1086/303972.

[106] Evan Schneider and Brant Robertson. "Cholla : A New Massively-Parallel Hydrodynamics Code For Astrophysical Simulation". In: *The Astrophysical Journal Supplement Series* 217 (Oct. 2014). DOI: 10.1088/0067-0049/217/2/24.

[107] Michele Maggiore. *Gravitational Waves. Vol. 1: Theory and Experiments*. Oxford Master Series in Physics. Oxford University Press, 2007. ISBN: 978-0-19-857074-5, 978-0-19-852074-0.

[108] P. C. Peters. "Gravitational Radiation and the Motion of Two Point Masses". In: *Physical Review* 136.4B (Nov. 1964), pp. 1224–1232. DOI: 10.1103/PhysRev.136.B1224.

[109] Benjamin P. Abbott et al. "Sensitivity of the Advanced LIGO detectors at the beginning of gravitational wave astronomy". In: *Phys. Rev. D* 93.11 (2016). [Addendum: Phys.Rev.D 97, 059901 (2018)], p. 112004. DOI: 10.1103/PhysRevD.93.112004. arXiv: 1604.00439 [astro-ph.IM].